Prediction of Deterioration of Concrete Bridges

Corrosion of Reinforcement due to Chloride Ingress and Carbonation

cover: Broadway bridge across Depot Street, constructed in ±1915, Ann Arbor, Michigan, U.S.A., photo by author.

Prediction of Deterioration of Concrete Bridges

Corrosion of Reinforcement due to Chloride Ingress and Carbonation

PROEFSCHRIFT

ter verkrijging van de graad van doctor
aan de Technische Universiteit Delft,
op gezag van de Rector Magnificus prof.dr.ir. J.T. Fokkema,
voorzitter van het College voor Promoties,
in het openbaar te verdedigen

op dinsdag 8 juni 2004 om 15:30 uur

door

Gerardus Cornelis Maria GAAL

civiel ingenieur
geboren te Alkmaar

Dit proefschrift is goedgekeurd door de promotoren:
Prof.dr.ir. J.C. Walraven
Prof.ir. A.C.W.M. Vrouwenvelder

Samenstelling promotiecommissie:

Rector Magnificus,	voorzitter
Prof.dr.ir. J.C. Walraven,	Technische Universiteit Delft, promotor
Prof.ir. A.C.W.M. Vrouwenvelder,	Technische Universiteit Delft, promotor
Prof.dr.ir. J.M. van Noortwijk,	Technische Universiteit Delft
Prof.dr.ir. A.S. Nowak,	University of Michigan, U.S.A.
Dr.ir. C. van der Veen,	Technische Universiteit Delft
Dr.ir. H.J.H. Brouwers,	Universiteit Twente
Dr. R.B. Polder,	TNO Bouw
Prof.dr.ir. K. van Breugel	Technische Universiteit Delft, reserve lid

This work has been financially supported by:
- Ministry of Transport, Public Works and Water Management
- Research School Structural Engineering
- TNO Building and Construction Research

Published and distributed by: DUP Science

DUP Science is an imprint of
Delft University Press
P.O. Box 98
2600 MG Delft
the Netherlands
telephone: +31 15 2785678
telefax: +31 15 2785706
e-mail: Info@Library.TUDelft.nl

ISBN 90-407-2500-4

Keywords: corrosion, chloride, spalling

Printed in the Netherlands

Acknowledgements

This thesis reports on a research project carried out at the Department of Mechanics Materials and Construction of Delft University of Technology. The financial support of the Research School of Structural Engineering, Ministry of Transport, Public Works and Water Management, and TNO Building and Construction Research is gratefully acknowledged.

I would like to thank my advisors Joost Walraven, Ton Vrouwenvelder and Cor van der Veen for the fruitful cooperation, giving me the opportunity to conduct this Ph.D. research project and providing a lot of freedom in my research. Further I would like to thank Ton van Beek, Joost Gulikers, Ben Jansen, Ying Li, Hessel Voortman and Geert Henk Wijnants who took time to review and comment on this thesis. They gave me insight, resources, suggestions, and help, all of which have made this a better document. With my good friend Hessel Voortman, I had numerous discussions on my research usually while enjoying a beer in the sunshine. I thank Boyke Djorai for his support to this project in co-ordinating matters related to the Ministry of Transport, Public Works and Water Management.

I am aware of the fact that this research project was only possible with the help and experience of all my colleagues. Especially, I would like to thank Ger Nagtegaal and Fred Schilperoort for their technical support that proved to be essential to produce and publish this thesis, and Plonia Wardenier for her dedication by analyzing the chloride concentration of over 400 concrete samples. For preparing most drawings in this thesis, I thank Theo Steijn.

I would like to express my sincere recognition to all those who are not mentioned in the acknowledgements but who graciously assisted me by providing service life performance information. Without their assistance this study could not have been performed. In particular I wish to acknowledge the help of numerous employees of Delft University of Technology, the Ministry of Transport, Public Works and Water Management, and TNO Building and Construction Research.

Finally, I would like to thank my parents and sister for their love, support and patience.

Summary

The first reinforced concrete structures were built at the end of the 19th century. These structures were mostly sewers, floors, water tanks etc. In the early 20th century, when the first concrete bridges were built, the general idea was that concrete made with sufficient cement would prevent the reinforcement from corroding. In those days, it was assumed that an everlasting protective layer would prevent the reinforcement from corroding.

During the 1980s and 1990s, a strong increase of the need for maintenance for concrete bridges was observed in the United States and Great Britain. It was therefore not surprising that in the U.S. approximately 150 – 200 bridges, out of 600,000 bridges, suffer partial of full collapse each year. However, long before a bridge will collapse, parts of concrete may come off due to spalling. These loose parts of concrete might already endanger passing traffic. In this thesis failure is therefore defined as the undesirable event of an intolerable amount of spalling. The scope of this thesis is limited to deterioration that results in damage to concrete bridges due to cracks and concrete spalling that are the result of corrosion of the steel reinforcement.

The main problem of estimating the future maintenance of bridge stocks is the heterogeneous composition of bridge stocks. A few examples of the heterogeneity are:

- during a number of years in the 1960s or 1970s a large number of bridges has been built in most countries;
- over the years, in most European countries, the cover depth that is required by the standard has increased from 15mm to 35mm;
- concrete quality, with respect to durability, has shown a considerable improvement over the last decades.

Because of the changes quoted above, each bridge will show a different pattern of deterioration in time. Therefore, a simple extrapolation of present inspection data will not lead to an accurate estimate of future deterioration.

So, the main question to be answered is: ‘What is the rate of deterioration of a concrete bridge stock, taking into account the history of bridge design and construction?’.

A large number of mechanisms, like sulphate attack, freeze-thaw action, alkali silica reaction, chloride ingress or carbonation might lead to deterioration of concrete structures. Based on numerous publications, it was learned that chloride ingress and carbonation cause the majority of deterioration at concrete structures. The effect of the increased use of chloride-based de-icing agents is dramatically illustrated by the fact that surface spalls were quite rare in California until the late 1960s when the use of chemical de-icers was introduced in this state.

It is commonly accepted to model the ingress of chlorides as a diffusion process. The ingress of chlorides is, however, affected by a number of phenomena, like absorption, various exposure conditions etc. An extensive literature review showed that the drawbacks are limited and can be overcome by assuming an effective chloride diffusion coefficient.

Once the chloride concentration at the reinforcement reaches the critical chloride concentration, corrosion of the reinforcement is initiated. A universal well-defined threshold value appears not to exist, because the lowest reported value is 0.2% whereas the highest is 2.0% by mass of binder. By analyzing the definition, the test set up, chloride binding and cation the reported values could be narrowed down to an acceptable value with a small scatter.

At first it was assumed that the chloride diffusion coefficient would be a constant value in time. However, on-site tests proved that the diffusion coefficient shows a considerable reduction in time. Because of the reduced diffusion coefficient, the amount of chlorides that can penetrate into the structure is considerably reduced. This phenomenon is especially important for bridges that are constructed before salt (sodium chloride) was used to keep bridges free of ice. The use of common salt to keep roads and bridges free of ice was carried out since the 1940s, in the U.S., and since the 1960s in Europe. The reduced coefficient of chloride diffusion in time and the subsequent reduced chloride ingress, explains the rather good condition of the pre World War II bridges compared to the bridges that were constructed during the early 1970s. In this thesis a model is proposed that is able to determine the chloride ingress, when a structure is not exposed to chlorides shortly after casting.

The input parameters determine to a large extent the quality of the outcome of the predictive model. Besides the critical chloride concentration and ageing coefficient, an extensive research program was carried out to determine the chloride diffusion coefficient and surface chloride concentration of a representative set of Dutch concrete bridges. From nine concrete bridges over 100 cores were taken to determine the resistance to chloride ingress. The locations of the cores were chosen in such a way that different structural elements and both concrete made of portland cement and blast furnace slag cement was tested. The slag content could not be retrieved from the design specification and was therefore determined by visual (microscopy) inspection of a number of thin sections of the drilled cores. The results indicated that the cement used could be classified as CEM III/A.

By analyzing the chloride ingress, a chloride diffusion coefficient and surface chloride concentration was obtained for each core. Both parameters were derived by fitting Fick's second law of diffusion to the observed chloride profile. Every drilled core was sliced into discs of which the chloride concentration was determined, this resulted in a chloride profile for each core. Not all observed chloride profiles fitted nicely to Fick's law, the differences increased for blast furnace slag cement compared to portland ce-

ment, and for structural elements in a relative dry environment (column) compared to the bridge deck. The suggested outstanding resistance of concrete made of blast furnace slag cement to chloride ingress was not observed at the analysed bridges. These bridges were constructed during the 1940s and 1960s. Both portland cement and blast furnace slag cement showed similar resistance to chloride ingress. The surface chloride concentration for blast furnace slag cement was somewhat higher than that of portland cement.

Finally, the amount of spalling of a concrete bridge is determined from the selected model and determined input parameters. The amount of spalling is determined by using the stochastic parameters combined with a first order reliability method. Besides input parameters like diffusion coefficient, also the age distribution and the size of the decks are taken into account when the amount of spalling is determined. To validate the results of the predictive method the results are compared to the observed spalling at 81 Dutch concrete highway bridges. A number of bridges were inspected twice, which resulted in 91 inspection results of 81 bridges. The comparison between the predicted and observed spalling showed that the predicted spalling closely matched the observed spalling. When the predictive method was used to determine the need for maintenance of the Dutch highway bridges, it showed that the amount of spalling will double over the coming decades.

Samenvatting

De eerste betonnen constructies zijn gebouwd aan het einde van de 19e eeuw. Deze constructies waren voornamelijk riolen, vloeren, water reservoirs etc. In de vroege jaren van de 20e eeuw, toen de eerste betonnen bruggen zijn gebouwd, was een breed gedragen gedachte dat beton dat gemaakt is met voldoende cement, het corroderen van de wapening zou voorkomen. In die dagen werd verondersteld dat een beschermde laag de wapening eeuwigdurend zou vrijwaren van corrosie.

Tijdens de jaren 80 en 90 van de 20e eeuw, werd voor betonnen bruggen in de Verenigde Staten en Groot-Brittannië een sterke toename van de onderhoudsbehoefte gesignaleerd. Het was daarom niet verrassend dat, in de Verenigde Staten, jaarlijks 100 tot 200 bruggen, van de 600.000 bruggen, geheel of gedeeltelijk instorten. Echter lang voordat een brug instort, zullen stukken beton van de constructie loskomen. De stukken beton kunnen reeds gevaar opleveren voor het passerende verkeer. Daarom is in dit proefschrift het falen van de constructie gedefinieerd als een ontoelaatbare hoeveelheid van de dekking die los komt van de constructie. Het kader van dit proefschrift is beperkt tot schade dat het gevolg is van scheuren en afgedrukte dekking ten gevolge van corrosie van de wapening.

Een groot probleem bij het bepalen van toekomstig onderhoud van een serie van bruggen is de heterogene samenstelling van het bestand. Een paar voorbeelden van de heterogeniteit is:

- gedurende een aantal jaren in de jaren 60 en 70 van de 20e eeuw, zijn een groot aantal bruggen gebouwd;
- in de loop der jaren is de voorgeschreven dekking volgens de norm toegenomen van 15mm tot 35mm;
- de betonkwaliteit, met betrekking tot duurzaamheid, heeft een aanzienlijke verbetering vertoond tijdens de afgelopen decennia.

Wegens de hierboven beschreven veranderingen zal elke brug een verschillend verloop van de veroudering in de tijd vertonen. Daarom zal een eenvoudige extrapolatie van de huidige inspectiegegevens niet leiden tot een betrouwbare voorspelling van toekomstige schade.

Uit het bovenstaande volgt de hoofdvraag van dit onderzoek: ‘Hoe is het verloop van de veroudering van een bruggenbestand, waarbij de verandering in ontwerp en bouwwijze wordt meegenomen?’.

Een groot aantal verouderingsprocessen zoals, sulfaataantasting, vorst-dooi schade, alkali-silica reactie, chloriden-indringing en carbonatatie zou tot schade aan betonnen constructies kunnen leiden. Op basis van een groot aantal literatuurbronnen is geconcludeerd dat het grootste gedeelte van de schade wordt veroorzaakt door

chloriden-indringing en carbonatatie. De desastreuze gevolgen van het toegenomen gebruik van dooizouten wordt geïllustreerd door het feit dat afgedrukte dekking zeldzaam was in Californië, tot het einde van de zestiger jaren, toen dooizouten voor het eerst op grote schaal zijn gebruikt in deze staat.

Het is algemeen geaccepteerd om chloriden-indringing te modelleren als een diffusie proces. Echter, diffusie wordt beïnvloed door fenomenen als absorptie, expositie omstandigheden etc. Het is algemeen geaccepteerd dat de beperking van de diffusie hypothese overwonnen kan worden door uit te gaan van een effectieve diffusie coëfficiënt.

Corrosie van de wapening wordt geïnitieerd als het gehalte aan chloriden bij de wapening het kritisch chloriden-gehalte overschrijdt. Het lijkt er op dat een algemeen geaccepteerde definitie van het kritische chloriden-gehalte niet bestaat, doordat het laagste gerapporteerde gehalte 0.2% is, terwijl de hoogste waarde 2.0% chloriden op basis van het cement gewicht is. Door het analyseren van de definitie, test methode, binding van chloriden en het soort ingemengd zout, kon de spreiding van de gerapporteerde waarden teruggebracht worden tot een acceptabel niveau.

Aanvankelijk werd verondersteld dat de chloriden diffusiecoëfficiënt niet zou veranderen in de tijd. Echter, praktijktests wezen uit dat de diffusiecoëfficiënt aanzienlijk afnam in de tijd. Wegens de reductie van de diffusiecoëfficiënt zal de indringing van chloriden afnemen. Dit verschijnsel is in het bijzonder van belang voor constructies die gebouwd zijn voordat zout gebruikt werd om wegen vrij van ijs te houden. Dooizouten om wegen en bruggen ijsvrij te houden worden toegepast sinds de jaren ‘40 in de Verenigde Staten en sinds de jaren ‘60 in Europa. De reductie van de diffusiecoëfficiënt en daardoor de afname van de indringing van chloriden verklaart de relatief goede conditie van de bruggen die gebouwd zijn voor de Tweede Wereldoorlog in vergelijking tot de bruggen die gebouwd zijn in de jaren ‘70. In dit proefschrift is een model voorgesteld om de indringing van chloriden te bepalen, waarbij rekening wordt gehouden met de periode waarin de constructie niet is blootgesteld aan dooizouten.

De invoerparameters bepalen voor een groot gedeelte de kwaliteit van het resultaat van de voorspelling. Naast het kritische chloridengehalte en de verouderingcoëfficiënt, is een uitgebreid onderzoek uitgevoerd naar de diffusiecoëfficiënt en het oppervlakte chloridengehalte door middel van onderzoek aan een serie Nederlandse bruggen. Uit negen bruggen zijn meer dan 100 kernen genomen voor het bepalen van de weerstand tegen het indringen van chloriden. De locatie van de te boren kernen is zo gekozen dat diverse constructie onderdelen en zowel portlandcement als hoogovencement is onderzocht. Het slakgehalte kon niet bepaald worden uit de bestekken en is daarom werd het slakgehalte bepaald uit microscopisch onderzoek aan slijpplaatjes van een aantal kernen. Deze resultaten

wezen uit dat het cement dat gebruikt is in de geteste bruggen uit de jaren 40 en 60 tegenwoordig geclassificeerd zou worden als CEM III/A.
Door het analyseren van de chloridengehaltes in de kernen, kon de diffusiecoëfficiënt en oppervlakte-chloridengehalte worden bepaald voor iedere kern. Elk van de geboorde keren is in schijfjes gezaagd waarvan het chloridengehalte werd bepaald, waardoor voor elke kern een chloridenprofiel werd verkregen. De diffusiecoëfficiënt en het oppervlakte-chloridengehalte zijn verkregen door Fick's tweede wet van diffusie passend te maken aan de waargenomen chloridenconcentraties in de boorkernen. Niet voor alle kernen sloot het chloridenprofiel aan bij Fick's tweede wet van diffusie. De verschillen waren groter voor hoogovencement dan voor portlandcement, en voor droge constructieonderdelen zijn de verschillen groter dan voor het brugdek. De vaak gesuggereerde uitstekende weerstand van hoogovencement tegen indringing van chloriden is niet vastgesteld aan de onderzochte bruggen. Deze bruggen zijn gebouw in de jaren '40 en '60 van de 20^{e} eeuw. Zowel portlandcement als hoogovencement vertoonden een gelijke weerstand tegen indringing van chloriden. Het oppervlakte-chloridengehalte van hoogovencement heeft een enigszins hogere waarde dan het oppervlakte-chloridengehalte van portland cement.

Tenslotte is de hoeveelheid afgedrukte dekking bepaald aan de hand van het gekozen model en de bepaalde invoerparameters. De hoeveelheid afgedrukte dekking is bepaald door het gebruikt van stochastische parameters gecombineerd met een *first order reliability method*. Naast de invoerparameters zoals diffusiecoëfficiënt, zijn ook de leeftijdsverdeling en de afmetingen van het brugdek meegenomen bij het bepalen van de hoeveelheid afgedrukte dekking. Ter controle van het voorspellingsmodel is het resultaat vergeleken met de waargenomen afgedrukte dekking van 81 Nederlandse betonnen bruggen. Een aantal van deze bruggen is tweemaal geïnspecteerd waardoor er in totaal 91 inspecties zijn verkregen. De vergelijking tussen de voorspelde en waargenomen afgedrukte dekking gaf aan dat het model de waargenomen schade nauwkeurig voorspelt. Bij het toepassen van het voorspellende model op betonnen bruggen in Nederlandse snelwegen, bleek dat de hoeveelheid afgedrukte dekking zal verdubbelen gedurende de komende decennia.

Table of contents

ACKNOWLEDGEMENTS ..... **V**

SUMMARY ..... **VII**

SAMENVATTING ..... **XI**

1. INTRODUCTION **1**

1.1. THE FIRST BRIDGES 1
1.2. BRIDGE MAINTENANCE ANALYSIS 3
1.3. SCOPE OF THE THESIS 4
1.4. OUTLINE OF THE THESIS 5

2. DETERIORATION OF CONCRETE **7**

2.1. INTRODUCTION 7
2.2. MECHANISMS OF DIRECT DETERIORATION 8
2.2.1. Sulphate attack *8*
2.2.2. Freeze-thaw action *9*
2.2.3. Chemical deterioration by acids *10*
2.2.4. Chemical deterioration by salts *10*
2.2.5. Alkali-Aggregate Reaction *10*
2.3. MECHANISMS OF INDIRECT DETERIORATION 12
2.3.1. Corrosion of reinforcement *12*
2.3.2. Chloride ingress *14*
2.3.3. Carbonation *15*
2.4. OBSERVED MECHANISMS OF DETERIORATION 16
2.5. DISCUSSION 17

3. CHLORIDE INGRESS AND CARBONATION; THEORY AND MODELLING **19**

3.1. INTRODUCTION 19
3.2. CHLORIDE INGRESS 19
3.2.1. Chloride diffusion *19*
3.2.2. Critical chloride concentration *23*
3.2.3. Chloride ingress model *30*
3.2.4. Evaluation of chloride ingress models *37*
3.3. CARBONATION 38
3.3.1. Carbon dioxide diffusion *38*
3.3.2. Carbonation model *39*
3.3.3. Evaluation of carbonation models *42*
3.4. MODELLING DETERIORATION 43
3.4.1. Modelling corrosion *44*
3.4.2. Initiation phase *45*
3.4.3. Propagation phase *45*
3.5. DISCUSSION 50

4. MATERIAL PROPERTIES **51**

4.1. INTRODUCTION 51
4.2. CRITICAL CHLORIDE CONCENTRATION 52
4.3. AGEING OF CONCRETE 53
4.4. CHLORIDE DIFFUSION COEFFICIENT 55

4.4.1. Examined bridges ... *56*
4.4.2. Slag content of cores ... *57*
4.4.3. Chloride profiles ... *59*
4.4.4. Derived diffusion coefficients ... *61*
4.5. SURFACE CHLORIDE CONCENTRATION ... 65
4.6. COMPRESSIVE AND TENSILE STRENGTH ... 67
4.7. CARBONATION ... 68
4.8. DISCUSSION ... 69

5. STRUCTURAL PARAMETERS ... 71

5.1. INTRODUCTION ... 71
5.2. COVER DEPTH ... 71
5.3. AGE DISTRIBUTION OF DUTCH BRIDGE STOCK ... 74
5.4. BRIDGE CHARACTERISTICS ... 74
5.5. DISCUSSION ... 77

6. PREDICTION OF DETERIORATION OF DUTCH HIGHWAY BRIDGES ... 79

6.1. INTRODUCTION ... 79
6.2. PREDICTIVE METHOD ... 79
6.2.1. Advantages of stochastic parameters ... *79*
6.2.2. Description of the predictive method ... *80*
6.3. VALIDATION OF PREDICTIVE METHOD ... 84
6.4. DETERIORATION OF DUTCH CONCRETE BRIDGE STOCK ... 88
6.5. VARIATION IN INPUT PARAMETERS ... 89
6.5.1. Cover depth ... *90*
6.5.2. Initial chloride concentration ... *90*
6.5.3. Critical chloride concentration ... *91*
6.5.4. Ageing coefficient ... *92*
6.5.5. Diffusion coefficient ... *92*
6.6. DISCUSSION ... 93

7. CONCLUSIONS AND RECOMMENDATIONS ... 95

7.1. CONCLUSIONS ... 95
7.2. RECOMMENDATIONS ... 96

REFERENCES ... 97

NOTATIONS AND SYMBOLS ... 111

APPENDICES ... 115

APPENDIX A DIFFUSION EQUATIONS ... 117
APPENDIX B TERMS RELATED TO CHLORIDE INDUCED CORROSION ... 121
APPENDIX C DEFINITIONS FOR COEFFICIENT OF CHLORIDE DIFFUSION ... 127
APPENDIX D REVIEW MINIMUM COVER DEPTH (DUTCH STANDARDS) ... 129
APPENDIX E COVER DEPTH ACCORDING TO DUTCH STANDARDS ... 133
APPENDIX F COMPRESSIVE AND TENSILE STRENGTH ... 135
APPENDIX G HISTORY OF BLAST FURNACE SLAG CEMENT ... 137
APPENDIX H NATIONAL BRIDGE INVENTORY ... 139

RESUME ... 145

1. Introduction

Since the first bridges had been built, their decay is a constant worry to their owners. Over the years, many types of bridges have been built and all those types show a different pattern of deterioration. In this introduction the necessity of a sound understanding of the changes in bridge condition in time is emphasized. To explain why today's bridge owners are often confronted with decay of bridges, which have been built since the late sixties, whereas older bridges are still in good condition, and the history of bridge construction is described in this introduction. The last section of this chapter gives an outline of this thesis.

1.1. The first bridges

The need for wide span bridges was not evident in the ancient Egyptian and Greek civilization. The Egyptian Empire was confined to the Nile River, and the Greek Empire consisted of a limited number of cities. In those days a fordable place was sufficient to cross the river, because there was only little need for transport.

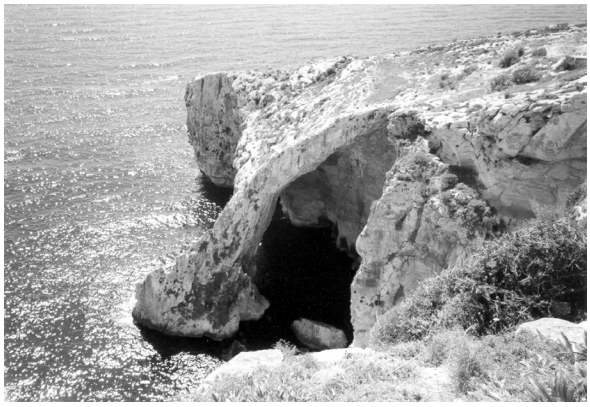

Figure 1: Bridge constructed by Mother Nature (Malta, photo by author)

However, this situation changed with the rise of the Roman Empire that included a vast area comprising Europe, North Africa and parts of Asia. Only a modern army that could be directed quickly to rebellious parts of the empire could control this gigantic area. For common use a fordable place in the river or stone steps were sufficient. However, a Roman legion comprising 5000 soldiers equipped with weapons and other equipment needed a solid solution to cross a river. A temporary bridge would never be ready in time; the solution to this problem was an extensive infrastructure comprising roads and bridges.

The bridges on the outskirts of the Roman Empire were constructed in wood, which allowed easy break down when the enemy was approaching. In contrast, the bridges in the centre of the Roman Empire were constructed of natural stone.

The Romans probably did not have any knowledge of the mechanical behaviour of a bridge structure. It is most likely that they obtained the skill of erecting bridges by trial and error. Most of the Roman stone bridges were built during the period of 50 BC until 150 AC.
Eventually, the West Roman Empire collapsed 476 AC, when the last emperor was forced to step down, after many decades of chaos. Subsequently during the Middle Ages the skill to build bridges was lost. Illustrative of the quality of the bridges in those days is that people preferred to use a fordable place in the river rather than crossing a bridge with their horse wagon [de Jong 1983]. During the Middle Ages, management including maintenance of bridges was usually charged to the closest village or city. The maintenance works were executed using the toll people paid when they passed the bridge. In those days it was common that bridges were in poor condition; probably because the toll was used for other goals or the maintenance tasks were just too difficult to carry out. In the early 16th century in many countries, the maintenance of bridges was taken over by the Government to ensure proper bridge management. After the Middle Ages the knowledge of bridge building gradually came back at the level of the Romans (figure 2). Similar to what the Romans did, the experience of bridge construction appears to be developed through trial and error.

Figure 2: Pont Neuf (Paris, photo by author)

Initially, bridges with smaller span were constructed in wood. Starting from the 13th century wood was also used for bridges with wider spans. However, maintaining wooden bridges proved to be costly because these bridges generally needed to be replaced after 20 years of service. Starting from the 16th century most bridges were constructed of stone, even though the construction of stone-arch bridges was costly and difficult.

The industrial revolution introduced the use of a new construction material: cast iron. The main advantage of this material was that slender bridges could be designed. The first cast-iron bridge was erected at Coalbrookedale (U.K.) across the Severn River in 1779. The bridge still exists today and was designated by UNESCO as a world heritage site in 1986.

The first reinforced concrete structures were built at the end of the 19th century. These structures were mostly sewers, floors, water tanks etc. With the introduction of this new combination of materials, the designers of bridges were no longer limited to arch bridges. New bridge types like slab and beam bridges came within reach. After the Second World War, the material mostly used for bridge design shifted from iron to reinforced concrete because of shortage of iron and the presumed higher durability of reinforced concrete. In the early 20th century, the general idea was that concrete made with sufficient cement would prevent the reinforcement from corroding. It was assumed that the concrete and steel would react to form iron silicate. This material would form a layer around the reinforcement and prevent corrosion [Verhey 1912]. Based on these assumptions a small cover depth was supposed to be adequate to prevent corrosion of the reinforcement.

Practice, however, has proven otherwise. During the corrosion process the reinforcement reacts with oxygen and water. The volume of iron oxide is about 3 times larger than that of the original iron. The corrosion and subsequent expansion due to the formation of iron oxide causes a reduced effective bar diameter, cracks and delamination of the cover. Due to the deterioration process described above, the structural characteristics of the structure change, which might lead to an unsafe condition.

1.2. Bridge maintenance analysis

In the last decade of the 20th century, the Departments of Transportation (DOTs) in the United States observed a strong increase of the need for maintenance of concrete bridges. At the end of the 20th century, the backlog in maintenance was estimated to be more than 90 billion US$. An example of a seriously deteriorated bridge is given in figure 3.

Figure 3: Deteriorated bridge, constructed in ±1915 (Ann Arbor, MI, U.S., photo by author)

It is therefore not surprising that in the US, approximately 150-200 bridges, out of 600.000 bridges, suffer partial or full collapse each year [Dunker 1993]. In other

countries the Ministries of Transport wondered what the future costs of maintenance would be, to keep their bridge stock in a serviceable condition.
The main problem of estimating the future maintenance of bridge stocks is the heterogeneous composition of bridge stocks. A few examples of the heterogeneity are:

- during a number of years in the 1960s or 1970s a large number of bridges has been built in most countries;
- over the years, in most European countries, the cover depth that is required by the standard has increased from 15mm to 35mm;
- concrete quality, with respect to durability, has shown a considerable improvement over the last decades.

Because of the changes quoted above, each bridge will show a different pattern of deterioration in time. Therefore, a simple extrapolation of present inspection data will not lead to an accurate estimate of future deterioration.

So, the main question to be answered is: 'What is the rate of deterioration of a concrete bridge stock, taking into account the history of bridge design and construction?'.

1.3. Scope of the thesis

In general, bridge failure is defined as the undesirable event of collapse of such a structure. Therefore reliability studies have focused on loss of structural strength as being the governing limit state for structural performance [e.g. Estes 1999, Mori 1994]. However, long before a bridge will collapse, parts of concrete may come off due to spalling. These loose parts of concrete might already endanger passing traffic.

In a study in Japan, a deteriorated beam that showed severe spalling was taken from a 40 year old bridge. When this beam was tested in a laboratory the ultimate load bearing capacity was still higher than the design strength [Oshiro 1985]. A first conclusion is that spalling is a greater threat to the users than full collapse of the bridge, since spalling normally occurs at an earlier age.

Although fewer than a dozen people die every year due to bridge collapses in the U.S., another 1,000 are killed in accidents involving bridges that are deficient, obsolete or have inadequate traffic-control provisions [Dunker 1993]. It is therefore not surprising that spalling of the concrete cover is a common problem in bridges, representing a hazard to passing vehicles and even to life safety [Stewart, 1998].

In this thesis failure is therefore defined as the undesirable event of an intolerable amount of spalling. The scope of this thesis is limited to deterioration that results in damage to concrete bridges due to cracks and concrete spalling that are the result of corrosion of the steel reinforcement.

This thesis intends to define the need for maintenance for a given stock of concrete bridges because of spalling. The results will be displayed in graphs that give the abso-

lute and relative quantity of spalling as a function of the year of construction. With this thesis a bridge owner can allocate funds that are needed to carry out maintenance with respect to spalling for the coming decades.

1.4. Outline of the thesis

Deterioration of concrete structures consists of numerous aspects; this thesis deals with damage due to corrosion of the reinforcement as a result of chloride ingress and carbonation.

Chapter two describes the processes that could cause deterioration of concrete structures. Based on numerous publications this chapter draws the conclusion that deterioration of concrete bridges is mainly caused by chloride ingress and carbonation.

Chapter three gives a qualitative description of chloride ingress, carbonation and eventually corrosion of reinforcement. The third chapter also provides equations to determine both the ingress of chlorides and carbon dioxide, and corrosion of the reinforcement that results in spalling. The models that are available to model chloride ingress and carbonation are introduced and adjusted in this chapter. The models are adjusted by introducing ageing and limited exposure to chlorides in time.

In Europe, little experience is available with corroding reinforcement at structures. However, the output of predictive models is as good as the input. Therefore, chapter four describes on-site tests that are carried out to determine the resistance of concrete to chloride ingress. In chapter five parameters like cover depth and age distribution are obtained from an extensive literature search.

Finally, in chapter six a concept is suggested to determine the deterioration of concrete bridges. The observed spalling of nearly 100 inspections at Dutch bridges is used to calibrate the suggested concept. Eventually the calibrated parameters are used to predict the amount of spalling that will evolve over the coming decades. Since the predicted spalling is derived from physical models, the models will be used to perform a parameter study.

A thesaurus of the most frequently used deterioration terms is given in appendix B.

2. Deterioration of concrete

2.1. Introduction

A sound understanding of deterioration processes is necessary before one can predict development of deterioration. This chapter provides a selection of frequently observed deterioration mechanisms for concrete structures. For each mechanism the cause and consequences will be described.

The first steel reinforced concrete bridges have been built in the early 20th century. During the first decades when reinforced concrete was used, it was assumed that iron and concrete would react and form iron silicate. As a result this material would develop a layer around the reinforcement, which effectively prevents corrosion of the reinforcement [Verhey 1912]. Nowadays, it is generally accepted that this was an erroneous assumption due to obvious signs of lack of passivity of the reinforcement. An example of the lack of a passive state after several decades of exposure to a severe winter climate is given in figure 4. The processes that take place when reinforcement is corroding are described later in this chapter.

Figure 4: Severe spalling at bridge pier (Ann Arbor, MI, U.S., photo by author)

There are many processes that lead to damage of concrete structures. These mechanisms of deterioration can be ordered in many different ways. This chapter will order the mechanisms by direct and indirect deterioration of concrete.
Direct deterioration is defined as the deterioration of cement and aggregate phase of the concrete itself due to exposure to harmful substances. These substances weaken

the cement matrix, which is followed by abrasion. Indirect deterioration is defined to occur if the concrete shows cracks and spalling due to the volume increase that arises from the corroding steel reinforcement. In the case of indirect deterioration the cement matrix itself is not affected by the harmful substances that penetrate the concrete.

2.2. Mechanisms of direct deterioration

Direct deterioration of concrete due to sulphate attack, freeze-thaw action, exposure to acids, alkali silica reaction and direct deterioration by salts is described in this section.

2.2.1. Sulphate attack

The presence of sulphates in the cement matrix can cause an expansive reaction that leads to cracks in the affected concrete. The sulphates usually originate from aggregate that contains sulphate or from exposure to contaminated groundwater, soils, seawater, decaying organic substance or industrial effluent. Another source of sulphates is recycled concrete that is used as aggregate. During the demolition of old concrete structures, gypsum ($CaSO_4$) that is used as plaster or wallboard could end up in the demolished concrete or masonry rubble that is reused as aggregate in new concrete.

The development of ettringite is preceded by the reaction that supplies gypsum. The chemical reaction is represented by equation 1. The combination of sulphate ions, aluminate phases in cement and water may result in the formation of ettringite (equation 2) [Bijen 1996].

$$Ca^{2+} + SO_4{}^{2-} + 2H_2O \rightarrow CaSO_4 \cdot 2H_2O \qquad (1)$$

The poor formation of (crystalline) ettringite from gypsum and aluminate and a low amount of water results in highly voluminous solids [Mehta 1992]. If sufficient pressure inside the concrete matrix is generated, the concrete will crack.

$$\underset{\text{gypsum}}{3\,(CaSO_4 \cdot 2H_2O)} + \underset{\text{calcium aluminate}}{3CaO \cdot Al_2O_3} + \underset{\text{water}}{26H_2O} \rightarrow \underset{\text{ettringite}}{3CaO \cdot Al_2O_3 \cdot 3CaSO_4 \cdot 32H_2O} \qquad (2)$$

The formation of ettringite can be prevented with blast furnace slag cement if the slag content is at least 65%. The high slag content results in less calcium oxide and calcium aluminate ($3CaO \cdot Al_2O_3$). Due to the higher density of concrete made of blast furnace slag cement than ordinary portland cement, the sulphate ingress will be retarded [Mehta 1992].

A special case of sulphate attack is delayed ettringite formation. During hardening of concrete, ettringite is formed around each cement particle to retard or slow down set-

ting of concrete. The ettringite that is formed during the plastic stage does not result in cracks. This type of ettringite is commonly referred to as primary ettringite.

If the temperature during steam curing is over 70˚C, primary ettringite is thermally decomposed to mono-sulphate aluminate. If, in a later stage, these sulphates react to form ettringite, concrete will crack due to the expansion that accompanies the formation of ettringite and the absorption of water. This process is called 'Delayed Ettringite Formation', or secondary ettringite [Collepardi 2003]. Correctly speaking the term delayed ettringite formation should include both internal sulphate attack, as is described in this paragraph, and external sulphate attack.

2.2.2. Freeze-thaw action

Freeze-thaw deterioration of concrete is caused by the expansion of pore water due to freezing. Concrete structures freeze from the outside inwards. If the pores in the outer layer of concrete are blocked by frozen pore water, expansion of the pore water underneath the frozen shell is prevented. If the pressure builds up, the outer concrete layer is damaged which often results in scaling. An example of damage due to freeze thaw is presented in figure 5.

Figure 5: Freeze-thaw deterioration (Owen Sound, ON, Ca, photo by author)

Not in all instances freezing of the pore water will lead to damage to the concrete structure. If sufficient space is available to enable the expansion, no damage will occur. An indication of possible damage is the amount of pores that are filled with water. If the pores are filled for more than approximately 92%, critical saturation, damage is likely to occur during the winter season [Powers 1975].

2.2.3. Chemical deterioration by acids

Hydrated cement shows a poor resistance to acids. Nearly all types of strong acids, like sulphuric acid, will affect these cement hydrates. At badly maintained structures, decaying organic materials can release sulphuric acid. Acid attack involves conversion of calcium compound to calcium salts after attacking acid. The chemical process of the effect of acids on cement hydrates is presented in equation 3.

$$\underset{\text{sulphuric acid}}{2H^{+} + SO_4^{2-}} + \underset{\text{cement hydrates}}{CaO \cdot SiO_2 \cdot nH_2O} \rightarrow \underset{\text{silica}}{SiO_2} + \underset{\text{gypsum}}{CaSO_4 \cdot (n+1)H_2O} \qquad (3)$$

The newly formed material silica, which replaces the cement hydrates, shows less strength than the original material. As a consequence the concrete structure will easily deteriorate due to abrasion or any other mechanical load [Roskam 1994].

2.2.4. Chemical deterioration by salts

The decay of concrete by salts is similar to the decay due to acids; the cement matrix is affected by salts to which it is exposed. An example of the salts that reduces the strength of concrete is ammonium chloride. Ammonium chloride is one of the chemical components of artificial fertilizers. The chemical process of the damaging effect of ammonium chloride to cement hydrates is presented in equation 4 [Roskam 1994].

$$\underset{\textit{ammoniumchloride}}{2NH_4^{+} + 2Cl^{-}} + \underset{\text{cement hydrates}}{CaO \cdot SiO_2 \cdot H_2O} \rightarrow \underset{\text{ammonia}}{NH_3} + \underset{\text{calcium chloride}}{CaCl_2} + \underset{\text{silica}}{SiO_2} + \underset{\text{water}}{2H_2O} \qquad (4)$$

The newly formed material silica, which replaces the cement hydrates, shows a smaller strength than the original cement hydrates. Therefore, the concrete structure will easily deteriorate due to abrasion.

2.2.5. Alkali-Aggregate Reaction

The presence of certain aggregates and alkali in the cement can lead to an expansive reaction that is called alkali aggregate reaction (AAR). The alkali silica reaction (ASR) is by far the most common of the alkali-aggregate reactions. Alkali and silica react at the surface of aggregate particles to form a non-expansive reaction product. Although the reaction itself results in a chemical shrinkage, the gel product has a great capacity to swell upon absorption of moisture. Because of the water absorption and subsequent volume increase of the silica gel, pressure builds up in the cement matrix and eventually cracks will develop.

In addition to the crack pattern, the Alkali Silica Reaction can also be recognized by the characteristic gel reaction product. This gel has been recognized as a glassy-clear or white powder deposit. However, the white reaction product, as shown in figure 6,

could also indicate other deterioration processes, like sulphate attack [Helmuth 1992, Stark 1993] or harmless calcium carbonate deposits.

The chemical process of the alkali silica reaction is presented in equation 5 [West 1996].

$$\underset{\text{alkali}}{2NaOH} + \underset{\text{silica}}{SiO_2} + \underset{\text{water}}{H_2O} \rightarrow \underset{\text{alkali - silica gel}}{Na_2SiO_3 \cdot 2H_2O} \qquad (5)$$

Figure 6: Damaging cracking and exudation of gel (Sherbrooke, QC, Ca, photo by author)

Not all concrete structures are prone to alkali aggregate reaction. This reaction will only occur under certain conditions. These conditions are [CUR 1998]:

- Poorly crystallized silica (SiO_2) will more easily take part in the ASR reaction.
- Sufficient water has to be available to cause expansion.
- Sufficient alkali ions have to be available to cause gel formation (cement type).
- The transport rate of sodium and potassium ions needs to have a relatively high value to ensure that a sufficient amount of reaction products are available for reaction.

The Alkali-Aggregate reaction can, in general, be prevented by the use of blast furnace slag cement instead of portland cement. Because of the low diffusion coefficient (high resistance to transport), the expansive reaction is most likely postponed past the end of the design lifetime [CUR 2002].

2.3. Mechanisms of indirect deterioration

The most important cause of indirect deterioration is corrosion of reinforcement. In case of indirect deterioration, cracks and spalling arise from the volume increase when iron reacts with oxygen. There are eleven minerals known to date that are composed essentially of the elements: iron, oxygen and hydrogen. The type of rust that is formed depends on the temperature, pressure, moisture, pH-value and availability of oxygen. For the most commonly observed corrosion products, the volume increase for iron oxides ranges from 100% for iron(II) oxide, to 300% for iron(III) hydroxide [Liu 1998]. Firstly, a general description of the corrosion process is given; a comprehensive description of corrosion of reinforcement is available elsewhere [e.g. Schießl 1988]. In this thesis, corrosion is restricted to carbon steel reinforcement excluding stainless steel and coated carbon steel.

2.3.1. Corrosion of reinforcement

Corrosion of reinforcement is an electrochemical process involving anodic and cathodic reactions. The reaction site where the metal dissolution takes place is called the anode. In the anodic reaction iron atoms lose electrons and enter the electrolyte (pore water). The chemical formulation of this process is:

$$2Fe \rightarrow 2Fe^{2+} + 4e^{-} \qquad (6)$$

Pore water is not only needed to form the electrolyte, it is also takes part in the oxygen reduction. At the cathode, the free electrons released at the anode react with oxygen and water to form hydroxyl ions according to:

$$4e^{-} + 2H_2O + O_2 \rightarrow 4OH^{-} \qquad (7)$$

The net reaction of the processes at the cathode and anode is the formation of iron hydroxide:

$$2Fe^{2+} + 4OH^{-} \rightarrow 2Fe(OH)_2 \qquad (8)$$

This newly formed iron hydroxide has a low solubility and will precipitate near the reinforcement. If sufficient oxygen is available, the iron(II)hydroxide will react to iron(III) (hydr)oxides, such as hematite as presented in equation 9.

$$4Fe(OH)_2 + O_2 \rightarrow \underset{\text{hematite}}{2Fe_2O_3} + 4H_2O \qquad (9)$$

If a limited amount of oxygen is present at the steel, magnetite (Fe_3O_4) is formed. The reaction products like hematite and magnetite are commonly known as more or less

porous and hydrated forms of rust. The process of corrosion is schematized in figure 7.

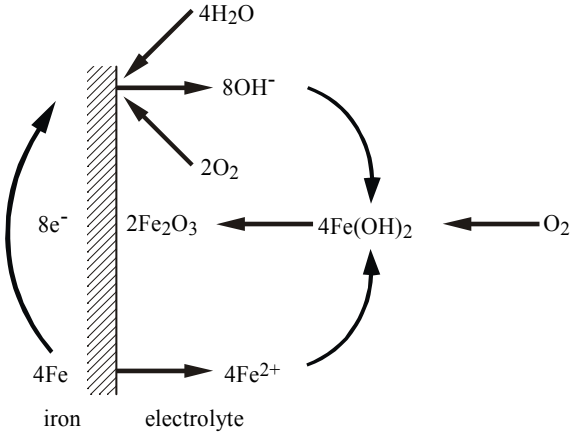

Figure 7: Corrosion process

In recently cast concrete pore water has a pH-value of about 13.5 [Fraay 1990]. In this alkaline condition, the ferrous oxides hematite and magnetite are in a stable condition, which prevents corrosion. This stable layer of ferrous oxides has a thickness of only a few nanometres and should not be confused with ordinary rust layers [Berke 1992, Schießl 1988].

If chlorides are present at the reinforcement, the dissolved iron atoms not only react with hydroxyl ions, the chlorides also react with iron to form iron chloride.

$$Fe^{2+} + 2Cl^{-} \rightarrow FeCl_2 \qquad (10)$$

This compound is colourless or has a greenish colour and is highly soluble. It may migrate far away from the reinforcement, for instance to the surface of the concrete, where it is oxidized to iron(III)(hydr)oxides, which have a red/brown colour. These brown stains at the concrete surface indicate chloride-initiated corrosion [CUR 1998]. In figure 8 different stages of corrosion damage: like brown stains, cracks and eventually spalling can be observed. In particular inside corrosion pits, iron chloride reacts partially with water to form hydrochloric acid and iron hydroxide. Hydrochloric acid causes a further drop of the pH-value, accelerating the local dissolution of iron.

$$FeCl_2 + 2H_2O \rightarrow 2HCl + Fe(OH)_2 \qquad (11)$$

The passive state of the reinforcement depends on the pH-value and the chloride concentration. The pH-value of the pore water is reduced by carbonation. If the pH-value drops below 10, more and more iron atoms dissolve from the passive oxide layer and

corrosion propagates. The reduction in alkalinity by carbon dioxide is called carbonation. If the chloride concentration in the pore water near the reinforcement exceeds the critical chloride conconcentration the passive state is lost, which is called chloride-induced corrosion. Both processes of carbonation and chloride-initiated corrosion are discussed in the next sections.

Figure 8: Corrosion process (Ann Arbor, MI, US, photo by author)

2.3.2. Chloride ingress

The ingress of chlorides can lead to chloride-initiated corrosion of the reinforcement. The chloride ions originate from the sodium chloride which is the most important salt in seawater and of de-icing agents. Once the chloride concentration at the reinforcement exceeds the critical chloride concentration, corrosion of the reinforcement is initiated (figure 9). The critical chloride concentration is discussed in detail in section 3.2.2.

The time until initiation of corrosion is determined by the concrete quality, the distance between the concrete surface and the reinforcement and the amount of chlorides to which the structure is exposed. These structural properties are discussed in detail in the chapters 4 and 5. Transport of chloride ions is discussed in chapter 3.

Figure 9: Corroded railway bridge column (Sherbrooke, QC, Ca, photo by author)

2.3.3. Carbonation

The alkaline environment of concrete is the result of hydroxyl ions that arise from the cement hydration. Carbonation is the process in which carbon dioxide, from the atmosphere, enters the concrete and reacts with the hydroxyl ions, which leads to a reduction of the pH-value below 9.0. The depth over which the pH-value has dropped is called the carbonation depth. In this zone the passive state of the reinforcement is lost and corrosion develops if sufficient oxygen and moisture are present. Carbonation is further discussed in chapter 3. An example of deterioration due to carbonation induced corrosion is the roof slab shown in figure 10.

Figure 10: Corrosion due to carbonation (Bloemendaal, the Netherlands, photo by author)

Corrosion damage due to carbonation in reinforced concrete can, in general, be prevented by sufficient cover depth, low to moderately low water to binder ratios and a dry environment.

2.4. Observed mechanisms of deterioration

In this chapter a number of mechanisms of deterioration are listed. To predict future deterioration for a whole bridge stock, it is not feasible to model all the listed mechanisms. Based on published results of practical experience, the dominating mechanisms of deterioration of concrete bridges appear to be corrosion of the reinforcement due to chloride ingress and carbonation. This hypothesis has been confirmed by observations in many countries in North America, Europe and Asia. In table 1, a number of articles are listed which describe chloride initiated corrosion. The effect of the increased use of chloride-based de-icing agents is dramatically illustrated by the fact that surface spalls were quite rare in California until the late 1960s when the use of chemical de-icers was introduced in this state [Cady 1977].

Table 1: Authors that observed chloride-initiated corrosion in listed countries

Country	**Author**
Finland	Söderqvist 2000
Great Britain	Bamforth 1994, Roberts 2000, Vassie 1986, Hobbs 1998
Japan	Mutsuyoshi 2001
the Netherlands	Roskam 1996
Switzerland	Roelfstra 2000
U.S.A.	Hyman 1983, Kilareski 1980, Kirkpatrick 2002, Cady 1977

From the information that is gathered in Japan, a detailed description of the mechanisms is given in figure 11.

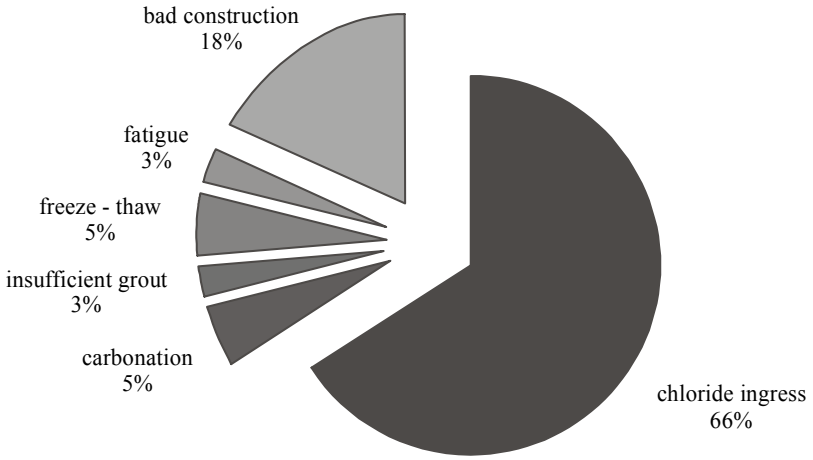

Figure 11: Number of observed deterioration in Japan [data: Mutsuyoshi 2001]

As a basis for this study it is assumed that the most relevant mechanisms for deterioration are corrosion due to chloride ingress and carbonation. Carbonation is also as-

sumed as one of the leading mechanisms of deterioration because it might affect bridges that have been built before World War II, which have a small cover depth.

2.5. Discussion

This chapter discussed a number of well-known mechanisms of deterioration. Adopting all these mechanisms of deterioration to model future decay would be unfeasible. Therefore it is assumed in this thesis that corrosion due to chloride ingress and carbonation are the leading mechanisms of deterioration. This choice is inspired by the numerous studies that analysed decay of concrete structures in many countries.

Chloride ingress and carbonation will be described in detail in the next chapters and used to predict future deterioration of a bridge stock.

3. Chloride ingress and carbonation; theory and modelling

3.1. Introduction

Numerous mechanisms of deterioration can occur in concrete structures. Of all the mechanisms of deterioration, it appears that chloride ingress and carbonation are the dominating mechanisms of deterioration, as is described in the previous chapter.

The next two sections will subsequently describe the mechanisms of chloride ingress and carbonation that are selected as the leading mechanisms of deterioration. Each section makes a distinction between the process, the accompanying material or environmental parameters that predominantly control deterioration, and the mathematical models that are used to calculate the rate of deterioration. In this chapter the material parameters are described both qualitatively and quantitatively. Finally, section 3.4 describes in what way the models are used to predict deterioration.

3.2. Chloride ingress

3.2.1. Chloride diffusion

Chloride ingress into concrete is usually modelled as a diffusion process[1]. However, other transport mechanisms like convection and absorption may contribute to the ingress of chloride ions. This section lists the reasons why diffusion is selected as the predominant transport process in the concrete cover. Fick's first and second law of diffusion, treated in section 3.2.3, describe the process of diffusion in a mathematical way. The mathematical formulation assumes a constant load of chlorides, which leads to a uniaxial permeation into a homogeneous semi-infinite medium.

There are a number of objections to modelling chloride ingress into concrete as a process of diffusion. These objections concern:

- convection / capillary flow;
- the heterogeneity of concrete;
- the various exposure conditions;
- the role of cracks;
- the influence of temperature differences;
- partially saturated pores;
- limited exposure to de-icing agents.

The next sections elaborate on the objections with respect to the simplification of only considering diffusion.

[1] A detailed description of diffusion is given in appendix A.

3.2.1.1. Convection / capillary flow

Chlorides may also penetrate by absorption (capillary forces) and convection. While the larger part of a concrete structure tenaciously retains capillary moisture, even in arid environments, the partially saturated surface zone is prone to accelerated chloride ingress due to capillary forces. However, the harsh winter season, where de-icing agents are used, is preceded by the fall where structures are exposed to moisture without chlorides. Even in relatively dry concrete, exposure to moisture results in rapid filling of the accessible pore space, after which bulk moisture movement virtually ceases because of the loss of driving potential (capillary attraction). Therefore, the primary mode of transport of chloride ions to the level of the reinforcement is diffusion [Cady 1983].

The convective zone is likely to be caused by the high cement content in the near surface layer, carbonation and the presence of micro cracks. The influence of cracks on the ingress of chlorides is discussed in section 3.2.1.3. In general, the near surface zone is poorly cured compared to the inner concrete and shows micro cracks due to drying shrinkage. The thickness of the zone where convection is the leading transport mechanism is not clearly defined. The thickness of the convective zone is determined from chloride profiles. The suggested thickness in literature is between 5 and 15 millimetres [Paulsson-Tralla 2002]. Other authors suggest the thickness of the convective zone to be 7-8 millimetres for concrete structures of two years old, and 10 millimetres for concrete of 8 years old. The study did not show a further increase of the thickness of the convective zone at older structures [Nilsson 2000, Paulsson-Tralla 2002].

The higher porosity in the wall effect zone might indicate that the leading transport mechanism in this zone is convection instead of diffusion. Due to the higher porosity of the cover concrete, chloride ions move with the free water. As a result chloride easily penetrates into concrete. A portion of the chloride, however, is ‘washed out’ of the convective zone during periods of rain. During periods without applying de-icing salts, chlorides continue to move inwards by diffusion. Once a concentration is established in the convective zone it will act as a buffer stock of chlorides. In that case, diffusion will be the dominating transport mechanism for the pores at greater depths.

Even though the convective zone is reported in literature, there is no solid evidence about the depth of the convective zone. For now, it is assumed that diffusion is the leading transport mechanism over the cover depth.

3.2.1.2. The heterogeneity of concrete

Chloride ions are carried by moisture through pores in the cement hydrates. However, concrete is far from homogeneous as it mainly contains impervious aggregates, and porous cement hydrates. If the water to binder ratio of the concrete mixture is reduced, the pores are reduced in size and number, subsequently the diffusion coefficient is reduced [Bamforth 1994]. The outer layer of a concrete structure contains less

aggregate and more cement than the bulk of the structure. This so-called wall effect results in a higher porosity in the near surface zone than in the bulk of the structure. In case of a monodisperse mix, where all grains have the same diameter, the wall effect layer has a thickness of half this diameter. The packing density in the wall effect zone is reduced by 12% for round grains and 27% for crushed grains [Sedran 1994]. In structures with a non-monodisperse mixture, small grains and a relatively large amount of cement hydrates are observed near the wall (figure 12).

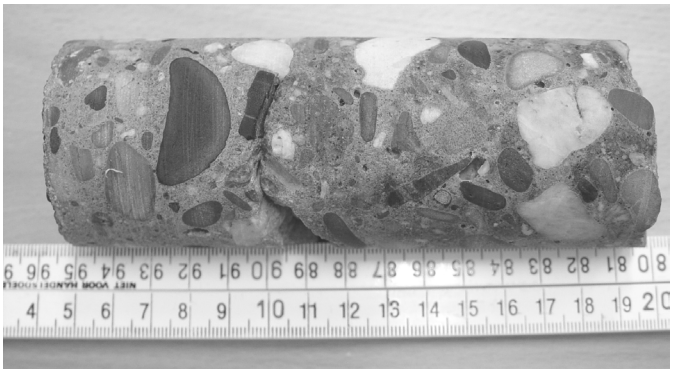

Figure 12: Smaller grains near surface (left side) i.e. higher cement content (photo by author)

3.2.1.3. The role of cracks

Cracks do accelerate ingress of chlorides into concrete. The question is, whether or not, the diffusion hypothesis is still valid in a structure that shows cracks. Chloride ingress into cracked concrete is not well understood; for now the crack width is suggested as a criterion for the durability of concrete. It is assumed that the additional chloride ingress, because of the cracks, is negligible in case of small crack widths. Laboratory studies showed that the chloride ingress rate, associated with water absorption into cracks with a width of 0.05mm to 0.50mm, could be considered to be similar to the ingress rate in sound concrete (table 2).

Table 2: Limiting crack widths for regular diffusion

author	**crack width [mm]**
Paulsson-Tralla 2002	0.05
Li 2002	0.10
Rehm 1964	0.15
Mangat 1987a / 1987b	0.20
Boulfiza 2003	0.20
Schießl 1986	0.25
François 1999	0.50

The crack width criterion, however, disregards the depth and the number of cracks. Since the chlorides penetrate into the concrete through the concrete crack surface area, a better understanding of the vulnerability of concrete to accelerated chloride ingress could be obtained by using the specific crack surface area [e.g. Locoge1992].

3.2.1.4. The influence of temperature differences

At high concrete temperatures the ingress of chlorides is faster than at low temperatures. Usually the increased movement of ions is considered with an increased diffusion coefficient. Many literature studies have been carried out, however, the results differ considerably, from a 100% increase at 50˚C temperature difference [Andrade 2003] to a 20% increase at a 60˚C temperature difference [Jooss 2002]. In these studies the specimens were heated up to a temperature of 80˚C, whereas most structures never experience these temperatures. Because of the limited temperature variations in Dutch bridges, the temperature dependency in the rate of chloride ingress is overcome by assuming an effective diffusion coefficient as is discussed in section 3.2.1.7

3.2.1.5. Partially saturated pores

The presence of a pore solution is indispensable to facilitate the diffusion of chlorides to greater depths. It is clear that the moisture content in the pores determines to what extent diffusion will occur. Even though the concrete is not saturated, as in laboratory tests, it is clear that sufficient moisture is present in the concrete to facilitate diffusion of chloride towards the reinforcement [Nilsson 2000]. However, the degree of saturation will influence the chloride ingress rate and this relationship between the moisture content and diffusion coefficient cannot accurately be defined. The somewhat reduced rate of ingress of chlorides is overcome by adopting an effective diffusion coefficient.

3.2.1.6. Limited exposure to de-icing agents

Most concrete bridges are, in contrast to laboratory specimens, only exposed to chlorides during several months each year. However, the cumulative duration of salt application to the highway bridges is unknown. Therefore it is assumed that highway bridges are exposed to chlorides all year long.

3.2.1.7. Concluding remarks

It is generally accepted that the concept of diffusion gives a sufficiently accurate description of the of ingress chlorides. Near the concrete surface the observed chloride concentrations deviate from the diffusion model. The drawbacks like cracks, heterogeneity, cyclic nature of exposure to de-icing agents, partial saturation and wash-off are only observed in the near surface zone, while diffusion complies with the observed chloride ingress at greater depths [Cady 1984, Takewaka 1988]. From a practical point of view, utilization of the above-mentioned phenomena is often difficult because there are in general too many unknown parameters [Maage 1996]. Therefore the surface chloride concentration and diffusion coefficient are usually referred to as effective surface chloride concentration and effective diffusion coefficient. The term effective emphasizes that the coefficient is not in exact agreement with the definition

of Fick's laws. However, all the known and unknown environmental and exposure conditions, which in reality act upon structures, are included in this effective surface chloride concentration and effective diffusion coefficient. Because of the reasons outlined above it is assumed that, in a de-icing salt environment, diffusion is the leading transport mechanism in concrete once the chloride has passed the surface zone. Other phenomena that might contribute to the movement of chlorides are included in the effective diffusion coefficient and effective surface chloride concentration.

3.2.2. Critical chloride concentration

Steel reinforcement is protected against corrosion by a passive oxide layer. The passive layer is only a few monolayers thick and is formed in the alkaline environment of concrete. However, chloride ions are able to form a complex with iron(II); these complexes can migrate from the steel surface and subsequently convert into an expansive corrosion product. The probability of chloride ions complexing iron(II) ions is increased with an increased chloride over hydroxyl ion ratio [Berke 1992]. To model the phenomena of initiation of corrosion, it is assumed that chloride ions present in concentrations in excess of a so called threshold level destroy passivation and promote the dissolution of iron [Schießl 1988], if sufficient oxygen and moisture is available at the reinforcement. Depassivation is a stochastic process due to the influence of many chemical and physical phenomena at the steel/concrete surface. Consequently, the threshold level is not a deterministic value, but is usually expressed as a mean value, which indicates a gradual increased probability of corrosion for increasing chloride concentrations at the reinforcement.

A universal well-defined chloride threshold value for corrosion initiation appears not to exist. The lowest reported threshold is 0.2% whereas the highest is 2.0% by mass of binder [Glass 1997, Petterson 1994]. This huge gap between the reported values questions the reliability of the critical chloride concentration. The used definition of the threshold value, the material studied and the ways the tests are carried out will most likely influence the final judgment about the critical chloride concentration. Based on published critical chloride concentration values, a most likely value of the critical concentration is suggested in this section.

The amount of chloride ions and the pH-value of the concrete pore solution determine the threshold value. A frequently used criterion of corrosion is the chloride-to-hydroxyl ion ratio of the pore water. It is suggested that the probability of corrosion is mainly dependent on the mass ratio of chloride to hydroxyl ions, which is about 0.6 [Hausmann 1967, Saremi 2002]. However, retrieving pore water from concrete is laborious and is mainly used in laboratory studies. Since the pH-value of the concrete is roughly related to the cement content, it is generally accepted to relate the probability of corrosion to the total chloride-to-binder (mass) ratio. Thus, in terms of currently used representations, chloride threshold levels are best presented as total chloride concentrations expressed relative to the mass of cement. In addition, it is found that

the smallest range of threshold levels is achieved when they are presented as total (free and bound) chloride concentration [Glass 1997].

The next sections successively discuss possible causes of the scatter in the threshold values that are reported in literature and give an overview of reported values subdivided by the causes discussed.

3.2.2.1. Definitions of threshold value

Before the values of the threshold values are discussed, the definitions that are used in the numerous studies should be clear. The three, mostly used, definitions of the critical chloride concentration are [CUR 1992, CUR 2000b]:

1. The chloride level at the depth of the steel, which initiates corrosion, independent from any damage to the structure.
2. The chloride level at the depth of the steel that results in developing damage (cracking, spalling) due to corroding reinforcement.
3. The chloride level at the depth of the steel that, within the intended life span of the structure, results in corrosion that causes spalling and cracking which results in a need for repair.

The differences between the definitions are considerable. The second and third definitions describe the initiation and propagation phase of the deterioration, whereas the first definition describes the end of the initiation phase. With regard to the third definition, initiation of corrosion can be indicated by the corrosion potential (<−350 mV $Cu/CuSO_4$ [ASTM 1999, van Daveer 1975]) or corrosion current density (>2 mA/m^2 [Alonso 2000, Glass 1997]) or by visual inspection of the reinforcement after the cover has been removed.

3.2.2.2. Laboratory test versus field construction

Many studies have been carried out in laboratories to investigate the critical chloride concentration. The aim of these studies generally was to assess the critical chloride value in real structures. It is important to recognize the differences between a laboratory test and a real structure operating under field conditions. The most important differences are:

- chloride source (added to mixing water versus permeation from the environment);
- cation of chloride salt (sodium chloride versus calcium chloride);
- preparation of reinforcement (clean versus rusted bars)
- compaction (air voids)

Preparation of reinforcement

The degree of surface preparation of the reinforcement has a strong influence on the outcome of the critical chloride concentration. In many laboratory studies, the mill scale of the bars was removed or the bars were polished to a mirror-like finish. The type of preparation of the reinforcement is sometimes not reported which makes it

difficult to compare the outcome of the tests. If the mill scale is removed the critical chloride concentration may be a factor of two higher than the as-received mill scale covered rebar (often called black bar) [Glass 2002, Sagüés 2001]. If the reinforcement is polished to a mirror like finish, no corrosion may be observed in a simulated pore solution even at high chloride concentrations [Mammoliti 1996].

The sensitivity of the critical chloride concentration to the compaction, as indicated by other authors, is not discussed in this thesis [e.g. Glass 2002]. The influence of the source of chloride and the cation are discussed in the next section in association with chloride binding.

3.2.2.3. Chloride binding

The chloride ions that are present in the hardened cement paste can be subdivided in free and bound chlorides. Only the free chlorides will move towards the reinforcement and may cause initiation of corrosion. The binding of chlorides is either physical or chemical. It was found that the proportion of bound chloride remained approximately constant regardless of the water-cement ratio [Mohammed 2003, Tang 1993, Tuutti 1982].

Chemically bound chlorides

One of the dominating parameters of chemical chloride binding is the tricalcium aluminate (C_3A[2]) content of the cement. The chlorides are partially bound by C_3A and form Friedel's salt (chloro aluminate[3]). Depending on the tricalcium aluminate content, 50 to 80% of chloride ions, which are added to the mix, may be bound by aluminate phases [Justnes 1983, Polder 2002a]. The bound chlorides are 'released' if the concrete is carbonated or if the concrete is exposed to sulphates [Hussain 1994]. It is found that if the pH value drops below 11.0, due to carbonation, most of the bound chlorides are released [Reddy 2002]. The release of the bound chlorides most likely accelerates the corrosion of the reinforcement. This phenomenon of increased corrosion when both chloride ingress and carbonation occur is called carbonation accelerated chloride initiated corrosion.

Physically bound chloride

Physical binding takes place when the amorphous calcium silicate hydrate (CSH) gel adsorbs the chlorides. The CSH-gel is formed during the cement hydration. The physically bound chlorides will move towards lower concentrations on the gel surface at a much slower rate than the free chlorides in the pore water. This indicates that the free chlorides will dominate the diffusion [Justnes 1983].

The chloride ions present in concrete can originate from exposure to a chloride-laden environment or from adding them to the fresh concrete mixture. The origin of the

[2] $3CaO \cdot Al_2O_3$

[3] $3CaO \cdot Al_2O_3 \cdot CaCl_2 \cdot 10H_2O$

chloride determines the ratio of free to bound chlorides. The degree of binding of chlorides, which are admixed, is also strongly influenced by the binder type. Blast furnace slag cement shows more binding during the first month than ordinary portland cement (table 3).

Table 3: Binding of chlorides added (sodium chloride or calcium chloride) to cement paste as a function of cement type for concrete samples with an age of 28 days at testing; w/b-ratio: 0.5, the content of C_3A in both ordinary portland cement (OPC1) and high alkali portland cement (OPC2) being 9% [Arya 1990]

Cement type	replacement	total Cl^- added [% by mass of binder]	bound Cl^- [% by mass of binder]	bound/total (%)
OPC1	-	1.0	0.385	39
OPC2	-	1.0	0.523	52
OPC1	15% PFA	1.0	0.532	53
OPC1	35% PFA	1.0	0.605	61
OPC1	70% GGBS	1.0	0.711	71
OPC1	15% CSF	1.0	0.322	32
SRPC1	-	1.0	0.283	28

Note: SRPC1: sulphate resisting portland cement (C_3A: 0% by weight); CSF: condensed silica fume; PFA: pulverized fuel ash; GGBS: ground granulated blast furnace slag

If concrete is exposed to permeation of chlorides from the environment, the binding is hardly influenced by the binder type (table 4).

Table 4: Binding of chlorides as a function of cement type for samples submerged in sodium chloride-solution (20g Cl^-/l) during 28 days (same cements as table 1) [Arya 1990]

Cement type	replacement	total Cl^- added [% by mass of binder]	free Cl^- [% by mass of binder]	bound Cl^- [% by mass of binder]	Bound/total [%]
OPC1	-	1.635	0.831	0.804	50
OPC2	-	1.779	0.811	0.968	54
OPC1	30% PFA	1.887	0.818	1.069	57
OPC1	70% GGBS	1.750	0.830	0.920	53
OPC1	10% CSF	1.265	0.684	0.581	46
SRPC1	-	1.659	0.885	0.774	47

In Japan, similar results were found for concrete specimens that are exposed to sea-water for 10 to 30 years (table 5).

Table 5: Binding of chlorides from exposure to seawater [Mohammed 2003]

binder type	**bound/total chloride [%]**
OPC	58
high early strength PC	57
moderate heat PC	56
aluminate cement	74
BFSC (5 - 30% slag)	56
BFSC (30 - 60% slag)	58
PFA (5 -10% FA)	61

It is suggested by Mohammed [2003] that not only tricalcium aluminate chemically binds chlorides but that all aluminate phases bind chlorides.

3.2.2.4. Cation of chloride salts

The de-icing agent that is used on the Dutch highways or the salt in seawater is mainly made up of sodium chloride. Another salt is calcium chloride that was used as an admixture until 1974, to accelerate hardening. Even though sodium chloride and calcium chloride show a different binding behaviour, both salts have been used in laboratory tests to determine the critical chloride concentration.

The cation causes a significant difference in binding. Chloride from calcium chloride is bound more strongly than from sodium chloride because calcium ions reduce the pH of the pore water by consuming hydroxyl ions due to precipitation of calcium hydroxide. The reduced pH value leads to an increased amount of bound chloride [Rasheeduzzafar 1991]. The difference of binding of chlorides that originate from different salts is listed in table 6.

Table 6: Binding of penetrated chlorides as a function of salt type [Arya 1990] for concrete samples having an age of two days at start of exposure; w/b-ratio: 0.5, cement type: OPC

Samples submerged in salt-solution (20gram Cl^-/l) during 28 days				
Cl^- concentration (% by mass of binder)	NaCl	Sea-water	$CaCl_2$	$MgCl_2$
Free	0.831	0.776	0.765	1.480
Bound	0.804	0.577	1.408	2.347
Total	1.635	1.353	2.173	3.827
Bound/total (%)	50	43	65	61

Note: Seawater has a chloride concentration of 18.5 gram Cl^-/l. The chloride in seawater originates from sodium chloride for 90%; the other salts are magnesium chloride ($MgCl_2$), magnesium sulphate ($MgSO_4$), calcium sulphate ($CaSO_4$) and potassium sulphate (K_2SO_4)

The relatively low binding of chloride that originates from seawater is caused by the presence of sulphates in seawater that show a stronger binding with C_3A than chlorides [Hussain 1994].

3.2.2.5. Literature review

This section lists the critical chloride concentrations given by various sources. The results are subdivided by those given in standards and other publications. Standards may be supposed to give a conservative value of the chloride corrosion threshold, because they most likely give an 'allowed' value that contains a certain amount of reserve. The other publications may be supposed to give an average value for the critical chloride concentration. These publications are subdivided by threshold definition, salt type and chloride permeation into hardened concrete or addition to fresh concrete, since all these variables influence the critical chloride concentration.

The critical chloride concentration is used in many service life prediction models to determine the time to initiation of corrosion. Since most models do not include the propagation phase, it is preferable to use the first definition that is listed in section 3.2.2.1. Thus, the adopted definition of the critical chloride concentration is: 'The concentration at which corrosion is initiated, independent from any damage to the structure'.

The results from various sources in the literature are classified by the previously mentioned differences in table 7. The values apply to concrete structures where oxygen can reach the reinforcement since oxygen is needed to form the passive layer [Buist 1982]. The results from table 7 indicate that the most likely critical chloride concentration that is associated with initiation of corrosion is on average 0.5% by mass of binder (cement). This conclusion agrees with two studies where corrosion was observed at structures with a chloride concentration of about 0.5% by mass of cement [Gaal 2001a, Polder 2002b].

The common perception is that blended cements like blast furnace slag cement or portland fly ash cement give a higher threshold level than ordinary portland cement [CUR 1997]. This perception probably originates from the fact that reinforcement in concrete, made of blended cements, is less likely to corrode. Blended cements show more binding of inter mixed chlorides and a reduced coefficient of diffusion in laboratory conditions. Concrete made of blended cements, however, show a lower concentration of hydroxyl ions in the pore water than portland cement because of the replacement of clinker by slag or fly ash [e.g. Glass 2002]. This indicates that blended cements will show a reduced threshold level compared to non-blended cements. Studies on fly ash blended cements showed an increase in chloride over hydroxyl ion ratio compared to portland cement, which indicates a higher probability of corrosion [Kawamura 1988, Thomas 1996].

Table 7: Review of critical corrosion threshold for atmospherically exposed structures [Gaal 2003c]

author / reference	condition	salt	definition*	salt added	value
Literature					
Stuvo, 1989	-	-	-	-	0.40%
Fluge, 2001	OPC, sea exp.	NaCl	initiation (1)	no	0.47%
Breit, 1997	OPC	-	initiation (1)	-	0.48%
Li, 2002	PFA	NaCl	initiation (1)	no	0.49%
Gaal, 2001a	OPC	NaCl	initiation (1)	no	0.50%
Polder, 2002a	OPC	NaCl	initiation (1)	no	0.50%
Polder, 2002b	OPC, sea exp.	NaCl	initiation (1)	no	0.50%
Mohammed, 2001	OPC	NaCl	initiation (1)	yes[4]	0.50%
Thomas, 1990	PFA, sea exp.	NaCl	initiation (1)	no	0.50%
Li, 2002	OPC	NaCl	initiation (1)	no	0.53%
CUR 1997	OPC, w/b=0.65	NaCl	initiation (1)	yes	1.25%[5]
CUR 1997	BFSC, w/b=0.65	NaCl	initiation (1)	yes	1.60%[5]
CUR 1997	BFSC, w/b=0.45	NaCl	initiation (1)	yes	2.00%[5]
CUR 2000a (DuraCrete)	OPC, w/b=0.5	-	initiation (2)[6]	no	0.50%
CUR 2000a (DuraCrete)	OPC, w/b=0.4	-	initiation (2)[6]	no	0.80%
CUR 2000a (DuraCrete)	OPC, w/b=0.3	-	initiation (2)[6]	no	0.90%
Fluge, 2001	OPC, sea exp.	NaCl	initiation (2)	no	0.80%
CUR 1992	OPC	$CaCl_2$	propagation (3)	yes	1.00%
CUR 1992	BFSC	$CaCl_2$	propagation (3)	yes	1.00%
Fluge, 2001	OPC, sea exp.	NaCl	propagation (3)	no	1.20%
National Standards					
ACI Building Code 318, 1999	free chlorides	-	-	-	0.15%
SAA 1990 (Austr, AS 3600)	total chlorides	-	-	-	0.22%
BSI 1972 (UK, CP 119)	total chlorides	-	-	-	0.35%
NNI 2001 (NEN-EN 206-1)	total chlorides	-	-	-	0.40%
NSF 1999 (Norway NS 3474)	total chlorides	-	-	-	0.60%

*The number refers to the definition of the critical corrosion threshold:

1 initiation without visible damage
2 initiation + propagation until visible damage
3 initiation + propagation until repair needed

[4] Critical chloride content refers to free chlorides.
[5] The critical chloride content is not adjusted because of chloride binding.
[6] Chloride level that leads to detectable levels of corrosion; in general this will be much earlier than the occurrence of wide cracks or spalling of concrete.

3.2.3. Chloride ingress model

Enough indications suggest that ingress of chlorides can be best modelled by a diffusion process (section 3.2.1.7). The next sections give the partial differential equation for diffusion and a number of solutions of this equation for specific conditions.

3.2.3.1. General model

Chloride permeation into concrete is commonly described as a one-dimensional diffusion process. Diffusion is mathematically represented by the partial differential equation that is called Fick's second law of diffusion [Crank 1975]. Fick's second law of diffusion is given in equation 12.

$$\frac{\partial C(x,t)}{\partial t} = D\frac{\partial^2 C(x,t)}{\partial x^2} \qquad (12)$$

Where: C(x,t) = concentration of diffusing substance at depth x and time t, t = time, D = diffusion coefficient, x = depth coordinate from the concrete surface into the concrete.

3.2.3.2. Solution – Collepardi

Collepardi was the first to apply Fick's 2nd law of diffusion to chloride ingress into concrete. Collepardi described the analytical solution to Fick's second law of diffusion on the condition that the diffusion coefficient and the surface chloride concentration are constant. The mathematical formulation for uniaxial permeation into a semi-infinite medium is represented by equation 13 [Collepardi 1972].

$$C_{cl}(x,t) = C_{cl;i} + (C_{cl;s} - C_{cl;i})erfc\left(\frac{x}{\sqrt{4D_{cl}t}}\right) \qquad (13)$$

Where: $C_{cl}(x,t)$ = concentration of chloride ions at depth x and time t, $C_{cl;i}$ = initial uniform chloride concentration in the concrete, $C_{cl;s}$ = concentration of chlorides at the surface, x = depth co-ordinate from the concrete surface into the concrete, D_{cl} = chloride diffusion coefficient, t = time. The initial chloride concentration represents the chloride that is present in the fresh concrete, which originates from tap water, binder and aggregate. The error function (erf) and complementary error function (erfc) are special cases of the incomplete gamma function (the error function is discussed in appendix A).

The analytical solution given by Collepardi assumes a uniaxial permeation into a semi-infinite medium. However, this assumption disregards the existence of for instance the beam edges. The analytical solution to calculate chloride ingress into concrete in a two dimensional situation is given by [Suryavanshi 2002]:

$$C_{cl}(x,y,t) = C_{cl;s} \cdot \left(1 - erf\left(\frac{x}{\sqrt{4D_{cl}t}}\right) erf\left(\frac{y}{\sqrt{4D_{cl}t}}\right)\right) \quad (14)$$

Two-dimensional ingress of chlorides is calculated for a fictitious beam. The results of this analysis are plotted in figure 13. The two-dimensional chloride ingress leads to increased chloride ingress. However, the chloride profile seems to follow the curvature of the stirrup as is shown in figure 13. According to the Dutch Standard, the radius of the stirrups should be at least two and a half times the diameter of the stirrup [NNI 1995b]. Therefore, chloride ingress is limited in the rest of this thesis to uniaxial permeation.

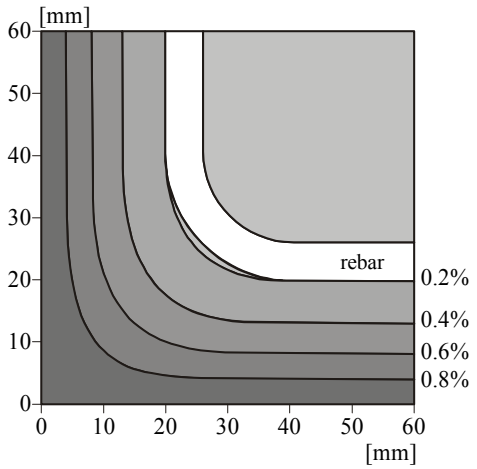

Figure 13: Cross section of two-dimensional chloride ingress

De-icing agents are only applied during the winter season, and this process is repeated every winter. Under these conditions an alternative solution to Fick's 2nd law of diffusion has been suggested by Crank (equation 15) [Crank 1975]. The solution given in equation 15 satisfies the condition that the total amount of chlorides (M) remains constant.

$$C_{cl}(x,t) = \frac{M}{\sqrt{\pi D_{cl}t}} \exp\left(\frac{-x^2}{4D_{cl}t}\right) \quad (15)$$

Where: $C_{cl}(x,t)$ = concentration of chloride ions at depth x and time t, x = depth coordinate from the concrete surface into the concrete, D_{cl} = chloride diffusion coefficient, t = time, M = total amount of diffusing chlorides. However, the total amount of chlorides is deposited at time t=0, therefore equation 15 is not suitable for the repeated chloride loads during successive winters.

The boundary conditions under which the solutions of equation 13 and 15 are derived from Fick's second law of diffusion (equation 12) are listed in appendix A.

3.2.3.3. Solution – time dependent diffusion coefficient

One of the boundary conditions that is used by Collepardi is a constant diffusion coefficient and surface chloride concentration. Until the mid 1990s, it was commonly accepted practice to model the diffusion coefficient as a constant value over time [e.g. Brodersen 1982, Collepardi 1972]. However, observations at structures suggested otherwise. The resistance to chloride ingress appears to increases over time, because the pores are blocked or reduced in width due to:

- A gradually increasing degree of hydration, in particular for hydration of slag and fly ash.
- A possible interaction between seawater (if present) and concrete, where precipitation of $CaCO_3$ and brucite may block some of the smallest pores in the surface layer of the concrete. Brucite ($Mg(OH)_2$) forms due to the permeation of sea salts ($MgCl_2$) that react with calcium hydroxide (equation 16). It is rather insoluble and clogs the pores of concrete. [Buenfeld 1986,Tong 2001].

$$MgCl_2 + Ca(OH)_2 \rightarrow Mg(OH)_2 \downarrow + CaCl_2 \qquad (16)$$

Consideration must be given to the ability of the cementitious system to refine its pore structure as it matures, thereby decreasing transport rates. Due to continued hydration of cement (i.e. ageing), the porosity is reduced, which results in a reduced diffusion coefficient. The diffusion coefficient and the surface chloride concentration are determined from a measured chloride profile; this is the so-called chloride profile method. However, by applying equation 13 to field data, it was found that the effective diffusion coefficient changed with exposure time [Bamforth 1999, Sandberg 1998, Thomas 1999]. In the past, the changing diffusion coefficient in time was overcome by changing the value of the diffusion coefficient. However, this approach leads to an underestimation of the chloride ingress at young ages or to an overestimate at higher ages. As a consequence the use of a time-dependent diffusion coefficient in predictive models is necessary to accurately predict the actual deterioration in concrete structures [Gaal 2001b, Thomas 1999].

A first attempt to include the effect of ageing of concrete on the diffusion coefficient is given in equation 17 [Takewaka 1988, Mangat 1994a]:

$$D_{cl}(t) = D_{cl;i}\, t^{-n} \qquad (17)$$

Where: $D_{cl}(t)$ = time-dependent chloride diffusion coefficient, $D_{cl;i}$ = initial chloride diffusion coefficient, t = time (year), n = ageing parameter.

Based on eight years of research at concrete exposed to an outdoor climate in Folkestone (U.K.), Bamforth derived input parameters for equation 17 [Bamforth 1999]. Deduced from field data a reference diffusion coefficient was introduced that could be

transformed to a time dependent diffusion coefficient by equation 17 or 18. The trend of the coefficient of diffusion over time is presented in figure 14. For blast furnace slag cement and portland fly ash cement, it seems that the water-binder ratio has an influence on the initial chloride diffusivity, while the level of replacement influences the slope, i.e. the development of chloride diffusivity in time [Maage 1996].

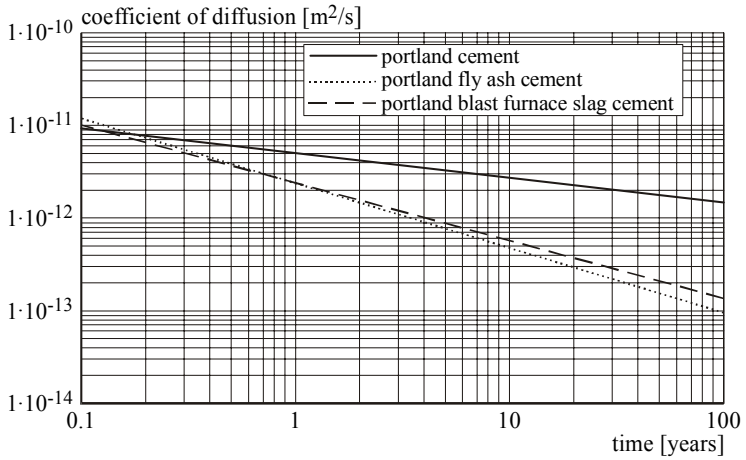

Figure 14: Time dependent diffusion coefficient of BFSC (70% slag), PFA and PC, $n_{bfsc}=0.621$, $n_{pfa}=0.699$, $n_{pc}=0.264$ [after: Bamforth 1999]

The disadvantage of equation 17 is that the units at both sides of the equality sign are dissimilar and the initial diffusion coefficient represents a diffusion coefficient at a certain age. A further developed time dependent model to predict the coefficient of diffusion at a given age is equation 18 [Maage 1996]. This model has the advantage that the initial reference diffusion coefficient can be taken at any point in time, usually a reference period of 28 days is chosen. In this thesis, equation 18 is used to model the ageing of the diffusion coefficient.

$$D_{cl}(t) = D_{cl;0}\left(\frac{t_0}{t}\right)^n \qquad (18)$$

Where: $D_{cl}(t)$ = time-dependent diffusion coefficient, $D_{cl;0}$ = reference chloride diffusion coefficient (associated with t_0), t_0 = reference period, t = time of exposure, n = ageing coefficient ($0<n<1$).

To determine chloride ingress with the time-dependent diffusion coefficient of equation 18, this equation is substituted in equation 13 to obtain a relationship for the time dependent prediction of the chloride profile (equation 19).

$$C_{cl}(x,t) = C_{cl;i} + (C_{cl;s} - C_{cl;i}) \cdot erfc \frac{x}{\sqrt{4 \cdot D_{cl;0} \left(\frac{t_0}{t} \right)^n \cdot t}} \qquad (19)$$

However, this substitution is mathematically inconsistent, because one of the preconditions of the solution of Fick's second law is the constant coefficient of diffusion in time. The total history of the changing diffusion coefficient is only included correctly by solving Fick's second law anew. It results in a time-history of the diffusion coefficient given by integrating equation 18 [Visser 2002]:

$$\int_0^t D_{cl}(t)dt = \frac{D_{cl;0}}{1-n} \left(\frac{t_0}{t} \right)^n \cdot t \qquad (20)$$

The factor 1/(1-n) is missing in most models, as noted earlier [Mangat 1994a]. Due to the integration it is now valid to substitute equation 20 into equation 13 resulting in equation 21. The complete derivation of equation 21 from Fick's second law of diffusion is given in Appendix A.

$$C_{cl}(x,t) = C_{cl;i} + (C_{cl;s} - C_{cl;i}) \cdot erfc \frac{x}{\sqrt{4 \cdot \frac{D_{cl;0}}{1-n} \left(\frac{t_0}{t} \right)^n \cdot t}} \qquad (0 < n < 1) \qquad (21)$$

This section discussed three types of diffusion coefficients, i.e. a constant diffusion coefficient (equation 13), a semi time-dependent diffusion coefficient (equation 19) and a full time-dependent diffusion coefficient (equation 21). The differences between the three types of diffusion coefficient are displayed in figure 15. The diffusion coefficient of equation 19 is usually referred to as time-dependent diffusion coefficient. However, the preposition of equation 19 is that the diffusion coefficient is constant in time. As a consequence the diffusion coefficient is not time-dependent, but it assumes that the diffusion coefficient at the end of the evaluated period is applicable to the whole lifetime, as is presented in figure 15. In this thesis, the time-dependent diffusion coefficient of equation 19 is referred to as semi time-dependent. Only the full time dependent diffusion coefficient (equation 20) gives an accurate description of the history of the diffusion coefficient.

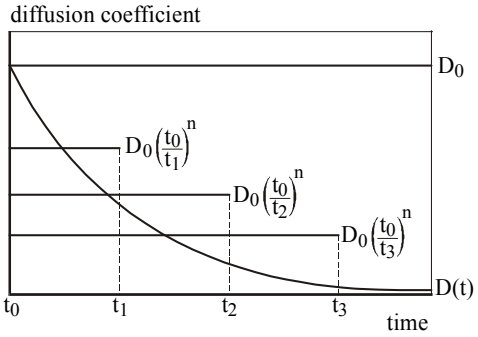

Figure 15: Time-dependent diffusion coefficients

3.2.3.4. Solution – limited exposure to chlorides

Bridges are exposed to chlorides as a result of the application of de-icing agents. A second source of chlorides could be seawater spray. In this thesis it is assumed that chlorides originate from de-icing agents and not seawater spray, since marine structures are not considered.

In the United States and Canada highways have been constructed since the 1920s. During the winter season, sleigh traffic was a common means of transportation because driving on icy roads was difficult for the early generation of cars. To accommodate the rapidly growing number of vehicles, the major highways were kept open to traffic by snowploughs and the use of abrasives like sand, during the winter season. By the mid 1930s, these materials were no longer sufficient because of an increased public demand for ice and snow free roads and bridges.

At first, this problem was overcome by adding common salt (sodium chloride) to the abrasives. However, over the years, the increased usage of abrasives mixed with salt led to costs associated with the clean up of roads and drainage facilities. The use of straight granular sodium chloride was pioneered by the New Hampshire State Highway Department on an experimental basis in 1938 [Hogan 2001]. By the mid 1950s many states in the United States used salt without abrasives to keep the roads free of ice. In Europe, the wide scale use of salt with abrasives started in the early 1960s and subsequently the use of salt without abrasives started in the late 1960s [Goltermann 2003, Vassie 1984, Vulpen 2000].

The age of the structure when the application of de-icing agents started has a significant influence on the chloride ingress, because of the reduction of the coefficient of diffusion in time. A graphical representation of the development is given in figure 16.

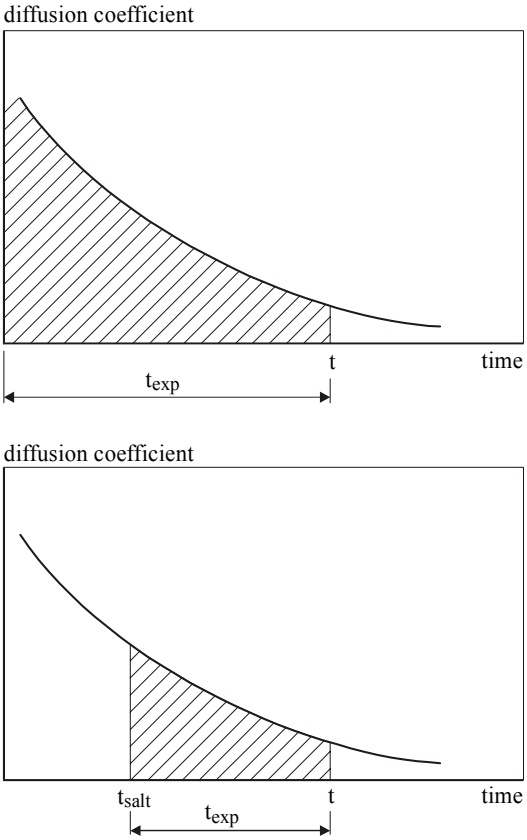

Figure 16: Ageing vs. exposure to de-icing[7]

Due to the reduction of the diffusion coefficient over time combined with the postponed exposure to chloride, the total amount of chlorides that will penetrate into the structure is reduced. The total history of the changing diffusion coefficient and the age at which the structure was first exposed to chlorides is only included when Fick's second law of diffusion is solved with the right prepositions of the time-dependent diffusion coefficient and the exposure to chlorides at a certain point in time (equation 22).

$$\int_{t_s}^{t_s+t_{exp}} D_{cl}(t)dt = \frac{D_{cl;0}}{1-n} t_0^{\,n} \left[(t_s + t_{exp})^{1-n} - t_s^{\,1-n} \right] \qquad \left(t_s + t_{exp} = t \right) \qquad (22)$$

Where: t_s = age at which the exposure to de-icing agent starts, t_{exp} = duration of the exposure to the de-icing agent, t = time (age of the structure).

Due to the integration it is now possible again to substitute equation 22 into equation 13, resulting in [Gaal 2003a]:

[7] t_s = age at which exposure to deicing started

$$C_{cl}(x,t) = C_{cl;i} + \left(C_{cl;s} - C_{cl;i}\right) erfc \frac{x}{\sqrt{4 \frac{D_{cl;0}}{1-n} t_0^{\,n} \left[t^{1-n} - t_s^{\,1-n}\right]}} \qquad \left(t > t_s\right) \tag{23}$$

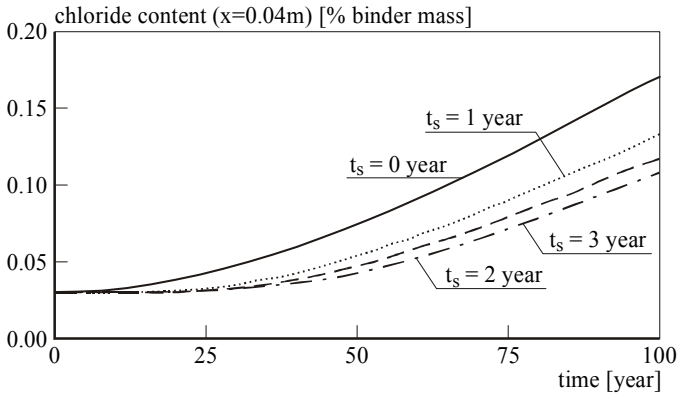

Figure 17: Influence of the start of application of de-icing salt

If the structure is exposed to de-icing agents several years after completion, the concrete shows a lower diffusion coefficient and consequently a decreased ingress of chloride. This effect is presented in figure 17 where the chloride concentration is determined at a depth of 0.04m for different scenarios of first exposure to de-icing salts, respectively 0, 1, 2, 3 years after completion. The reduced levels of the chloride ingress in figure 17 express the ageing of the concrete before the de-icing salt is first applied. The initial chloride concentration, of 0.03% of the mass of binder, is caused by the chlorides that are present in the mixing water and binder.

3.2.4. Evaluation of chloride ingress models

It has been suggested that only finite element models are capable of predicting chloride ingress with sufficient accuracy [Reinhardt 1985]. However the knowledge of finite element models by far exceeds the knowledge of the input values for the finite element calculations. Therefore in this thesis the main processes, like ageing and chloride ingress are modelled with Fick's second law of diffusion.

It is observed from structures exposed to de-icing agents, that old bridge structures contain lower chloride concentrations than more recently constructed bridges [Goltermann 2003]. Only by using equation 23, where both the start of application of de-icing salts to concrete structures and the change in diffusion coefficient in time is taken into account, chloride ingress is modelled correctly.

3.3. Carbonation

The alkaline environment in concrete is the result of calcium, sodium and potassium hydroxides that arise from cement hydration. Especially sodium and potassium hydroxides give the high pH-value to the pore water in concrete [Fraay 1990]. Carbonation is the process where carbon dioxide, from the atmosphere, enters concrete and reacts with the hydroxides to form carbonates and water (equation 24, 25 and 26). Due to the consumption of these hydroxides the pH-value is reduced below 9.0.

$$Ca(OH)_2 + CO_2 \rightarrow CaCO_3 + H_2O \quad (24)$$

$$2NaOH + CO_2 \rightarrow Na_2CO_3 + H_2O \quad (25)$$

$$2KOH + CO_2 \rightarrow K_2CO_3 + H_2O \quad (26)$$

The depth over which the pH-value has dropped below 9.0 is called the depth of carbonation. In general, this depth is 1-2mm for portland cement after 2 years of exposure [Jones 2001]. To facilitate the ingress of carbon dioxide the pores should not be blocked by pore water. The reasons outlined before make clear that corrosion due to carbonation can only arise in a situation where there is a small cover depth and a relatively dry environment. However, sufficient moisture is necessary to facilitate corrosion.

The rate of carbonation depends on: type of cement, cement content, grain size of aggregate, water/cement-ratio, temperature, moisture conditions and concentration of carbon dioxide of the ambient air. Corrosion damage due to carbonation in reinforced concrete can, in general, be prevented by sufficient cover depth and low to moderately low water to binder ratios.

3.3.1. Carbon dioxide diffusion

The resistance of concrete structures to carbonation can be determined indirectly by means of material tests (natural or accelerated carbonation test). In these types of tests concrete specimens are subjected to environmental conditions that accelerate carbonation, viz. increased carbon dioxide concentration, intermediate relative humidity and moderate temperatures. After a defined exposure time, the specimens are broken and the carbonation front is detected by the application of a suitable indicator solution (phenolphthalein). The result of such a direct measurement is a recorded carbonation depth, which represents both diffusion characteristics and carbon dioxide binding capacity of the material; the carbonation resistance[8] is hereby derived.

[8] Literature about the coefficient of carbonation be should read with great care, because three different variables are in use (D_{eff}, R_{acc}^{-1}; accelerated carbonation test, R_{nac}^{-1}; natural carbonation test).

It is well known that the cement type can have a significant influence on the rate of carbonation of concrete. In this respect a particularly strong influence on carbonation is noted for blast furnace slag cement. Various authors have shown that concrete made of blast furnace slag cement shows greater carbonation depths than those made of portland cements [Jones 2001, Parrott 1996]. The rate of carbonation is proportional to the replacement of portland cement with blast furnace slag. For concrete made of blast furnace slag cement with a replacement of 75%, the depth of carbonation is about three times larger than that of portland cement in an artificial climate (constant humidity) [CUR 1999]. The main cause of this higher rate is the lower lime content of the hydrated cement, which will be depleted more easily [Bijen 1998].

3.3.2. Carbonation model

This chapter gives the most often used models to predict the depth of carbonation that are available from literature.

3.3.2.1. General model

It is generally accepted that Fick's first law of diffusion (equation 27) describes the depth of carbonation as a function of time. If Fick's first law is adapted for carbon dioxide diffusion it results in equation 28 [Meyer 1967].

$$F = -D\frac{\partial C}{\partial x} \tag{27}$$

Where: F = rate of transfer per unit area of cross section, C = concentration of diffusing substance, x = space coordinate measured normal to the section, D = diffusion coefficient.

$$dQ = D_{cb} A \frac{\Delta C_{cb}}{x} dt \tag{28}$$

Where: Q = amount of diffusing carbon dioxide, A = penetrated area, ΔC_{cb} = difference between carbon dioxide concentration in the atmosphere and at the carbonation front, x = distance between carbonation front and concrete surface, t = time, D_{cb} carbon dioxide diffusion coefficient.

The diffusing carbon dioxide reacts with calcium, potassium and sodium hydroxides at the carbonation front. In a simplified form, this process is modelled by equation 29, where an amount of carbon dioxide (dQ) in a volume (dV) reacts with hydroxide. This equation is rewritten to equation 30.

$$dQ = a \cdot dV \tag{29}$$

$$dQ = a \cdot A \cdot dx \tag{30}$$

Where: Q = amount of diffusing carbon dioxide, a = carbon dioxide binding capacity of concrete, V = concrete volume.

The next equation is obtained if equation 30 is substituted in equation 28.

$$a \cdot A \cdot dx = D_{cb} A \frac{\Delta C_{cb}}{x} dt \quad (31)$$

$$x \cdot dx = \frac{D_{cb}}{a} \Delta C_{cb} dt \quad (32)$$

Integration of equation 32 yields:

$$x_{cb} = \sqrt{\frac{2 \cdot D_{cb} \cdot \Delta C_{cb}}{a}} \cdot \sqrt{t} \quad (33)$$

Where: x_{cb} = carbonation depth, D_{cb} = carbon dioxide diffusion coefficient, ΔC_{cb} = difference between carbon dioxide concentration in the air and at the carbonation front, a = carbon dioxide binding capacity of concrete, t = time.

The binding capacity of carbon dioxide of concrete, which is a parameter in equation 33, is determined by equation 34.

$$a = 0.75 \cdot C_{CaO} \cdot C_c \cdot \alpha_h \cdot \frac{m_{CO_2}}{m_{CaO}} \quad (34)$$

Where: a = carbon dioxide binding capacity of cement, C_{CaO} = content of calcium oxide in cement (table 8), C_c = cement content in concrete, α_h = degree of hydration, m_{CO2} = molar mass of carbon dioxide, m_{CaO} = molar mass of calcium oxide.

Table 8: Calcium oxide content (CaO) [CUR 1999]

type of cement	**content of CaO [%]**
CEM I portland cement	63.9
CEM I-SR portland cement	64.0
CEM III/B-LH/SR blast furnace slag cement	48.0

The content of calcium oxide in the cement should be known to determine the carbon dioxide binding capacity of the concrete. During cement hydration, calcium oxide reacts to calcium hydroxide, which subsequently reacts with carbon dioxide (equation 24, 25 and 26). An average content of calcium oxide is given in table 8.

The degree of hydration during the service life of the concrete is assumed to be constant (when carbonation is determined) and is proportional to the water to binder ratio (table 9). The assumption of a constant degree of hydration is not in line with the assumption of the time-dependent diffusion coefficient that is used to determine chloride ingress.

A number of researchers have tried to calibrate equation 33 as will be discussed in the next sections.

Table 9: Degree of hydration [CEB 1997]

w/b-ratio	degree of hydration
0.63	0.82
0.57	0.79
0.55	0.75
0.54	0.74

3.3.2.2. Model of CEB

The CEB-model [CEB 1997] takes into account that carbonation depends on wetting and drying of the cover. In wet concrete, the pores are filled with water and the carbon dioxide cannot penetrate into the concrete, where in relative dry concrete carbon dioxide can easily penetrate. The carbonation depth for specific environmental conditions can be determined with equation 35 and the parameters from table 10. The parameters from table 10 are calibrated at observed depths of carbonations in the accompanying environments.

$$x_{cb} = \sqrt{2 \cdot \psi_1 \cdot \psi_2 \cdot \psi_3 \cdot C_{cb;s}} \cdot \sqrt{\frac{D_{cb}}{a} \cdot t} \cdot \left(\frac{t_0}{t}\right)^{\psi} \qquad (35)$$

Where: x_{cb} = carbonation depth, ψ_1 = parameter for micro climatic conditions, describing the mean moisture content of concrete, (table 10), ψ_2 = parameter to describe the curing conditions, ψ_3 = parameter to describe the effect of water separation (local water to binder ratio), $C_{cb;s}$ = carbon dioxide content in the atmosphere[9], D_{cb} = effective carbon dioxide diffusion coefficient of dry carbonated concrete, which is the diffusion coefficient of dry concrete for carbon dioxide in a defined environment (T=20ºC RH=65%), a = amount of carbon dioxide for complete carbonation, (binding capacity for carbon dioxide) (equation 34), t_0 = reference period, t = time in service, ψ = parameter for micro climatic conditions, describing wetting and drying.

Table 10: Parameters CEB Carbonation model [CEB 1997]

class	I	II	III	IV	V
curing	bad	good	good	good	good
Ψ_1	0.3	0.3	0.4	0.5	0.6
Ψ_2	2.0	1.0	1.0	1.0	1.0
Ψ_3	1.5	1.2	1.2	1.0	1.0
Ψ	0.3	0.3	0.2	0.1	0.05
I, II: wet at any occasion III: wet when driving rain IV, V: sheltered parts					

[9] In general, the carbon dioxide content in the atmosphere is used in stead of the concentration difference between the carbon dioxide concentration at the carbonation front and in the air as is used in equation 33. This implicitly assumes a negligible carbon dioxide concentration at the carbonation front.

3.3.2.3. Carbonation model of Häkkinen

In general, the depths of carbonation at different structures show a large scatter. Häkkinen tried to overcome the scatter by relating equation 33 to the compressive strength of the concrete. The model of Häkkinen assumes a relation between the compressive strength and the resistance to ingress of carbon dioxide. The Häkkinen model takes the following form [Häkkinen 1993]:

$$x_{cb} = \xi_{env} \cdot \xi_a \cdot f_{cm}^{\xi_b} \cdot \sqrt{t} \text{ [mm]} \qquad (36)$$

Where: x_{cb} = depth of carbonation front [mm]; ξ_{env} = environmental coefficient, ξ_a = parameter relating to cement type, f_{cm} = mean compressive strength of the concrete at the age of 28 days, ξ_b = parameter relating to cement type, t = time.

The suggested values for the parameters of equation 36 are listed in table 11.

Table 11: Suggested values for carbonation model parameters [Häkkinen 1993]

environment		ξ_{env}
structures sheltered from rain		1.0
structures exposed to rain		0.5
cement type	ξ_a	ξ_b
portland cement (p.c.)	1800	-1.7
p.c. + fly ash 28%	360	-1.2
p.c. + silica fume 9%	400	-1.2
p.c. + blast furnace slag 70%	360	-1.2

3.3.3. Evaluation of carbonation models

The results of the different models give a relatively large scatter. The problem of the carbonation model is that it is unknown to which set of data the parameters are calibrated. This does not mean that the models are not good, but the parameters should be used with care.

The environment has a pronounced influence on the depth of carbonation as is described in chapter 2. Because the CEB model (CEB 1997) gives the best possibilities to adjust the model to the environment, this model is selected to simulate carbonation induced deterioration in this thesis.

3.4. Modelling Deterioration

Over the last decade of the 20th century, many research studies were carried out to model the deterioration of concrete structures [e.g. Frangopol 1997, Roberts 2000, Stewart 1998]. In these studies models of chloride ingress and carbonation were tuned to observed damage to concrete structures.

However, it has been suggested that modelling of deterioration will not lead to a satisfactory result because:

- bridges are often rated as functionally obsolete before becoming structurally deficient;
- pre WWII bridges are still in good condition, as compared to bridges constructed during the 1970s;
- small areas of bridge elements, like joints, need a lot of maintenance.

Some articles suggest that if a structure is designed according to the standards and does not show deterioration within 10 years after construction, the lifetime of the structure is infinite [de Sitter 2001]. However, this section together with chapter 6 will show that concrete structures do deteriorate over time.

Functionally obsolete structures

In general, according to the standards a design service life of 100 years is required. However, most structures show the first signs of deterioration after 25 years of service and therefore need maintenance [Hyman 1983, Markow 1993, Vorster 1991]. Because of the early end of the functional lifetime, long before concrete structures have reached the end of their design lifetime, it is questioned if the models for chloride ingress and carbonation are really suitable to predict deterioration. However, concrete structures begin to crumble long before they have reached the end of their design lifetime. To predict the gradually increasing risk of spalling, deterioration models are used. Only these models describe the changes in condition in time.

In the Netherlands, over the last two decades about 50 out of 3500 highways bridges have been demolished (in the year 2000). These bridges were mostly demolished because of a change in functional or economical requirements. The average age of these demolished bridges was about 40 years, which corresponds to the often-suggested functional lifetime of 40 years. However, if the lifetime distribution of these 50 demolished bridges is combined with the current age distribution of the 3450 existing bridges, it is found that the expected age of bridges is about 83 years [van Noortwijk 2002].

Old bridges in good condition

Analyzing the Dutch bridge stock, it is observed that bridges constructed before the Second World War are in a comparable condition, with respect to spalling, as the bridges from the early 1970s. The condition of these old pre-WW2 bridges is ex-

ploited to prove that concrete bridges have an infinite life span. The most likely reasons for the good condition of the pre-WW2 bridges, is that they were not exposed to de-icing agents until the 1960s.

In order to understand the way bridges deteriorate it is important to recognize that the use of sodium chloride as a de-icing agent to keep the roads and bridges free of snow and ice, started only in the 1960s. Together with the ongoing hydration of cement, it is explained in this thesis why pre-WW2 bridges generally are in a better condition than bridges constructed in the 1970s or later.

Maintenance of bridges

For young bridges, leaking bridge deck expansion joints and not corrosion of the reinforcement is the most important reason for maintenance expenses. Because of the small number of old bridges compared to the number of recently built bridges on Europe's mainland, maintenance of young bridges receives a lot of attention. Therefore leaking joints show up in the maintenance statistics more frequently than corrosion of reinforcement because bridges that show corrosion have probably already been demolished and not maintained before.

3.4.1. Modelling corrosion

The corrosion process consists of a number of sequential phases. The generally accepted model of Tuutti suggests an initiation and a propagation phase (figure 18). The initiation phase describes the permeation of aggressive agents through the concrete cover until they reach the reinforcement. The propagation phase describes the development of rust products that induce cracking and spalling of the concrete cover.

Models that includes the propagation stage generally states that the service life of the structure formally ends after a critical crack width has been developed. The service life of a concrete structure is mathematically modelled by equation 37 through 47 [Thoft-Christensen 2000, Tuutti 1982, Liu 1998, Bažant 1979a, Bažant 1979b]. The suggested values for the input parameters are tabulated in table 12 (p. 49).

$$t_{service} = t_{corr} + \Delta t_{crack} \qquad (37)$$

Where: $t_{service}$ = service life, t_{corr} = time of initiation of corrosion, Δt_{crack} = time from corrosion initiation to cracking of the concrete cover.

3.4.2. Initiation phase

In this thesis, it is assumed that the leading mechanisms of deterioration are due to chloride ingress and carbonation. The concentration of chlorides at the reinforcement is determined with equation 23, once this concentration reaches the critical chloride concentration it is assumed that corrosion of the reinforcement is initiated. The depth of the carbonation front is determined with equation 35. When the carbonation front

reaches the reinforcement it is assumed that corrosion is initiated. Both events cause the system (reinforced structure) to enter the propagation phase.

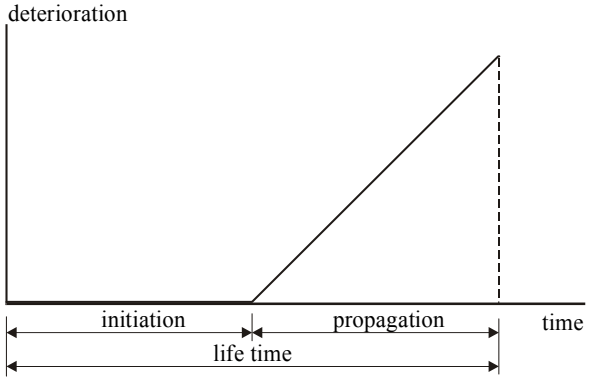

Figure 18: Schematic representation of steel corrosion in concrete as a function of age [after: Tuutti 1982]

3.4.3. Propagation phase

Service life of a bridge is usually defined as the time until initiation of corrosion [e.g. Clifton 1993]. In previous sections, the most important models for chloride ingress and carbonation were described. Equations 23 (p. 37) and 35 (p. 41) give the time until initiation of corrosion due to chloride ingress and carbonation, respectively. However, after initiation of corrosion the structure is still without any cracking or spalling. During the propagation phase, the concrete will eventually crack due to the tensile stresses that arise from the expansion that is caused by the corrosion of the reinforcement. The three stages that are considered in the propagation model are:

- free expansion;
- stress initiation;
- crack initiation.

The length of the propagation period depends on:

- the corrosion rate;
- the criterion (first crack, spalling);
- the amount on corrosion causing that the criterion is exceeded.

Initiation of corrosion does not lead to instantaneous cracking. When corrosion products are formed, first, the porous zone around the reinforcement is filled with corrosion products. The concrete porosity is at its largest close to the rebar, the so-called transition zone, as was discussed in section 3.2.1. For simple calculation, an equivalent zone with porosity one (100%) is assumed around the steel bar.

The total amount of corrosion products that is needed to cause cracking of the cover is calculated by:

$$w_{crit} = w_{porous} + w_{expan} + w_{steel} \quad (38)$$

Where: w_{crit} = amount of corrosion product needed to cause cracking, w_{porous} = amount of corrosion product necessary to fill the porous zone, w_{expan} = amount of corrosion products needed to create expansive pressure, w_{steel} = amount of corrosion products that causes actual cracking.

The amount of corrosion products necessary to fill the porous zone can be written as:

$$w_{porous} = \pi \cdot \rho_{rust} \cdot d_{por} \cdot d_r \quad (39)$$

Where: w_{porous} = amount of corrosion product necessary to fill the porous zone, d_r= initial diameter of the reinforcement, ρ_{rust} = density of corrosion products, d_{por} = thickness of equivalent zone with porosity 1.

The concrete will expand after the porous zone around the rebar has been filled with corrosive products. The amount of expansion of the concrete without causing any cracking is modelled by:

$$w_{expan} = \rho_{rust} \cdot \pi \cdot \left(d_r + 2 \cdot d_{por}\right) \cdot d_{crit} \quad (40)$$

Where: d_{crit} = the thickness of expansion at crack initiation

Liu and Weyers have estimated the thickness of the expansive zone at crack initiation by assuming that the concrete is a homogeneous material [Liu 1998]. This expansive zone can be approximated by a thick-walled concrete cylinder [Thoft-Christensen 2000] (figure 19).

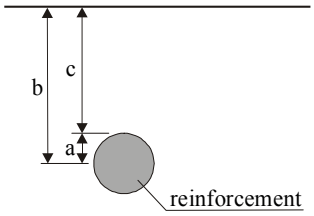

Figure 19: Input parameters of equation 41

The approximating value of the critical expansion is:

$$d_{crit} = \frac{c \cdot f_t^{'}}{E_{cf}} \cdot \left(\frac{a_{por}{}^2 + b^2}{b^2 - a_{por}{}^2} + \upsilon_c \right) \quad (41)$$

Where: d_{crit} = the thickness of the expansive zone at crack initiation, c = cover depth, f_t = tensile strength of concrete, E_{cf} = effective elastic modulus of concrete, a_{por} = inner radius of equivalent porous zone, b = outer radius of porous zone plus cover depth, ν_c = Poisson's ratio of concrete.

$$a_{por} = \frac{d_r + 2 \cdot d_{por}}{2} \quad (42)$$

$$b = c + a_{por} \quad (43)$$

Finally, the amount of corrosion products that causes actual cracking of concrete is calculated by:

$$w_{steel} = \frac{\rho_{rust}}{\rho_{steel}} \cdot m_{steel} \quad (44)$$

Where: ρ_{steel} = density of steel, m_{steel} = mass of corroded steel.

The critical amount of rust products to cause cracking (w_{crit}) is proportional to the amount of corroded steel (m_{steel}). The constant that relates these parameters depends on the type of corrosion products. Based on frequently observed corrosion products, the factor of proportionality is calculated as $m_{steel} = 0.57 \cdot w_{crit}$ [Liu 1998]. Therefore, equation 38 can be rewritten as:

$$w_{crit} = \frac{\rho_{steel}}{\rho_{steel} - 0.57 \cdot \rho_{rust}} \cdot \left(w_{porous} + w_{\exp an} \right) \quad (45)$$

The rate of formation of rust as a function of time t (years) from corrosion initiation can be written as:

$$\frac{dw_{rust}(t)}{dt} = k_{rust}(t) \cdot \frac{1}{w_{rust}(t)} \quad (46)$$

Where: w_{rust} = amount of rust products, k_{rust} = rate of rust production.

From this results equation 47 follows

$$\Delta t_{crack} = \frac{w_{crit}{}^2}{2 \cdot k_{rust}} = \frac{w_{crit}{}^2}{2 \cdot 0.383 \cdot 10^{-3} \cdot \phi \cdot i_{corr}} \quad (47)$$

Where: i_{corr} = corrosion current

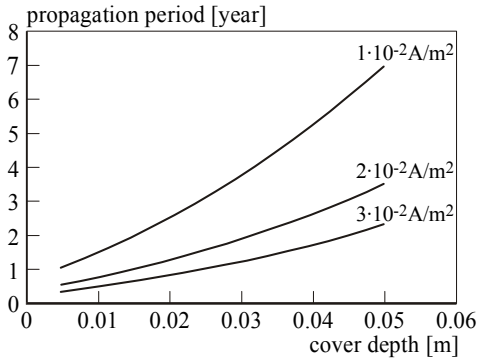

Figure 20: Duration of the propagation phase as a function of cover depth and corrosion current density

In this study, the equations above are used to determine the time from initiation of corrosion until cracking (i.e. duration of the propagation phase). To get an impression of the duration of the propagation phase in different conditions, corrosion current density cover depth and the duration of the propagation phase is displayed in figure 20 and 21. The input parameters are tabulated in table 12.

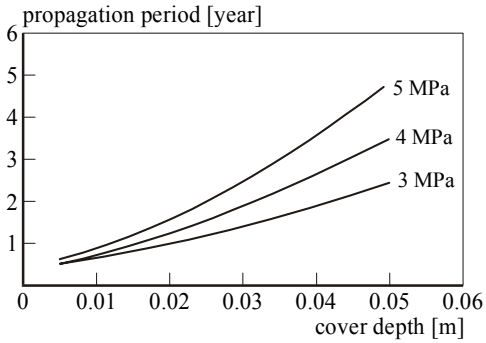

Figure 21: Duration of the propagation phase as a function of cover depth and concrete tensile strength

Experimental data showed that cracks joined together to create longitudinal cracking at crack widths of about 0.4 to 0.5mm [Vu 2002]. At this stage, it is likely that spalling would occur in a real slab with transverse reinforcement, especially if loads are applied to the structure.

Oxygen availability at the cathode and electrical resistivity are factors that affect the rate of corrosion. Corrosion is stopped if the concrete contains too little moisture because of the low permeability of the concrete, while the diffusion of oxygen through the concrete is reduced at relative high humidity. The threshold values for corrosion depend on a number of factors, many of which are still not well understood. However, the optimum relative humidity for corrosion is observed at 70-85% [Carrier 1975, Gardiner 2002, González 1993, Neville 1995, Novak 2001, Yalçyn 1996].

Table 12: Input parameters propagation phase [after: Thoft-Christensen 2000]

parameter	symb.	mean value	unit
diameter reinforcement	∅	16	mm
modulus of elasticity	E_{cf}	10	GPa
elastic modulus	f_t	4.0	MPa
rate of corrosion	i_{corr}	2	10^{-2} A/m^2
thickness of eq. zone	d_{por}	12.5	μm
poisson's ratio	ν_c	0.25	-
density of corr. product	ρ_{rust}	3600	kg/m^3
density of steel	ρ_{steel}	7800	kg/m^3

Research at a series of 11 bridges in Denmark and Sweden showed that the relative humidity is higher than 75% and builds up with increasing depth [Lindvall 2000]. At these 11 bridges no difference was observed between sheltered and unsheltered parts of the bridges or summer and winter season. Therefore, in this thesis, it is assumed that oxygen and moisture availability do not limit the corrosion of reinforcement in concrete bridges.

3.5. Discussion

This chapter described modelling of damage to concrete structures due to reinforcement corrosion caused by chloride ingress or carbonation. The models used might not be the most sophisticated models that are available at the moment, but in this thesis robust models are preferred. Robust models are preferred since these models consider the most important input parameters.

In this thesis it is assumed that diffusion gives an accurate description of ingress of chlorides and carbon dioxide. The question is to what extent the mathematical models comply with reality. Even though other transport mechanisms transfer chlorides as well, diffusion is demonstrated as the leading mechanism of transport of chlorides and carbon dioxide.

Since the outcome of the models is as good as the input allows, the estimation of the values of the input parameters should be determined with great care. In the next two chapters, values are suggested for the input parameters that are discussed in this chapter, based on extensive research.

4. Material properties

4.1. Introduction

In the early years of forecasting deterioration, the predicted bridge condition was entirely based on the judgment of past bridge maintenance trends. However, extrapolating this experience to predict a future condition is questionable since most concrete bridges are relative young of age.

Over the last decades, models have become available to simulate changes in bridge condition. A number of these models were given in the previous chapter. The knowledge of these models, however, by far exceeds the knowledge of the values of the parameters used in the models. An important precondition for predicting future deterioration is choosing the right input values, because the results of any prediction are as good as the input allows.

This chapter will give values for input parameters for the deterioration models that have been derived from realistic and accurate data representative for the Dutch stock of concrete highway bridges. Based on the input parameters given in this chapter, a simulation and prediction of deterioration will be carried out in chapter 6.

Deterioration of concrete structures usually starts at an isolated spot and expands over time. An example of the spatial variability of deterioration is given in figure 22 where different stages of corrosion are shown (sound concrete, first crack and finally spalling).

Figure 22: Observed variability of deterioration (Barcelona, Spain, photo by author)

There is a range of sources that contribute to the uncertainties that are encountered in modeling and predicting the development of the process of deterioration. These may include environmental conditions, material heterogeneity, execution (workmanship) and human errors, as is outlined in figure 23 (where: D = diffusion coefficient, c_{cl} = surface chloride concentration, y_{cl} = chloride ingress, c = cover depth). The inherent

stochastic behaviour of the deterioration processes is discussed in this chapter and chapter 6.

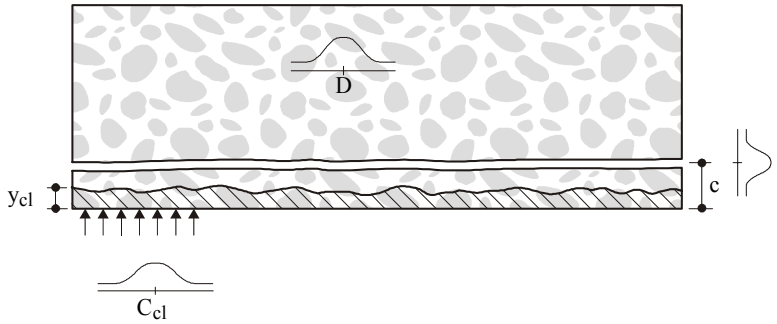

Figure 23: Sources of variability in deterioration processes

4.2. Critical chloride concentration

The critical or threshold chloride concentration was extensively discussed in section 3.2.2. On the basis of the literature review, that is listed in table 7 (p. 29), it is suggested that the most likely mean value of the threshold value is 0.50% by mass of binder. This section will suggest a value of the standard deviation for the threshold concentration. The standard deviation is derived from both samples taken from structures and a laboratory study.

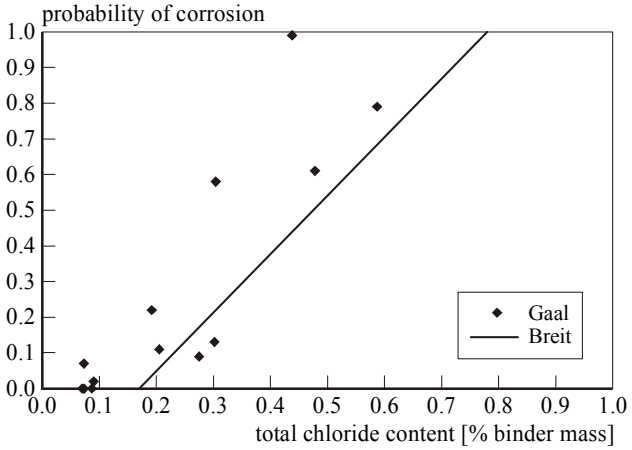

Figure 24: Chloride concentration at reinforcement as a function of the probability of corrosion (corrosion potential<-350mV) [Breit 1997, Gaal 2001a]

To determine the critical chloride concentration for concrete structures, inspection results from a survey in Scotland are analysed. On the A82 trunk road in Scotland, twelve concrete bridges were selected from which the year of construction ranged

from 1930 until 1932. Since the mid 1960s these bridges were exposed to de-icing salts. Between 1981 and 1983 the bridges were extensively examined with respect to cover depth, chloride concentration and corrosion potential [Vassie 1986]. From these results both the chloride concentration at the reinforcement and the corresponding probability if the corrosion potential is more negative than –350 mV ($Cu/CuSO_4$) are determined. A comprehensive description of the half-cell or corrosion potential measurement can be found in appendix B. The results from the bridges in Scotland are in agreement with the literature review in table 7, but indicate a slightly higher probability of corrosion for structures compared to laboratory specimens. The increased probability of initiation of corrosion for structures compared to laboratory specimens could be caused by, among other things, the preparation of the laboratory specimens, as was discussed in section 3.2.2.2. The results for the bridges in Scotland and results obtained under laboratory conditions are plotted in figure 24. Because of the limited number of results from the bridges in Scotland, the earlier assumed value of 0.5% is maintained. From the laboratory results of Breit a standard deviation of 0.2% by mass of binder is suggested and a normal distribution is assumed [Breit 1997].

4.3. Ageing of concrete

The ageing coefficient is usually derived from cores that are taken from structures that differ in age [Bamforth 1999, Gehlen 2000, Helland 2001]. Of each structure the diffusion coefficient is derived from chloride profiles. Subsequently the ageing coefficient is obtained by comparing the diffusion coefficients of all the structures that differ in age. However, over time the original concrete quality has changed which will influence the diffusion coefficient. In this section the ageing coefficient is derived from specimens that are made of the same type of cement and have the same mixture, but differ in the period of curing before exposure to chlorides.

In 1976, the Dutch foundation for Materials Research in the Sea initiated a long-term programme of concrete submerged in deep-sea water [de Lange 1984, Polder 1995]. Over 250 specimens were cured for 1, 4 or 14 weeks before they were exposed to seawater. Subsequently the specimens were placed 5 or 100 meters below sea level for 2, 8 and 16 years. Because of the different periods of curing prior to exposure to chlorides, this set of data is suitable to derive the ageing coefficient by using equation 23 (p. 37).

From the profiles obtained, the surface chloride concentrations and chloride diffusion coefficients are derived by fitting Fick's 2nd law of diffusion (equation 23) to the observed chloride profiles using the least square method. A detailed description of the method to derive the diffusion coefficient and surface chloride concentration from the cores is described in section 4.4.3. If the ageing coefficient, surface chloride concentration and diffusion coefficient are unknown, there are an infinite number of solutions when a single chloride profile is fitted to Fick's second law of diffusion. By, simultaneously, fitting two chloride profiles of e.g. 4 and 14 weeks of curing, a unique solution is found. The result from this analysis is the ageing coefficient, the diffusion

coefficient and two surface chloride concentrations for each curing period. A different surface chloride concentration is found for each period of curing; this corresponds to findings of other authors [Bamforth 1993]. The results that are obtained by simultaneously fitting three chloride profiles, with different periods of curing, are plotted in figure 25 and tabulated in table 13.

Table 13: Determined ageing coefficient and other parameters (cement type: CEM III B)

Exposure [months]	**Depth [m]**	**Diff coeff[10] [m²/s]**	**Ageing coeff. [-]**	**$C_{cl;s}$ curing 1 week**	**$C_{cl;s}$ curing 4 weeks**	**$C_{cl;s}$ curing 14 weeks**
89/98	100	$3{,}65 \cdot 10^{-12}$	0.40	2.84	2.03	1.30
96	5	$4{,}51 \cdot 10^{-12}$	0.52	2.88	2.34	1.38
23/32	100	$9{,}18 \cdot 10^{-12}$	0.58	2.11	1.27	1.37
26	5	$3{,}76 \cdot 10^{-12}$	0.31	2.20	1.48	1.30
Average			0.45			

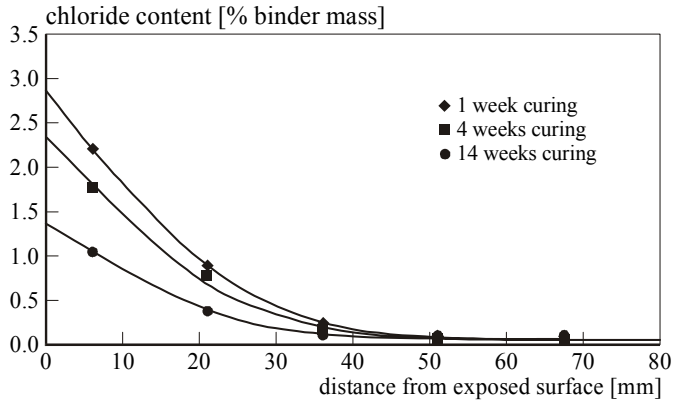

Figure 25: Chloride profiles obtained form specimen submerged in North Sea

The ageing coefficient that is found from the specimens that have been submerged in the North Sea is in close agreement with the results from Gehlen (table 14). To determine the deterioration of concrete bridges, the standard deviation found by Gehlen will be used.

[10] Reference diffusion coefficient at an age of 28 days.

Table 14: Ageing coefficient (n)

Author	Cement	Mean value	Stand. dev.
Gehlen 2000	CEM I	0.30	0.12
Gehlen 2000	CEM III/B	0.45	0.20
Polder 2003	CEM III/B	0.48	0.07
this work	CEM III/B	0.45	-

4.4. Chloride diffusion coefficient

Today's road authorities require bridge structures with an expected lifetime of 80 to 100 years. In Europe the average age of bridge structures is about 35 years. Experience with older structures is limited. To overcome this lack of experience, numerical models are used to predict future deterioration. Whereas the predicted lifetime should be of the order of 100 years, the input parameters used are derived from specimens that are mostly less than 1 year old [e.g. Brodersen 1982].

Published data of the diffusion coefficient of concrete are often based on small-scale specimens made from cement paste or mortar that are only exposed to chloride during several months. The exposure period is not the only limitation of laboratory specimens. Structures like bridges are in a permanent non-steady state with respect to the chloride exposure, which is far from laboratory conditions.

Figure 26: Taking cores from a bridge column (photo by author)

To overcome the relatively short exposure period and non-steady state environment in this study the diffusion coefficients are derived from structures that are up to 62 years of age. To recognize the difference in construction practice over the last decades, a distinction is made between three age groups and two cement types. The goal of this paragraph is to derive a coefficient of chloride diffusion and a surface chloride concentration from bridges that are up to 62 years old.

4.4.1. Examined bridges

The Dutch Ministry of Transport gave permission to take over 150 cores from a series of bridges, because those bridges were bound to be demolished (figure 26). Most bridges were located in or over highway 16, which is situated in the southern part of the Netherlands. In this study, 100 cores (∅=50mm) are analysed to quantify the chloride ingress and 50 cores (∅=75mm) are analysed to determine the compressive and tensile strength. These structures were owned and maintained by the Dutch Ministry of Transport. The examined bridges are tabulated in table 15.

Table 15: Examined bridges

Name	**constructed**	**cores drilled**
Landscheidingsweg	1989	Apr. 08, 2002
Riga	1987	Apr. 14, 2002
Klein Overveld	1967	Aug. 19, 2002
Dirk de Botsdijk	1967	June 05, 2002
Verlatendijk	1965	Aug. 19, 2002
Muntendam	1964	Feb. 08, 2002
Reevliet	1963	June 05, 2002
Langeweg	1940	Aug. 23, 2002
Brug over de Mark	1940	Aug. 23, 2002

Nearly all cores were taken from the structures in sets of two cores directly next to each other, as indicated in figure 27. Subsequently, each core was sliced into discs with a net thickness of 6 millimetres, to obtain a chloride profile. Next the set of chloride profiles is put together to a single chloride profile, as is shown in figure 29. With this method detailed information on the chloride concentrations is gathered for each tested location of the structure. For a number of sets, the chloride profiles could not be put together to a single profile because of differences in the chloride levels. No clear reason could be identified for the differences in chloride concentration for cores that were only a few centimetres apart.

When cores are taken from a structure and subsequently sliced into discs, water is used to cool the saw blade. One could argue that the outcome of the test is influenced by the method since chlorides might be washed out when the cores are drilled and sawn.

In a study about this phenomenon, concrete of both portland cement and blast furnace slag cement was tested at samples with an added chloride concentration of 0.2, 0.1 and 0.05% by mass of binder. To examine the influence of cooling water, samples were obtained by both crushing test cubes, and coring and subsequent slicing of the cores taken from the test cubes. The cores were drilled and sliced with the same diameter and in the same way as is done at structures. The chloride concentration was determined by the same method as is used to determine the chloride concentration of

the specimens in this thesis, the Volhard method. The found chloride levels deviated at most 0.01% by mass of binder from the intermixed amount of chlorides of 0.2, 0.1 and 0.05% by mass of binder. These results indicate that the water that is used to cool the drill and saw blade does not wash out the chlorides [Wardenier 1996].

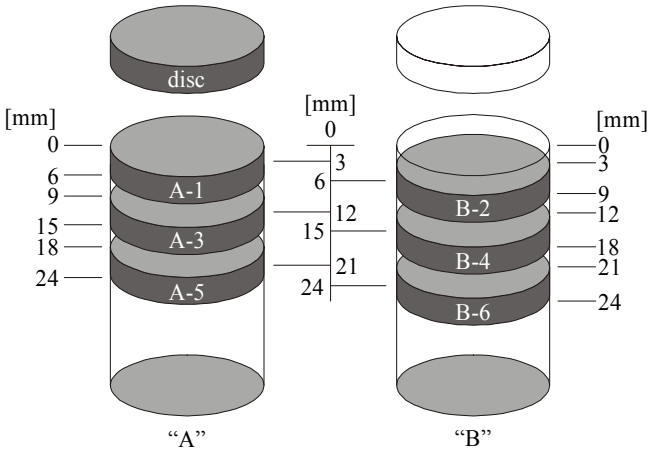

Figure 27: Discs from a set of cores [after: Taheri 1998]

From the cores that were taken from the bridges that are listed in table 15 it was learned that approximately 30% of the surface area of a bridge could be considered as sheltered surface, and approximately 40% of the concrete was made blast furnace slag cement.

4.4.2. Slag content of cores

The slag content of blast furnace slag blended cements strongly influences the diffusion coefficient [Brodersen 1982]. An arbitrary conclusion from figure 28 is that the slag content should be over 40% to result in a significant reduction of the diffusion coefficient. In the study of Brodersen, the mortar discs were exposed to chlorides in a steady state diffusion test, after 28 days of wet storage curing. The discs, with a thickness of 10mm, were exposed to a chloride solution of 175gr sodium chloride per liter for 15 weeks. The diffusion coefficient was determined from the amount of chlorides that passed through the disc. Since the results that are plotted in figure 28, are derived from laboratory tests, the conclusion above is only true if similar curing took place.

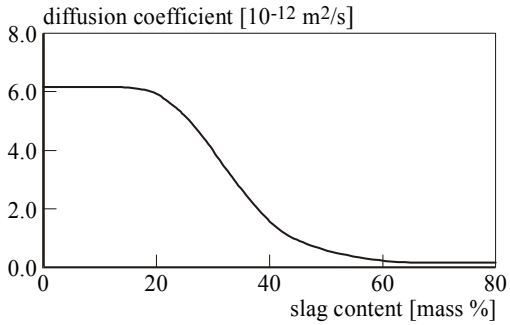

Figure 28: Diffusion coefficient as a function of the slag content [after: Brodersen 1982]

In order to be able to group the diffusion coefficients, which were derived from the tested cores by cement type, the slag content should be established. The slag contents of the examined bridges, which are listed in table 15, could not be found in the design specifications of the Dutch Ministry of Transport. The presence of a certain amount of slag in the concrete is inferred from the dark colour of the core. (The physical phenomenon that causes the blue discolouration is discussed in appendix G). To determine the slag content of the blue coloured cores, thin-sections have been made of 10 cores. The slag content is determined by optical microscopy, tabulated in table 16. This table lists both the observed slag volume-%, as observed and the slag mass-% as determined from the densities of slag and cement hydrates. The drawback of the visual method is that the finest slag particles are not visible on the thin sections. Therefore, the results from table 16 give a lower boundary of the true slag content.

Table 16: Established slag content of cores from microscopy

bridge	**year**	**sample**	**slag % by volume**		**slag % by mass**
			range	mean	
Reevliet	1963	RC093	30 – 45	35	33
		RC036	20 – 30	25	24
Mark	1940	BMC066	30 – 50	40	38
		BMC062	30 – 50	40	38
Langeweg	1940	LGC07	10 – 25	16	15
		LGC08	10 – 20	15	14
Verlatendijk	1965	VC16	45 – 60	52	50
Klein Overveld	1967	KC74	40 – 60	50	48
		KC95	25 – 35	31	30
Meeden	1964	MC02	45 – 60	50	48

The thin sections indicate low slag content for the bridges Reevliet and Langeweg. The other bridges show slag contents that will presumably result in a substantially reduced diffusion coefficient.

4.4.3. Chloride profiles

Despite the range of possible transport mechanisms, chloride ingress of concrete is analysed using the Fick's second law of diffusion. From the chloride profiles both the effective surface chloride concentrations and effective chloride diffusion coefficients are derived with curve fitting to Fick's 2nd law of diffusion (appendix A).

The chloride threshold levels are best presented as total chloride concentrations expressed relative to the mass of cement [Glass 1997]. Also the diffusion coefficient of acid-soluble chloride concentration in concrete shows a strong correlation of proportionality with the diffusion coefficient of free chloride concentration in the pore fluid [Mangat 1994b]. Therefore, each disc was analysed to determine the chloride concentration as a proportion of the binder content.

To determine the chloride and calcium content the following procedure was followed [Gulikers 1996]. Each disc was dried at a temperature of 105˚C until the weight of the disc remained constant. Next, the discs were ground and treated with boiling nitric acid to extract the acid soluble chloride from the cement hydrates. Carbon dioxide and hydrogen sulphide (H_2S) escaped from the mixture during boiling.

The next step is to separate the non-dissolved gravel and sand from the dissolved chlorides and cement hydrates by filtering. It is assumed that the hydrated cement weight is equal to the acid soluble part of the powder. This is only true if the sand and gravel do not dissolve in acid, which is not true for calcareous aggregates. The assumption that both gravel and sand are insoluble in nitric acid is valid for nearly all Dutch aggregates as they consist almost of quartz only.

The hydrated cement is separated from the aggregates to determine the ratio of chloride to cement. However, the hydrated cement contains non-evaporable water. In this analysis a non-evaporable water content of 20% by weight of cement was assumed to convert the reported chloride concentrations of the hydrated cement mortars to a percentage by original weight of cement [Wardenier 1995]. The amount of non-evaporable water depends on the clinker composition; Bentz reported a non-evaporable water content of 22 and 23% [Bentz 1995].

A number of methods are available to determine the chloride concentration of the filtrate. The most frequently used methods are determination by the chloride selective electrode or Volhard titration. The latter method has proven to be the most reliable of both methods [Johnson 1982] and has been selected to be used in this study. To determine the chloride concentration of the dissolved materials an amount of 10.0 ml of silver nitrate and 3.0 ml of ferric ammonium sulphate was added as an indicator. To determine the amount of chloride in the sample, ammoniumthiocyanate (NH_4SCN) was added to the sample until the colour changed. The reaction to determine the chloride concentration does not make a distinction between chloride, sulphide, iodide and

bromide. However, sulphide did already escape and iodide and bromide are in general not present in concrete.

The results of the discs gave the chloride concentration relative to the cement content for the examined location [Wardenier 2003]. From the obtained profiles the surface chloride concentrations and chloride diffusion coefficients are derived by fitting Fick's 2nd law of diffusion to the observed chloride concentration with the least square method [Nordtest 1995]. To derive the effective diffusion coefficient and surface chloride concentrations, the chloride profiles are fitted to equation 23 by using the parameters mentioned in this thesis. Deviations from Fickian behaviour are identified in the near surface region as is shown in figure 29. Therefore the coefficient of diffusion and surface chloride concentration are derived from the observed chloride concentrations, omitting the near surface zone.

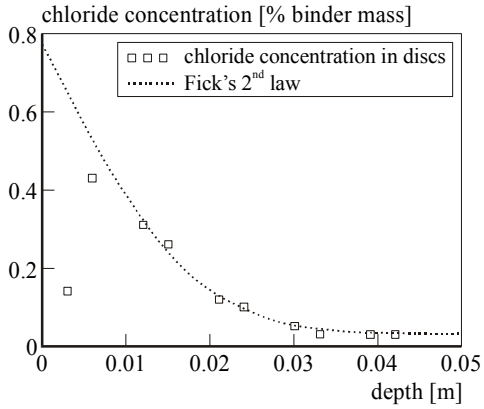

Figure 29: Chloride profile and model of 35-year-old bridge

For partially saturated mortar specimens under laboratory conditions, similar deviations from Fick's 2nd law of diffusion have been observed. When similar mortar specimens were vacuum saturated, the chloride profiles did not deviate from Fick's law [Nielsen 2003].

The physical processes that result in the deviation of the chloride concentration in the near surface region from ideal Fickian behaviour are not completely understood. To overcome the deviation from Fick's law, it is suggested to neglect approximately the first 10mm of the cover depth, and assume a surface chloride concentration at a depth of about 10mm [Andrade 2000]. In this study the deviations of the determined chloride concentrations from Fick's second law is registered. Figure 30, indicates the number of the first disc that complies with Fick's second law. Therefore considering the results of the individual chloride profile analysis that are displayed in figure 30, the reduction of the cover depth by a fixed distance is not generally applicable.

Most of the pairs of cores, as displayed in figure 27, showed small differences between the individual chloride profiles. Therefore, the diffusion coefficient and surface chloride concentration were obtained from the set of cores as is displayed in figure 29. If considerable differences were observed between the sets, each individual chloride profile was analysed to obtain the diffusion coefficient and surface chloride concentration.

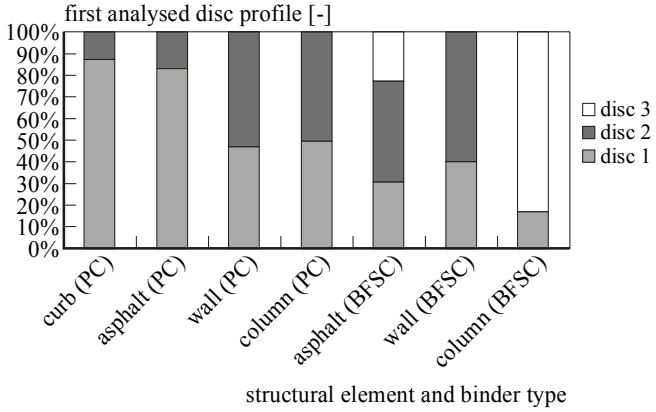

Figure 30: Compliance of discs of core to Fick's 2nd law as a function of structural element and binder type[11] (The structural element 'asphalt' refers to concrete underneath the asphalt pavement on the bridge.)

Concrete of structural elements that are sheltered from moisture, i.e. supporting wall or column, show a stronger deviation from Fick's second law of diffusion than concrete that is regularly exposed to moisture e.g. a curb. Also the binder type has a strong influence on the deviation from Fick's second law of diffusion. A first conclusion is that carbonation also has an influence on the chloride concentration of the outer zones since blast furnace slag cement shows more carbonation than portland cement.

4.4.4. Derived diffusion coefficients

In this study, the chloride diffusion coefficient is determined by fitting the solution of Fick's second law (equation 23) to the chloride profiles. The constants in equation 23 are the start of the application of de-icing agent and the ageing coefficient. From literature it is assumed that the application of de-icing salts started in 1965, as is discussed in section 3.2.3.4. Together with ageing coefficients from table 14; the reference diffusion coefficient at an age of 28 days was determined. The diffusion coefficients that are derived from each set of cores or single core is shown in figure 31.

[11] I.e. 75% of the profiles taken from curbs fully complied with Fick's second law, 25% of the chloride profiles were analysed omitting the first disc, i.e. the chloride profile fitted to Fick's law starting from the second disc.

From the derived diffusion coefficients it was observed that three groups could be distinguished, 1940s, 1960s and 1980s. From each of these three groups the average diffusion coefficient is determined and tabulated in table 17. It was chosen not to subdivide these results by the location where the cores were taken from the structure, since it did not reduce the scatter.

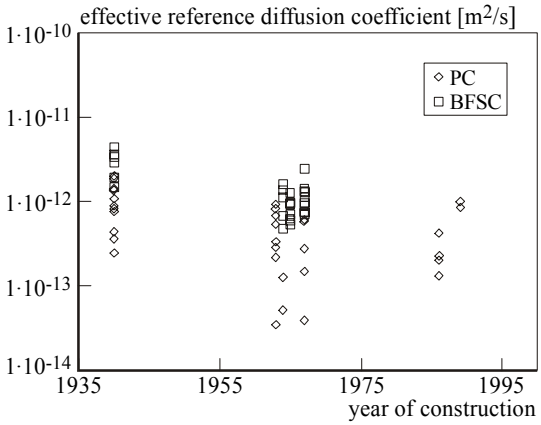

Figure 31: Effective diffusion coefficient at t_0 [Gaal 2003b]

The variability of the derived diffusion coefficients is modelled with a probability distribution having a mean value and standard deviation. The derived reference diffusion coefficient will be modelled as a lognormal distribution since this type of distribution appeared to agree with the distribution of the derived values. This choice is evaluated by visually comparing the cumulative distribution of the derived diffusion coefficient with the assumed lognormal distribution (figure 32).

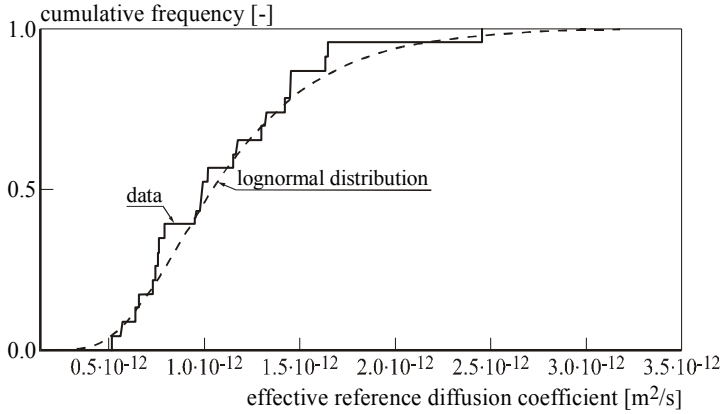

Figure 32: Observed and modelled diffusion coefficient (BFSC - 1960s)

The results are subdivided by cement type since it is generally accepted that blast furnace slag cement shows a higher resistance to chloride ingress than portland cement.

A laboratory study showed that the diffusion coefficient of concrete made of blast furnace slag cement depends on the degree of replacement of portland cement by blast furnace slag. The diffusion coefficient of a cement paste where 80% of the portland cement is replaced by blast furnace slag gives a 100-fold reduction of the diffusion coefficient. If the replacement by blast furnace slag is below 30-40%, there is hardly any effect of the blast furnace slag, as is displayed in figure 28 [Brodersen 1982 (mortar specimen)]. Other research projects found that cement paste made of blast furnace slag cement (50 to 65% slag) shows a 25 to 50% reduction of the diffusion coefficient compared to portland cement [Ellis 1991 (concrete specimen)]. However, in case of bad curing blast furnace slag cement showed a similar diffusion coefficient as portland cement [Wierig 1965 (mortar specimen)]. The studies that indicated the better performance of blast furnace slag cement, all examined mortar of concrete in laboratory conditions and moist or submerged curing conditions.

Table 17: Effective reference diffusion coefficients from Dutch highways bridges

period	**effective reference diffusion coefficient [10^{-12} m^2/s]**			
	binder	mean	st. dev.	coef. of var.
1940s	PC	1.039	0.531	0.51
1960s	PC	0.396	0.291	0.73
1980s	PC	0.478	0.372	0.78
1940s	BFSC	2.824	1.178	0.42
1960s	BFSC	1.117	0.532	0.48
1980s	BFSC	-	-	-

The results presented in figure 31 indicate that the blast furnace slag cement, that was used at the examined bridges, does not show the suggested lower chloride diffusion coefficient compared to portland cement. It is most likely that blast furnace slag cement similar to type CEM III/A was used at the examined bridges. The reported reduced diffusion coefficients for blast furnace slag cement are observed for mortar specimens. It is discussed in section 3.2.1 that the pore structure of paste development in the presence of aggregate is quite different from that of neat mortar specimen.

Using mercury intrusion porosimetry, it was shown that the pore structure of the paste developed in the presence of aggregate particle is quite different from that of the neat cement paste. More in detail, a higher porosity, together with larger pores and a higher volume fraction of calcium hydroxides is observed around each aggregate or sand grain, which has a decisive influence on the diffusion coefficient. When the transition zones overlap, a continuous path is created that leads to a low resistance to permeation of chlorides. This layer, with a thickness of approximately 50μm, is called the interfacial transition zone [Barnes 1979, Halamickova 1995, Scrivener 1989]. Because the average particle size of the cement is much smaller than the average particle size of the sand, the thickness of the interfacial zone is determined by the cement particle size [Garboczi 1995].

Also the curing conditions in a laboratory are quite different from those at a construction site. Curing of concrete on site may have been poor or at least less than optimal. Personal communication with inspectors of the Dutch Ministry of Transport indicated that the curing of blast furnace slag cement was not as it should be, during the 1970s. The negative effect of bad curing on the diffusion coefficient is found by numerous studies [Bonavetti 2000, Khatib 2002, Mangat 1999, Patel 1985]. A diffusion coefficient of blast furnace slag cement that is about 50% lower than OPC was reported [Bamforth 1993].

The deviations between the coefficients observed from structures and laboratory data could be caused by the reasons outlined above.

A similar study to obtain diffusion coefficients from concrete of highway bridges was carried out in Sweden and Denmark [Lindvall, 2000]. These coefficients are shown in figure 33 together with the results that are obtained from Dutch highway bridges. The diffusion coefficients from Sweden and Denmark are determined from chloride profiles under the assumption that the diffusion coefficient is constant over time. Therefore the diffusion coefficients from the Dutch structures were derived again with the same assumption as in Sweden and Denmark,

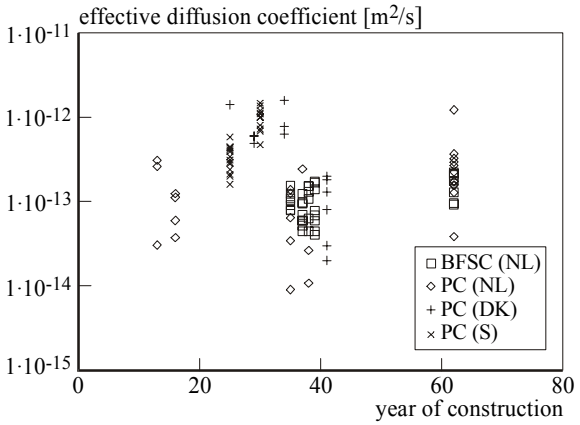

Figure 33: Comparison effective diffusion coefficients [after: Gaal 2003b, Lindvall 2000]

The results from the Dutch bridges indicate that the resistance to chloride ingress is approximately five times better than is observed for bridges in Denmark and Sweden. A clear explanation of the differences between the bridges in the mentioned countries is not available.

4.5. Surface chloride concentration

Like the diffusion coefficient, the surface chloride concentration is not a measurable unit but a proportionality constant in Fick's laws. When analyzing the surface chloride concentration, it should be taken into consideration that the exposure to chloride only occurs during the winter season, and depends on a number of material and environmental parameters like [Bamforth 1993]:

- sorptivity of the concrete if not saturated when firstly exposed to chlorides;
- cement content;
- period of curing.

Therefore the concentration is referred to as effective surface chloride concentration.
Together with the diffusion coefficient, the surface chloride concentration is derived from fitting Fick's 2nd law of diffusion to an obtained chloride profile in a concrete sample. To determine the surface chloride concentration of Dutch highway bridges that are exposed to de-icing salt, over 100 cores were taken from 9 bridges that were constructed between 1940 and 1986. To get a representative set of data, the locations of the cores were chosen in such a way that concrete made of both blast furnace slag cement and portland cement was taken, and that structural members like column, supporting wall, curb and deck (underneath asphalt) were tested. The results of the analysis are plotted in figure 34.

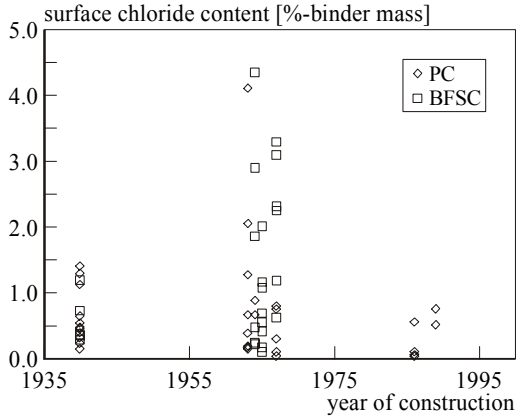

Figure 34: Surface chloride concentration derived from chloride profiles

The surface chloride concentrations in figure 34 show a wide scatter. It is often suggested that the location influences the surface chloride concentration. However, when the results are grouped by structural member, there is still a wide scatter.

The surface chloride concentrations that are derived from the cores taken from the investigated Dutch bridges are tabulated in table 18. Similar to the diffusion coefficients, the mean value and standard deviation is calculated for the three groups that could be distinguished in the determined results for both cement types.

The derived surface chloride concentrations are entered, as input parameters, into the method to predict deterioration. The observed surface chloride concentration will be modelled as a lognormal distribution. This choice is supported by the good agreement of the cumulative distribution of the observed surface chloride concentration with the assumed lognormal distribution (figure 35).

Table 18: Average surface chloride concentration from Dutch highways

period	**surface chloride concentration [%-mass of binder]**			
	binder	mean	st. dev.	coef. of var.
1940s	PC	0.59	0.40	0.68
1960s	PC	0.80	1.03	1.28
1980s	PC	0.34	0.31	0.90
1940s	BFSC	0.59	0.38	0.66
1960s	BFSC	1.45	1.16	0.80
1980s	BFSC	-	-	-

The increased surface chloride concentration of blast furnace slag cement concrete compared to ordinary portland cement concrete is also observed for structures in Great Britain [Bamforth 1993]. The observed surface chloride levels for British bridges are up to 40% higher for blended cements compared to pure portland cement concretes.

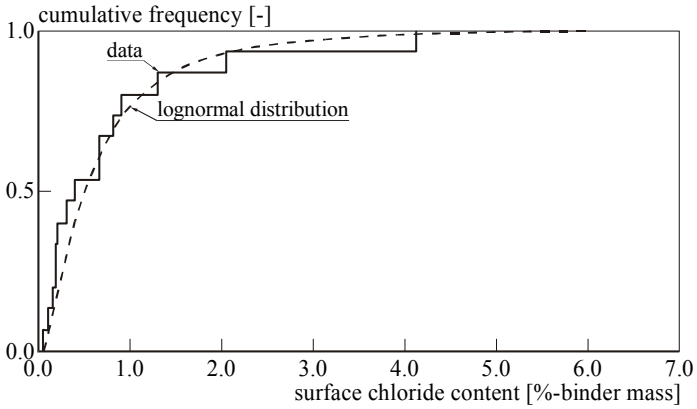

Figure 35: Observed surface chloride concentration and chosen distribution (PC - 1960s)

Analysis of all the cores learned that the mean value of the initial chloride concentration is 0.03% by mass of cement, the coefficient of variation is assumed to be 0.33.

4.6. Compressive and tensile strength

The tensile strength is one of the input parameters to determine the time until the first cracks will appear after corrosion of the reinforcement has initiated. There are three kinds of tests available to determine the tensile strength of concrete; the direct tensile test, the bending test and the splitting tensile test. The difficulty with the bending test is to derive the tensile strength from a bending load. Therefore the tensile strength of the test samples was determined by both the direct tensile and splitting tensile test. The results of the obtained tensile strengths as a function of the compressive strength are shown in figure 36.

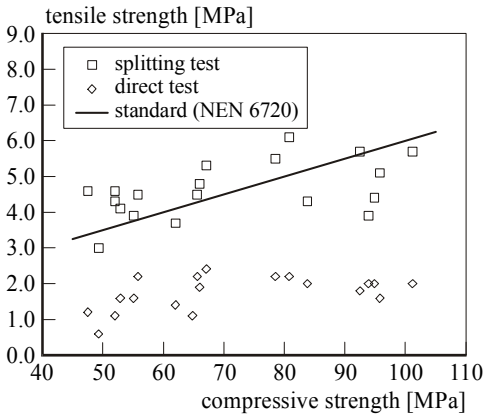

Figure 36: Tensile strength

The results of the tensile splitting strength correspond more or less with correlation expressed in the Dutch standard (NEN 6720) [NNI 1995b]:

$$f_{t;spl} = 1 + 0.05 f_c' \qquad (48)$$

where: $f_{t;spl}$ = tensile strength (split test), f_c' = compressive strength (cube).

However, the tensile strength is overestimated at relatively high compressive strengths and the other way around for low compressive strengths. NEN 6720 states that the tensile strengths that result from the uniaxial tensile test are 10% less than the tensile strengths that result from the splitting test. This ratio between the tensile strengths (splitting and direct) is not found in this study. Low uniaxial tensile strengths have also been found in other studies [McNeely 1963, Siemes 2002].

The splitting tensile strength is used in this study to determine the duration of the propagation phase since corrosion of the reinforcement will result in a crack at a specific location.

4.7. Carbonation

In this section, the carbonation model of CEB has been compared with measured depths of carbonation. The data is obtained from inspection reports of about 80 bridges in the Netherlands. In total, the depth of carbonation was determined at more than 1100 locations.
In figure 37, a comparison is made between the inspection data and the prediction result of the CEB-carbonation model. The small dots represent the inspection data of 80 Dutch bridges. The dashed line represents the average carbonation depth of the inspections. The inspection data show a large scatter. The scatter was not reduced if the data was divided into groups of structural member types. Larger carbonation depths occur if the structural member is sheltered from weather influences. This information could not be gathered from the inspection data since the test locations were not sufficiently specified. More detailed information is available from the Kaag Bridge [Rijkswaterstaat 2000]. The results from sheltered and unsheltered locations are shown respectively with squares and solids. The bottom side of the deck, columns and supporting walls are regarded as sheltered structural members. The unsheltered structural members are the topside of the deck and the supporting wall that is located at leaking bridge deck expansion joints or blocked drains.

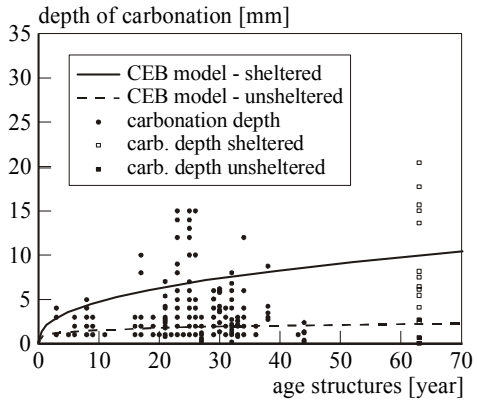

Figure 37: Carbonation, models versus. data for 80 bridges in the Netherlands

In figure 37 both the results of the CEB-model (equation 35) and the actual data from 80 bridges are presented. The model seems to describe the reality rather well, when the input parameters for the unsheltered environment were used (table 19). The data however were not verified at the location of the samples.

It appears that the theory and results obtained with the carbonation model agree reasonably well with the inspection data.

Table 19: Parameters used to model data in figure 37

Variable	symbol	value	unit	cov	distribution
parameter micro climate unsheltered (moisture content)	ψ_1	0.30	-	-	-
parameter micro climate sheltered (moisture content)	ψ_1	0.40	-	-	-
parameter curing condition	ψ_2	1.00	-	-	-
parameter water separation	ψ_3	1.20	-	-	-
parameter Micro climate sheltered	ψ	0.10	-	-	-
parameter Micro climate unsheltered	ψ	0.30	-	-	-
carbon dioxide concentration in the atmosphere	ΔC_{cb}	0.0005	kg CO_2/m^3	0.1	normal
reference period $D_{cb;eff}$	t_0	0.0767	year	-	-
effective CO_2 diffusion coefficient	D_{ch}	2.0	m^2/year	0.1	normal
cement content	C_c	280	kg/m^3	0.1	normal
CaO content in cement	C_{CaO}	0.65	-	0.1	normal
degree of hydration	α_h	0.75	-	0.1	normal

4.8. Discussion

Concrete quality results from the combination of workmanship and raw materials like sand, gravel and cement. The inherent variability of durability aspects are reflected by stochastic input parameters of the models that have been presented in chapter 3. This chapter gives the stochastic input parameters for critical chloride concentration, diffusion coefficient, surface chloride concentration and ageing coefficient based on test results obtained from on site-concrete.

Analysis of inspection results from 12 Scottish bridges confirm the stochastic nature of the critical chloride concentration, however the mean value seems to be lower than the mean values that has been found in chapter 3. Explanations for the deviation between results from on site tests and laboratory tests have been presented. In chapter 6 a conclusive value is chosen.

Over the years, numerous values have been suggested for the ageing coefficient. However, these values show a lot of scatter. Therefore this thesis analysed the results from numerous specimens again to derive the ageing coefficient. A new method is adopted in this thesis to obtain the ageing coefficient from carefully documented specimens. The advantage of this method is that all specimens are made by the same persons and according to the same design specifications. The results gave a value of the ageing coefficient that corresponds well to the values found in other research projects.

In the literature it is often claimed that concrete made of blast furnace slag cement shows superb resistance to chloride ingress compared to portland cement. In this thesis approximately 100 cores have been taken from Dutch bridges and analysed for chloride ingress. The results indicate a similar resistance to chloride ingress of concrete made of both blast furnace slag and portland cement. A literature study showed that only a limited number of publications claim the superb quality concrete made of blast furnace slag concrete. Furthermore these publications only researched mortar or concrete under laboratory conditions.

Besides the diffusion coefficient, the surface chloride concentration is of great importance to chloride ingress. Structures that have been built during the 1970s show a higher surface chloride concentration than structures that have been built during the 1940s and 1980s. One of the factors that influence the surface chloride concentration is the curing of the concrete, as was observed when the ageing coefficient was derived from specimens that are cured for different periods.

5. Structural parameters

5.1. Introduction

The choices made when concrete structures are designed determine the boundary conditions for the rate of deterioration of these structures. Where the previous chapter described the input parameters that are derived from samples to model deterioration, this chapter describes the input parameters that are obtained by observations (e.g. cover depth).

5.2. Cover depth

The periods of initiation and propagation of corrosion due to chloride ingress and carbonation are strongly influenced by the cover depth to the reinforcement. Over the years, the minimum cover depth, as specified by the successive standards, has changed. The history of cover depths for concrete in wet environment exposed to deicing agents according to the Dutch standards, is given in figure 38. Other countries show a similar increase of the minimum cover depths over the years.

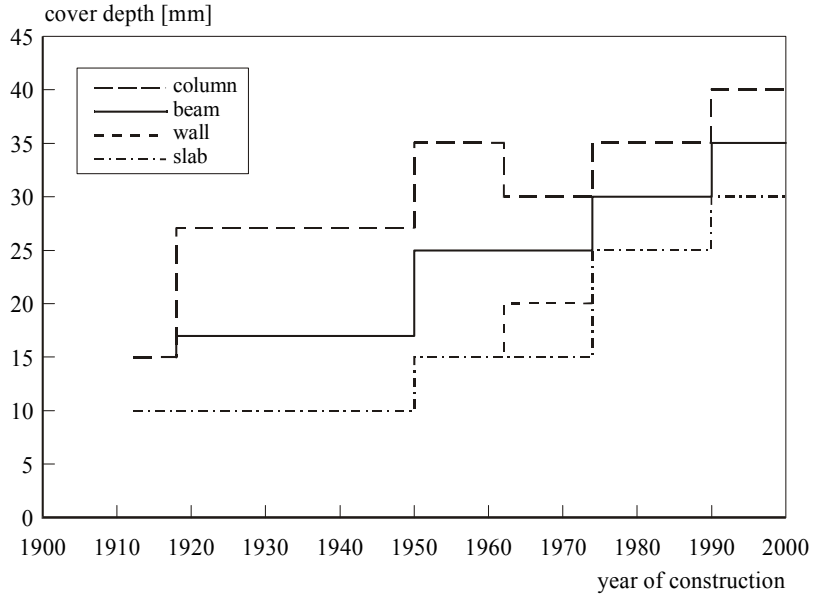

Figure 38: Required cover, according to the Dutch standards [Gaal 2001b]

There are most likely differences between the minimum cover depth according to the standard, and the cover depth that is actually achieved on site. To get an indication of the cover depth of the Dutch bridge stock, over 1100 measurements of the cover depth of 80 bridges were analysed. The measured cover depths apply to bridges at random locations in the Netherlands, and the year of construction ranges from 1950 to 1990. In this analysis a distinction has been made between different structural members

(beam, column, supporting wall, slab and curb) and the valid national standard at the time of construction. This distinction has been made to emphasize that the methods of construction and production have changed, over the years. The results from the analysis of cover depths are tabulated in table 20 and 21; detailed information on the analysis is listed in appendix D.

The observed mean values and minimum cover depth for each standard for specific structural elements are summarized in table 20. The cover depths given in table 20, show that the differences between minimum and achieved cover depth is more or less constant over the years. However, there is a strong difference between the structural members. The difference between the minimum cover depth and the observed cover depth of columns is only 7-8mm, whereas the additional cover depth of slabs and walls is 22mm. Over the years, the Dutch Ministry of Transport increased the minimum cover depth of the structural element curb en slab by 10mm [de Bruijn 1995].

Table 20: Results of cover depth: standard versus observed mean value (mm) [Gaal 2002]

standard	**beam**		**column**		**curb**[12]		**slab**		**wall**	
	$c_{stand.}$	c_{obser}	$c_{stand.}$	c_{obser}	$c_{stand.}$	c_{obser}	$c_{stand.}$	c_{obser}	$c_{stand.}$	c_{obser}
GBV 1950	25	42.0	35	-	15	44.4	15	36.5	15	36.6
GBV 1962	25	42.0	30	37.9	15	42.5	15	36.0	20	39.9
VB 74/84	30	46.9	35	43.1	25	48.2	25	46.6	25	48.5
VBC 90/95	35	-	40	-	30	53.2	30	-	30	53.7

The mean value and standard deviation that are used as input parameters to predict future deterioration are tabulated in table 21.

Table 21: Results of cover depth analysis (mm)

standard	**beam**		**column**		**curb**		**slab**		**wall**	
	μ[13]	σ[14]	μ	σ	μ	σ	μ	σ	μ	σ
GBV 1950	42.0	9.7	-	-	44.4	11.4	36.5	11.7	36.6	12.2
GBV 1962	42.0	9.7	37.9	6.1	42.5	9.1	36.0	5.9	39.9	5.5
VB 74/84	46.9	10.7	43.1	6.7	48.2	8.7	46.6	5.6	48.5	6.7
VBC 90/95	-	-	-	-	53.2	10.7	-	-	53.7	6.7

The variability of the observed cover depths is modelled as a lognormal distribution with a certain mean value and standard deviation. It is an arbitrary choice to represent the data by a lognormal distribution. The choice is visually evaluated by comparing the cumulative distribution of the observed data with the fitted lognormal distribution

[12] Dutch: schampkant
[13] mean value for cover depth at selected structural element and standard (lognormal distribution)
[14] standard deviation for cover depth at selected structural element and standard (lognormal distribution)

(figure 39). The choice for a lognormal distribution is confirmed by the observation that there are only minor differences between the observed cover depth and the cumulative distribution function of the cover depth in figure 39. The most frequently used type of structure of the main span is a slab (figure 41), therefore the accompanying cover depths and standard deviations from table 21 will be used in the analysis.

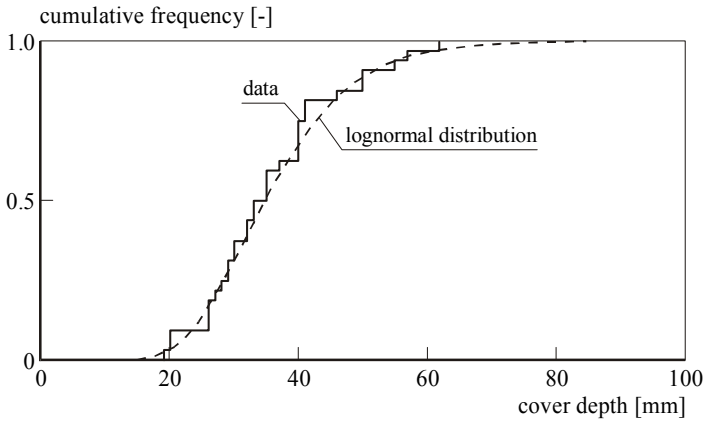

Figure 39: Observed and modelled cover depths of concrete slab bridges (1950-1961)]

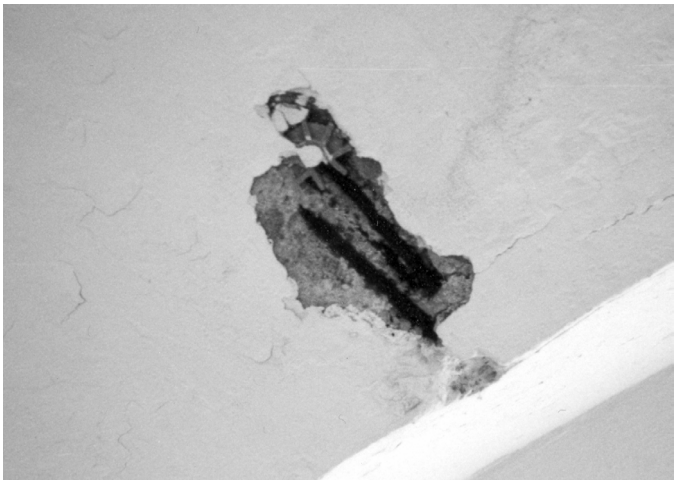

Figure 40: Corrosion due to tipped spacer (Berlin, photo by author)

5.3. Age distribution of Dutch bridge stock

This paragraph describes the Dutch concrete highway bridge stock that will be analysed to predict future deterioration (chapter 6). To predict future deterioration of the stock of Dutch concrete bridges, the age distribution gives important information. Over the years, about 3500 concrete bridges have been constructed over or in Dutch highways. Especially during the early seventies a massive number of bridges has been constructed. The prediction of deterioration in this thesis is limited to the deterioration of concrete bridges, since the Dutch highway bridges have mainly been made of concrete. Of all highway bridges in the Netherlands, about 95% are concrete bridges. The number and type of concrete bridges that are constructed in the Netherlands during the 20th century are given in figure 41.

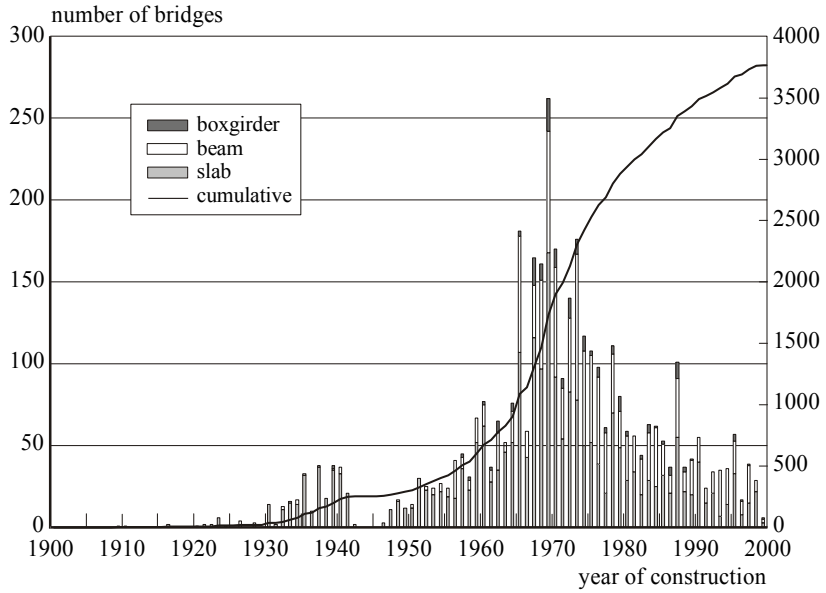

Figure 41: History of bridge construction in Dutch highways

5.4. Bridge characteristics

It can be questioned whether the amount of deterioration depends on the type of structure of the main span(s). However, from European countries insufficient inspection data are available to compare the structural types of the main span. Fortunately, the National Bridge Inventory (NBI) documents the condition of over 650.000 U.S. bridges (in the year 2000) and these bridges are, in general, older than the European bridges. Because of the massive number of inspection records and the higher probability of deterioration, the NBI-data are well suited for use in a statistical analysis of deterioration of bridges and to draw conclusions about the deterioration of each structural type of the main span.

The National Bridge Inventory has tracked the condition of all bridges in the United States. To make the data more consistent with the data of other bridge stocks, the inspection data was limited to interstate -, US numbered – and state highways and the material concrete. In the United States, there were in total 140783 concrete bridges in or over the above-mentioned highways, in the year 2000.

The data of the National Bridge Inventory was obtained by visual inspection. During a visual assessment, the condition of the bridges was rated with a number between 0 and 9, according to the visual level of deterioration. The number 0 indicates that the bridge is closed for all traffic due to durability problems, and condition 9 indicates that the bridge is in superior condition and meets all desirable criteria. A bridge is structurally deficient if the superstructure or substructure requires immediate repairs or rehabilitation or if the ability to carry normal live loads is severely impaired. Bridges with a rating of 4 or less are considered as structurally deficient. The relative number of deficient structures for each year of construction is given in figure 42.

The U.S. federal-aid highway program was initiated in 1916 and got off to a slow start. This explains why during the first two decades of the 20th century only a limited number of bridges were constructed (figure 43). Because of the limited number of bridges that were constructed during the first decades of the 20th century, the relative number of deficient bridges shows more scatter. Because of the scatter the analysis is limited to the years from 1920 to 2000.

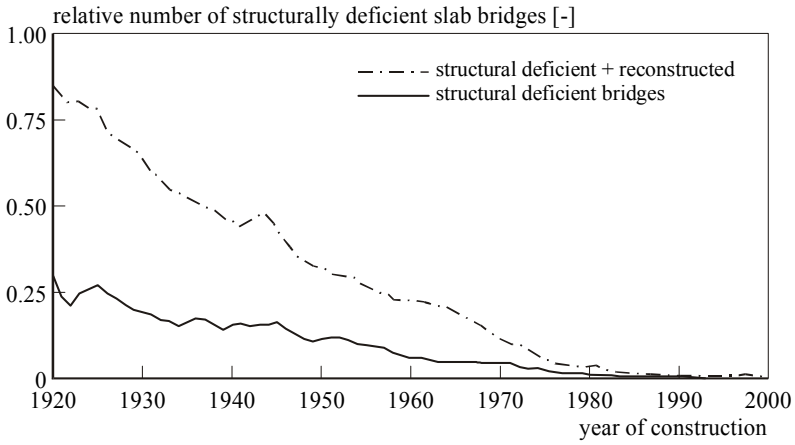

Figure 42: Deficient concrete bridges in US highways (in the year 2000)

A large number of bridges that has been constructed before the Second World War have been reconstructed. It is most likely that these bridges have been reconstructed because their condition was rated as structurally deficient. As a result of the maintenance that has been carried out, the present number of deficient bridges does not rep-

resent the total decay of concrete bridges. Some types of work are not considered as reconstruction, like [FHWA 1995]:

- replacement of safety features;
- painting of structural steel;
- overlay of bridge deck;
- utility work;
- emergency repair after an accident.

To give an indication of the total decay of concrete bridges in the U.S. highways the relative number of bridges that have been reconstructed is added to the number of structurally deficient bridges (figure 42). The absolute number of concrete highway bridges that has been constructed and reconstructed over the years is given in figure 43. The solid line gives the number of constructed bridges in each year. The dashed line gives the year of construction of the reconstructed bridges and the dotted line gives the year in which the bridges have been reconstructed.

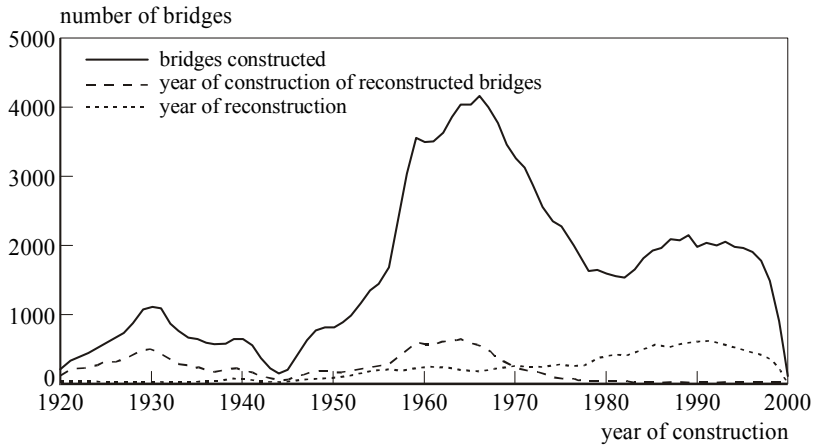

Figure 43: Constructed and reconstructed concrete bridges in the U.S.

Besides the type of material and route prefix also the type of structure of the main span is registered in the National Bridge Inventory. In this section the number of structurally deficient bridges is analysed by structural type of span. A detailed description of each type of structure versus the structural deficiency is given in appendix H. A summary of these results is given in figure 44. Since structures like precast beam bridges have been constructed since the 1960s, some of the lines in figure 44 do not start from the origin of the figure.

The results presented in figure 44 demonstrate that there are differences in deterioration between various types of bridges. However, on average the analysed bridge structures deteriorate with a similar rate. One could question whether the results from the United States are applicable to bridges in other countries. However, in general the different types of bridges are exposed to the same environment. For example in the

Netherlands, the observed general level of deterioration might deviate from that in the U.S., but the differences between the various types of bridges will be the same. Therefore it is assumed in this thesis that the results from the United States are representative for bridge stocks of other countries too.

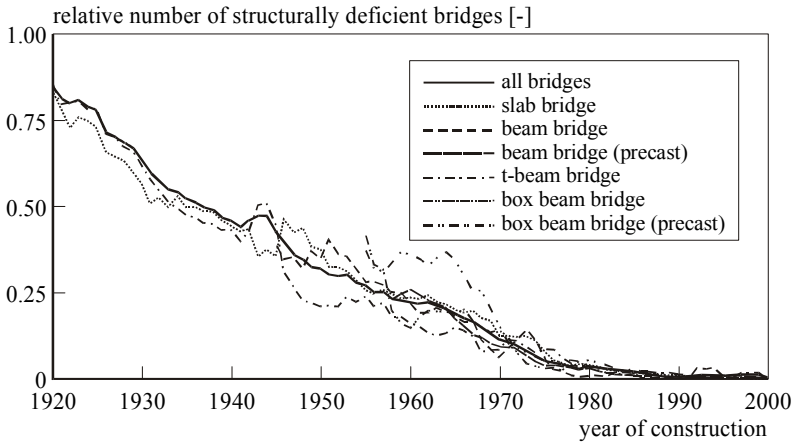

Figure 44: Relative number of structurally deficient bridges + reconstructed bridges in US highways

The conclusion that can be drawn from figure 44 is that on average slab-, beam- and T-beam bridges show a similar resistance against deterioration.

5.5. Discussion

In this chapter the influence of a number of design parameters i.e. cover depth, age distribution and type of structure of the main span(s) is discussed. The cover depth of Dutch bridges has been increased considerably during the last century: on average the cover depth doubled for most structural elements. The analysis of cover depths on site showed that the cover depths realized are approximately 20mm larger than the minimum cover depth according to the standard at the time of construction.

It was suggested in the past that the type of bridge influences the rate of deterioration [Roskam 1994]. A bridge inventory in the United States show that the relative number of structurally deficient bridges is not equal for all structural types in each year. On average, the relative number of structurally deficient bridges is equal for all types of structures. Therefore, this thesis does not distinguish between bridge types while modelling deterioration.

6. Prediction of deterioration of Dutch highway bridges

6.1. Introduction

Most Dutch bridges were constructed during the early 1970s, when most of the present highway network was effected in the Netherlands. Deterioration of these concrete structures has become an important issue over the last decade of the 20th century, when these bridges showed the first signs of deterioration.

The heterogeneous age distribution makes it clear that predicting future deterioration by extrapolating current trends does not lead to an accurate prediction. A sound predictive method is needed that regards the effects of bridge construction practice of the 20th century in order to predict deterioration for the first decades of the 21st century.

Current bridge deterioration models, which are used in bridge management systems, are not able to take account of the effects of the history of bridge construction practice during the last century. In this chapter a prediction will be made of deterioration of concrete bridges in the Dutch highway bridge stock, based on models and observed bridge characteristics that are described in the previous chapters. It is emphasized that in this thesis it is assumed that deterioration is limited to corrosion of the reinforcement due to chloride ingress or carbonation and subsequent spalling, as was discussed in chapter 1.

6.2. Predictive method

6.2.1. Advantages of stochastic parameters

A deterministic approach to the deterioration problem is a powerful way to assess a bridge stock. However, uncertainty due to the inherent stochastic behaviour of the infrastructure's deterioration processes makes a probabilistic approach to the problem a logical choice. The probabilistic approach to predict the deterioration of bridges is most commonly carried out by the Markov chain method [Hawk 1998, Thompson 1998]. The drawback of this technique is that this type of model assumes discrete transition intervals of bridge conditions, which neglects the gradual increase of deterioration that is observed for concrete structures.

With today's computers it is possible to use the first order reliability method, where the probability of deterioration of each bridge in a bridge stock is determined individually with complex deterioration models, instead of the Markov chain method. In

this chapter the probability of initiation[15] of corrosion is determined with a first order reliability method in which the limit state function is based on models for chloride ingress and carbonation. For most structures the duration of the initiation phase is much longer than the propagation phase. The length of the propagation phase, until spalling of the cover occurs, is usually 3 to 5 years (figure 20 and 21, p. 49) [Liu 1998]. Therefore, the time to initiation of corrosion is determined with a probabilistic method, whereas the period between initiation of corrosion and spalling of the concrete cover is determined deterministically.

The question is whether the calculated time until spalling can be compared with the observed time until spalling in existing bridges, since it is assumed that the input parameters are not related when the probability of initiation of corrosion is calculated. This assumption may not be valid for a single bridge, since in case of a single bridge both the cover depth and the diffusion coefficient can be below average due to bad workmanship. However, the quality of workmanship and materials of a series of bridges can be assumed to be independent of each other, since different construction workers and ready mix plants were employed to construct all the bridges of the bridge stock. In such a situation the predicted probability can be compared with the observed deterioration. A single bridge might deviate from the predicted deterioration due to related characteristics, but on average the model will hopefully meet the observed deterioration of a bridge stock.

6.2.2. Description of the predictive method

In this section the method is described that is used in this thesis in order to determine the rate of deterioration of a concrete bridge stock. The method determines the rate of deterioration based on the bridge characteristics, exposure conditions, selected deterioration processes and constants of the deterioration processes. A flow chart of the method, which leads to the results that are presented in the figures 46 and 47, is shown in figure 45.

Structure of the model

The method derives its input from three databases. The main database is filled with data of all, about 3500, Dutch concrete highway bridges. This database is property of the Dutch Ministry of Transport. The data consists of year of construction and possibly demolition, width and length of the bridge deck[16]. To grasp the full scale of deterioration it is necessary to take the width and the length of each bridge into account, since the dimensions of typical bridges increased over the years. The second database contains the input parameters, which are related to the concrete quality and design details, for each year of construction of Dutch bridges. These input parameters are

[15] The concept of the initiation and propagation phase will be used to model the need for maintenance of the Dutch concrete highway bridge stock in the 21st century, as is discussed in section 3.4.

[16] About fifty bridges were removed from the database because the year of construction or width and length of the deck were unknown

determined from site-concrete, like taking concrete cores from structures and cover depth measurements. The last database contains the constants that are used in the deterioration models, like corrosion current[17], critical chloride concentration and ageing coefficient.

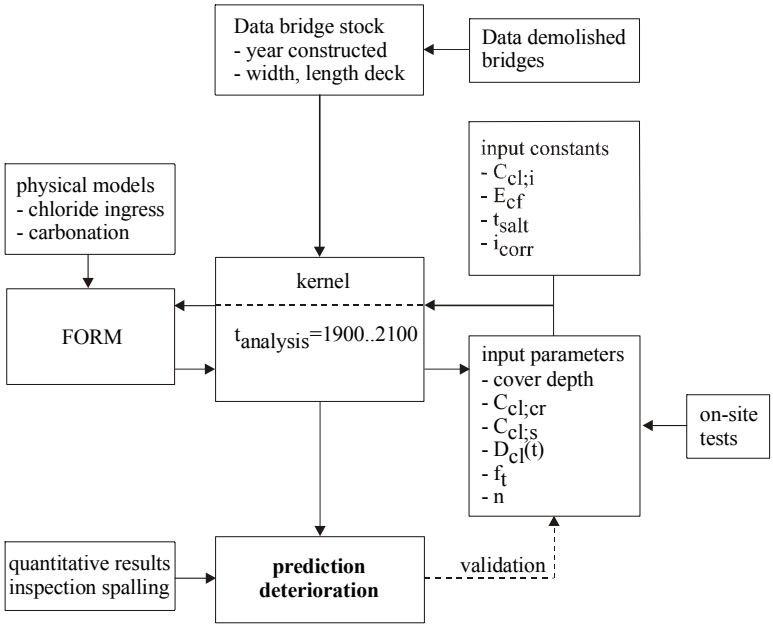

Figure 45: Flow chart of the predictive method used

The next step is to determine the probability of initiation of corrosion from the input parameters for each individual bridge from the bridge database. The probability of corrosion is determined from the stochastic input parameters, e.g. cover depth, diffusion coefficient, surface chloride concentration that are representative for the year of construction. These probabilities are determined with a first order reliability method programmed in Fortran90 [Voortman 2002]. The advantage of this method is that a more reliable prediction of the deterioration is obtained since the development of the variables over time, that influence deterioration, is included in the prediction. Since the superstructure represents the largest concrete surface area of a bridge, the spalling is determined for the span of the bridges. Subsequently the probability of initiation of corrosion due to chloride ingress and carbonation of each individual bridge is summed up to the total probability of corrosion. The result of this analysis is an arithmetic plot that gives the probability of initiation of corrosion on the vertical axis for each year of age on the horizontal axis, which is an ogive curve (figure 46).

[17] Results indicate that after corrosion has been initiated, the corrosion rate develops until a plateau value at which an increasing chloride content does not significantly increase the corrosion current [Dhir 1994]

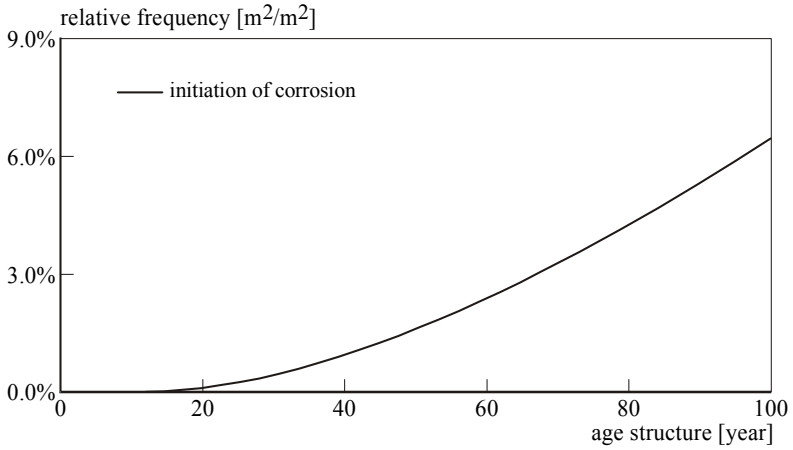

Figure 46: Indicative plot of probability of initiation of corrosion

There is a possibility that carbonation and chloride ingress might develop at the same location of a concrete structure. Because the probabilities of corrosion due to carbonation and chloride ingress are summarized and not corrected for being in the same place, the probability of deterioration is overestimated. However, since the intervention level is relatively low, the overestimation of the probability of corrosion initiation is small. It is assumed in this thesis that adding up the probability of corrosion due to carbonation and chloride ingress gives an accurate description of the deterioration of concrete structures.

The next step is to determine the time from initiation of corrosion to spalling. Once again the time is determined from the constants (corrosion current, modulus of elasticity etc.) and input parameters (cover depth, tensile strength) that are obtained from on-site tests as described in the chapters 4 and 5. To obtain the probability of spalling, the probability of initiation of corrosion of figure 46 is shifted by the duration of the propagation phase, the principle is illustrated in figure 47. After the time until spalling of each individual bridge is known, a combined probability of spalling is calculated for the whole bridge stock, as is represented in figure 53 (p. 88) .

In this study of the Dutch highway bridge stock, the reliability functions both take into account chloride initiated corrosion and carbonation initiated corrosion. It is suggested that the processes of carbonation might accelerate corrosion due to chloride ingress, because the chloride concentration at which corrosion starts is related to the pH-value [Jung 2003]. Since very little is known about the relation between carbonation and chloride initiated corrosion it is assumed in this thesis that there is no relation between carbonation and corrosion due to chloride ingress.

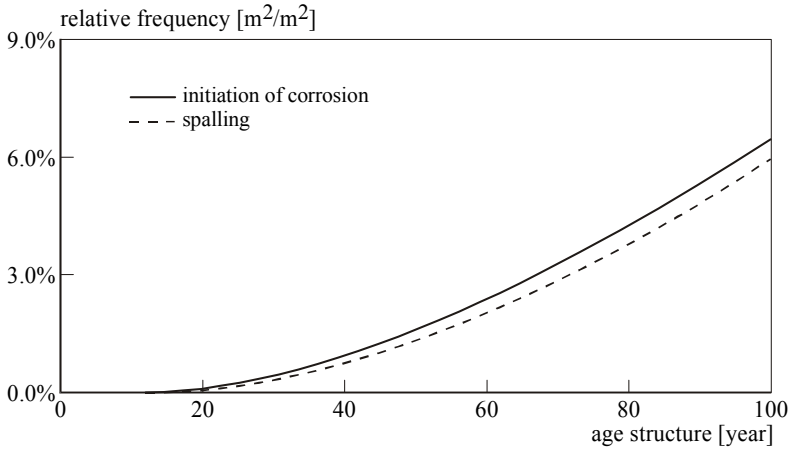

Figure 47: Indicative plot of probability of spalling

Table 22: Input parameters of predictive model as shown in figure 45

parameter	description	page
equations		
chloride ingress	equation 23	37
carbonation	equation 35	41
stochastic parameters		
critical chloride concentration	section 6.3, figure 24	52
ageing coefficient	table 14	55
diffusion coefficient	table 17	63
initial chloride concentration	section 4.5	65
surface chloride concentration	table 18	66
carbonation parameters	table 19	69
cover depth	table 21	72
deterministic parameters		
propagation phase	table 12	49
start application de-icing agent	section 3.2.3.4	35
other		
ratio sheltered/total	0.3 (section 4.4.1)	56
ratio OPC/(BFSC+OPC)	0.4 (section 4.4.1)	56
age distribution bridges	figure 41	74

The input parameters that have been used to predict deterioration of concrete bridges are shown in table 22. The outcome of the deterioration prediction, as is displayed in figure 47, gives the probability of spalling. This value does not represent the probability that the complete surface of the structure will show spalling or not, but represents the probability of spalling for each unit area. In the next section the predictive model

is calibrated with inspection results of the relative amount of spalling at 81 bridges in the Netherlands.

6.3. Validation of predictive method

The validation of the model that predicts deterioration is one of the most important elements of this thesis, which is important for its practical use. Most inspections, however, only give a qualitative judgment of the examined structure, whereas a predictive model can only be verified with quantitative data of spalling (or any other form of deterioration). The actual amount of spalling is, in general, rarely recorded, because of the shortage of available funds. Luckily, the actual amount of spalling was obtained from 81 bridges in the Netherlands, which is used to calibrate the predictive model that is presented in the previous section. The age of the inspected bridges ranged from 3 to 37 years, and some were inspected twice over a period of 10 years. The obtained data of 91 inspections of these 81 bridges are shown in figure 48, where each dot represents the damage of a single bridge. The inspection data are obtained by visual inspection at which the areas of spalling were reported. Subsequently the spalled areas were expressed relatively to the deck area of that specific bridge. The amount of spalling relative to the total area of the bridge structure is plotted on the vertical axis, and the corresponding age on inspection is plotted at the horizontal axis.

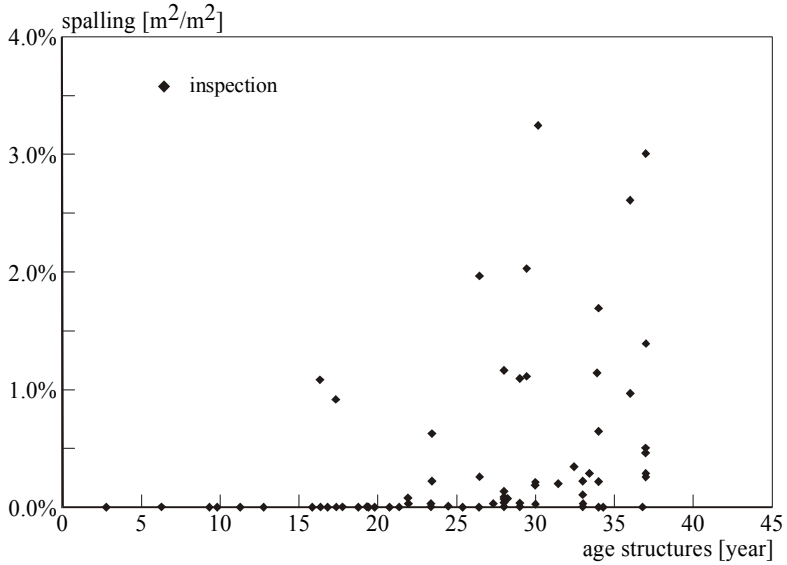

Figure 48: Observed spalling at 81 bridges in 91 inspections

The next step is to compare the outcome of the predictive method with the observed amounts of spalling. The large scatter of the observed spalling makes it difficult to compare the mean value of the predicted spalling with the observed spalling. There-

fore, for each year an average value of the observed spalling is determined and plotted in figure 49. The set of averages of each year indicate that a second order polynomial would best approach the observed damages. The second order polynomial, which is fitted to the observed spalling by using the least square fit procedure, facilitates easy comparison between the predictive model and the observations.

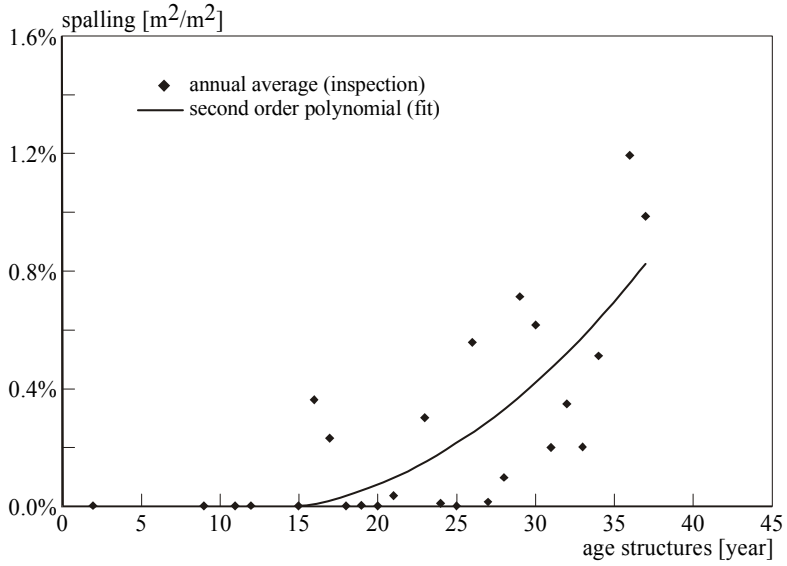

Figure 49: Annual average of observed spalling and second order polynomial

To compare the predictive method with the determined second order polynomial (figure 49), the amount of spalling is determined according to the method described in figure 45 based on the characteristics of the 81 bridges (design specification according to the standards at the time of construction).

At first, a small deviation was observed between the predicted and the observed spalling. Usually a predictive model is adjusted to the desired outcome by a model parameter. In this thesis it is preferred to re-examine the input parameters (figure 45). Where most of the input parameters of the chloride ingress model, like cover depth, diffusion coefficient etc., were derived from samples or inspections, the critical chloride concentration was based on laboratory results. However, as was mentioned in section 4.2, the threshold level in field conditions is lower than in laboratory conditions. Consequently the critical chloride concentration was chosen as a chloride concentration of 0.40% of the binder mass, instead of 0.5% as was discussed in chapter 4. A critical chloride concentration of 0.4% by mass of cement is more in agreement with the value that is observed at structures, than the value of 0.5% by mass of cement that is observed in laboratories. By changing only the value of the critical chloride concentration, the predictive method accurately matches the mean of the amount of observed spalling as is observed at the 81 bridges (figure 50).

For the selected values of the input parameters the predictive model is in exact agreement with the observed spalling at the 81 bridges in the Netherlands. The added value of the predictive model over the fit is that the influences of changes in one or more input parameters can be determined with the predictive model, as is performed in section 6.5.

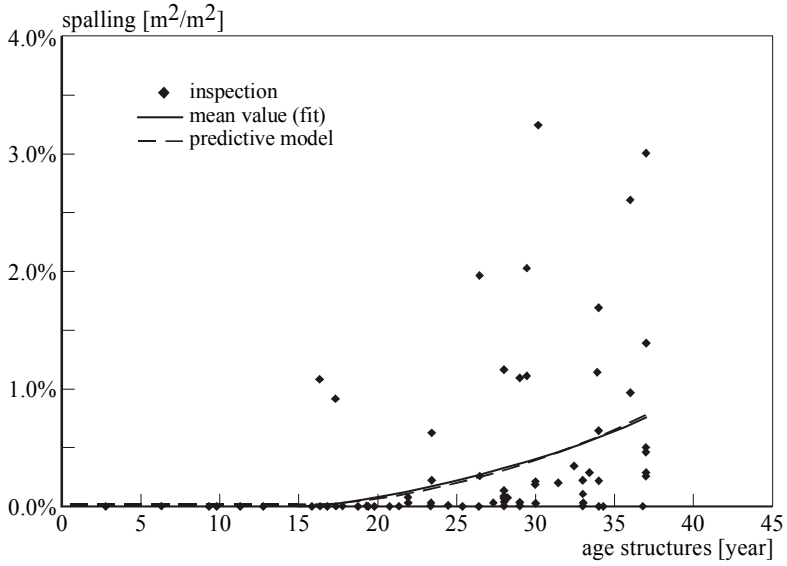

Figure 50: Observed and predicted spalling of 81 Dutch bridges.

As is mentioned earlier, the observed spalling shows a considerable scatter (figure 50), therefore the mean value of spalling does not give sufficient information to the bridge owner. The bridge owner wants to know when the first bridges are eligible for repair, in order to allocate sufficient funds, therefore 5% and 95% fractile levels are added to the prediction of spalling.

The fractile levels are derived from the observed spalling at the earlier mentioned 91 inspections. The inspection results were subdivided into four groups of which the age of the structure at inspection ranged from 0 to 10, 11 to 20, 21 to 30 and 31 to 40 years. From each set of inspection results the mean value and standard deviation is derived for an assumed lognormal distribution of the inspection results (figure 51). The average coefficient of variation of the four groups is 2.14, which is used to determine the fractile levels. With this information the 5^{th} and 95^{th} fractile levels are determined and plotted in figure 52.

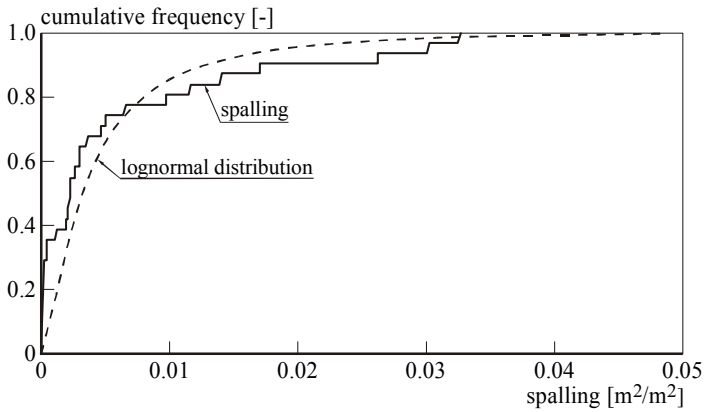

Figure 51: Observed and modelled spalling (age at inspection between 30 to 39 years)

The results of the analysis of the 81 Dutch bridges, as displayed in figure 52, indicated that at an age of 37 years:

- 5% of the bridges show more spalling than 2.9% of the surface area;
- 50% of the bridges show more spalling than 0.8% of the surface area;
- 95% of the bridges show more spalling than 0.04% of the surface area.

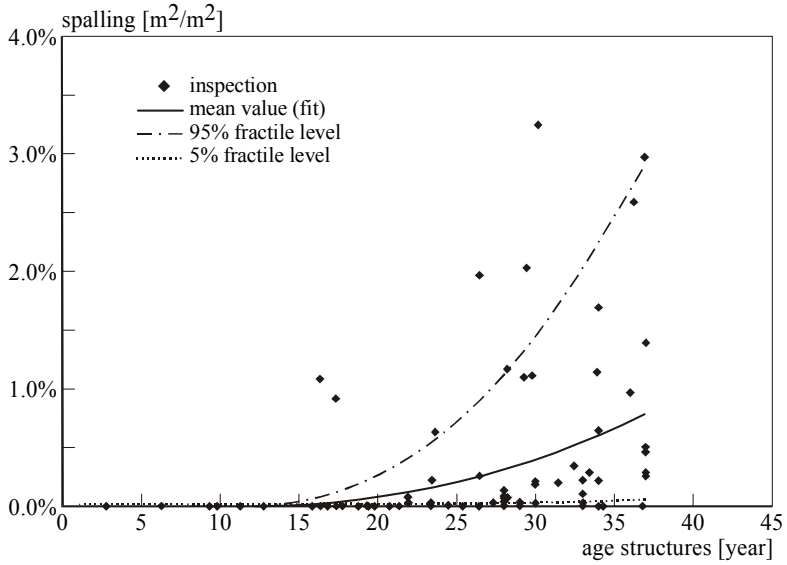

Figure 52: Confidence intervals of probability of spalling

6.4. Deterioration of Dutch concrete bridge stock

As discussed in chapter 1, the aim of this thesis is to determine the rate of deterioration of the Dutch concrete highway bridge stock, taking into account the history of bridge construction. The extent of deterioration for the coming decades is determined by combining the selected deterioration processes, input parameters and calibrated critical chloride threshold parameters.

The relative amount of spalling of an average Dutch highway bridge is plotted in figure 53. Together with the 5% and 95% fractile levels this figure gives and indication of the robustness of the Dutch bridge stock. The prediction as displayed in figure 53 gives the deterioration of the present bridge stock due to chloride ingress and carbonation. In figure 53, the spalling of a set of bridges is predicted beyond the period for which the model is calibrated. However, it is emphasized that the prediction is determined by physical models. Bridges that are constructed after 2003 are not included in this prediction, because the extended knowledge about deterioration, future bridges will hopefully be more resistant to deterioration.

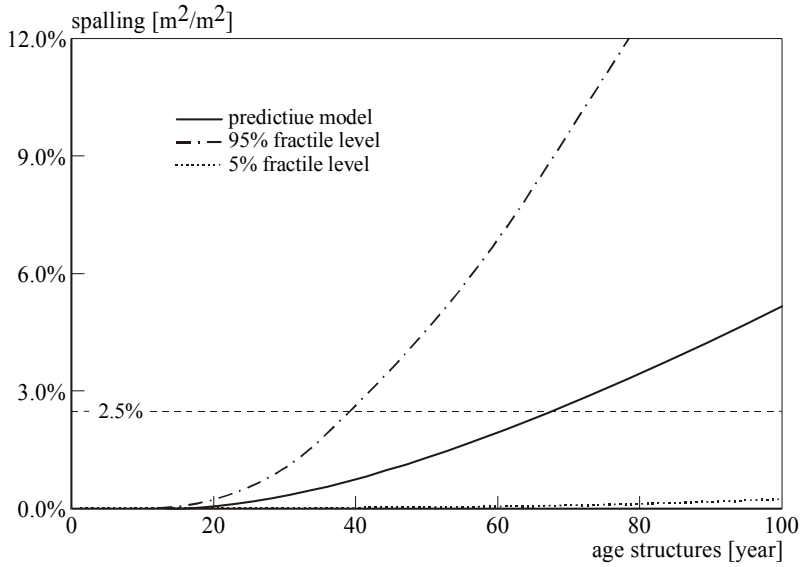

Figure 53: Relative average amount of spalling of Dutch bridges

When bridges are designed, one of the intentions is to achieve a certain design lifetime. However, the outcome of predictive models usually gives a probability of failure or spalling. The lifetime is obtained by selecting a certain upper threshold level of spalling as a criterion to define the end of the technical lifetime. Experts from the U.S. Departments of Transportation indicate that the time to first repair is reached when 2.5% of a structure surface area shows spalling [Weyers 1993]. This intervention level is added to figure 53. From this figure it is derived that 5% of the bridge stock is eligible for repair at an age of nearly 40 year, whereas half of the bridge stock is eligible

for repair after nearly 70 years of service. Due to the shortage of funds, bridge owners might decide to accept more spalling before intervention. It is emphasized that these lifetimes are only valid for bridges that are exposed to the Dutch climate of mild winters and are designed, owned and maintained by the Dutch Ministry of Transport.

Until now, all the results gave an relative amount of spalling, where the bridge owner would like to know what the total amount of damage to the bridge stock is. The total need of maintenance is determined by calculating the amount of spalling for any individual bridge in the Dutch bridge stock. Subsequently the amount of spalling is summarized for each year, as is displayed in figure 54. The figure indicates a steady increase of the yearly area of spalling at Dutch bridges for the coming decades.

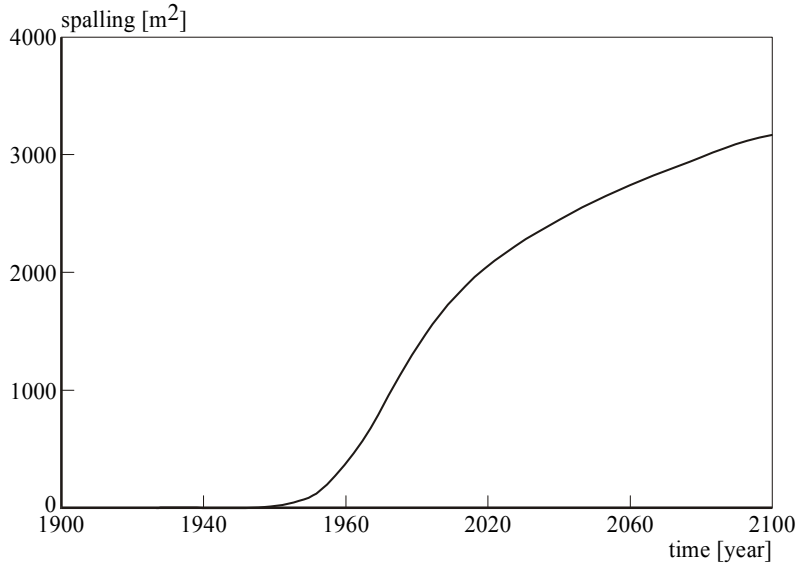

Figure 54: Annual amount of spalling of the Dutch bridge stock

6.5. Variation in input parameters

The predictive method that is presented in this thesis is based on mathematical models for the physical processes that take place. These processes are chloride ingress, carbonation and propagation of corrosion. Because the models are based on physical processes, it is possible to evaluate changes in the input parameters. The next sections will determine the influence of changes in cover depth, initial chloride concentration, critical chloride concentration, ageing coefficient and diffusion coefficient. The next sections give the results of a parameter study where one parameter is varied and the other parameters are chosen according to table 22.

6.5.1. Cover depth

The cover depth is one of the most important parameters because it affects both the initiation and the propagation phase. Over the years the minimum cover depth according to the standard increased considerably, as was discussed in chapter 5. The question is which cover depth is advisable to minimize spalling. In this section the relative amount of spalling is determined for cover depths ranging from 20 to 60mm. These upper and lower boundaries correspond to the maximum and minimum observed cover depths.

In the case of a cover depth of 60mm, a nearly non-existent amount of spalling is predicted. However, to prevent micro cracks in the cover, a cover depth of 50mm is advisable, as is practiced by the Dutch Ministry of Transport (section 5.2).

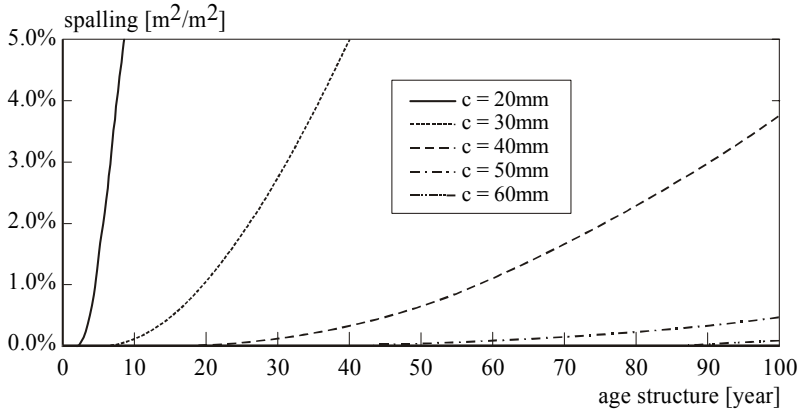

Figure 55: Spalling as a function of cover depth and age

6.5.2. Initial chloride concentration

The initial chloride concentration originates from the chlorides that are present in cement, aggregate or mixing water. It is surprising that some equations for determining the chloride ingress do not even consider the initial chloride concentration (e.g. equation 15). Even though the addition of calcium chloride to concrete is prohibited in most countries since the early 1970s, most standards still allow for chloride concentration up to 0.4% by mass of cement [e.g. NNI 2001]. The analysis from numerous structures in the Gulf region learned that corrosion of the reinforcement was caused by high internal chloride levels [O'Conner 1994].

The relative amount of spalling was calculated for an initial chloride concentration ranging from 0.0 to 0.4% by mass of cement. The results indicate that the initial chloride concentration should be limited to 0.1% by mass of cement in order to prevent unwanted spalling within the design lifetime of structures.

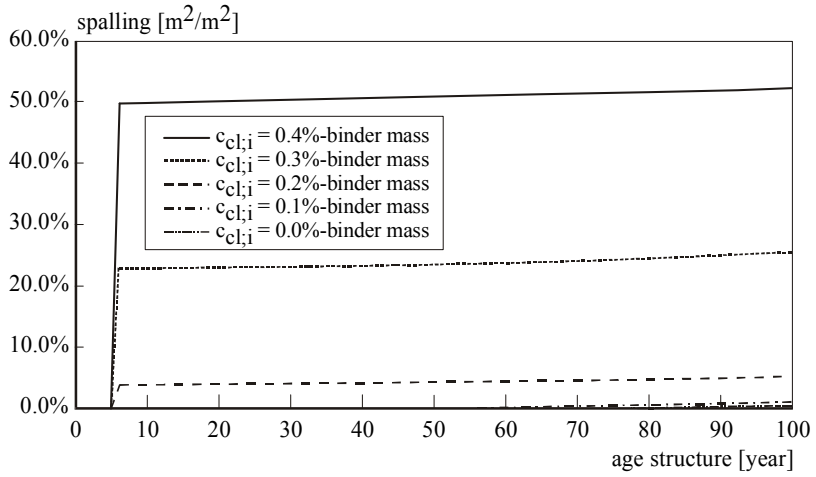

Figure 56: Spalling as a function of initial chloride concentration and age (cover depth 50mm)

6.5.3. Critical chloride concentration

The critical chloride concentration is one of the parameters that is generally not derived from on site tests but from laboratory specimens. In figure 57, the amount of spalling is predicted for the case of a critical chloride concentration ranging from 0.2 to 0.6% by mass of cement. These chloride concentrations form the upper and lower boundary of the critical chloride concentration as observed in on site tests, as derived in section 4.2.

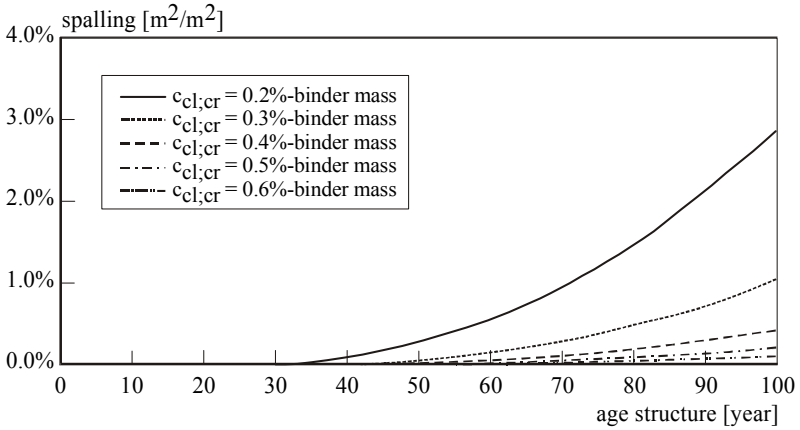

Figure 57: Spalling as a function of critical chloride concentration and age (cover depth 50mm)

The determined spalling at the suggested critical chloride concentrations indicates that the sensitivity of the outcome of the predictive model to changes is limited. However, the variation in the critical chloride concentration should be kept to a minimum to

prevent early initiation of corrosion. The variation of the critical chloride concentration can be minimized by proper compaction (section 3.2.2).

6.5.4. Ageing coefficient

The ageing coefficient is a parameter, which is surrounded by uncertainty, since identical specimens from different years of construction are difficult to obtain from bridges. To overcome this problem, the ageing coefficient is usually derived from moist or submerged cured specimens. One could question if these specimens are representative for concrete in bridges.

In this parameter study, the ageing coefficient is varied using values, which have often been suggested. The outcome of the parameter study indicates that relatively small differences in the ageing coefficient result in substantial differences in the predicted amount of spalling, figure 58.

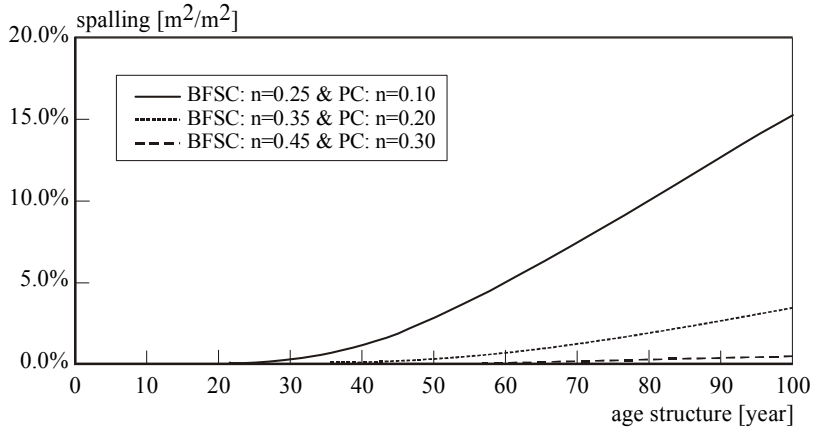

Figure 58: Spalling as a function of the ageing coefficient and the age (cover depth 50mm)

6.5.5. Diffusion coefficient

The diffusion coefficient is one of the parameters that are influenced by the concrete composition and workmanship. In this section the upper and lower boundary for the diffusion coefficient are chosen by respectively adding and subtracting the standard deviation from the mean value. These boundaries correspond to the upper and lower boundaries of the ageing coefficient and critical chloride concentration. The results of the parameter study are shown in figure 59.

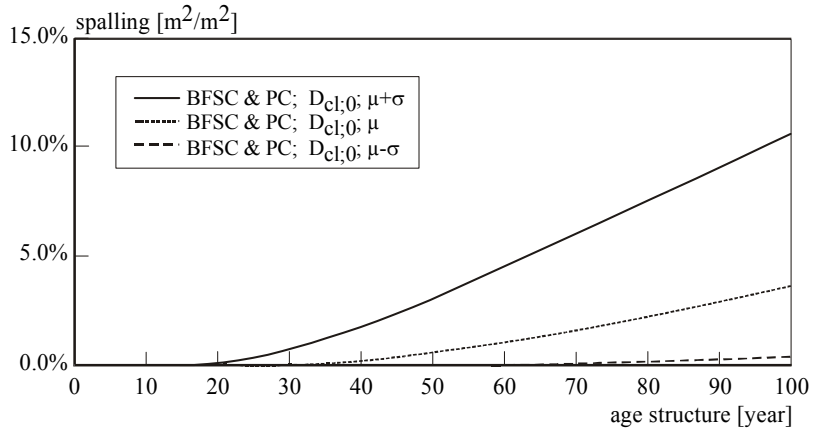

Figure 59: Spalling as a function of diffusion coefficient and age (cover depth 40mm)

6.6. Discussion

In this chapter the results of the model that predicts the development of spalling in time for concrete bridges are presented. The magnitude of spalling at these structures is determined by the first order reliability method, the input parameters of which are tabulated in table 22.

To verify the correctness of the method, the predicted spalling is compared to the results of 91 inspections of 81 bridges in the Netherlands. To obtain an exact match between the prediction and the inspections, the critical chloride was reduced to 0.4% by mass of cement.

The outcome of the parameter study makes clear that relatively small deviations may result in considerable changes. Therefore proper design and workmanship is required to reduce the variation in characteristics of a concrete structure.

7. Conclusions and recommendations

7.1. Conclusions

This thesis deals with predicting deterioration of concrete bridges. In general, it is assumed that deterioration leads to the undesirable event of collapse of such a structure. However, long before a bridge will collapse, pieces of concrete will come off due to spalling that might harm the passing users. Therefore in this thesis 'failure' is defined as the undesirable event of spalling.

From all possible mechanisms of deterioration it is assumed that corrosion due to chloride ingress and carbonation are the leading mechanisms. Illustrative is the effect of the sudden increase of spalling after sodium chloride was introduced as a de-icing agent in California, in the late 1960s.

Over the years it has been observed that older bridges perform better than recently constructed bridges. This thesis presents a theoretical background for the improved condition of bridges that are not exposed to chlorides for several years after construction. During the years that a bridge structure is not exposed to chlorides, the hydration continues and as a result concrete will show more resistance to chloride ingress.

Once the chlorides reaches the reinforcement, the critical chloride concentration determines when corrosion of the reinforcement is initiated. However, all critical chloride concentrations are derived from laboratory specimens. In chapter 4, a critical chloride concentration is derived from specimens obtained from structures. Due to the differences between laboratory and on-site specimens, e.g. cleaning reinforcement and compaction, a reduced critical chloride concentration was derived.

As is observed in chapter 6, the ageing coefficient exerts a large influence on the ingress of chlorides and subsequent spalling. In chapter 4 a new method is presented to derive the ageing coefficient. By exposing identical specimens to chlorides after various periods of curing, the ageing coefficient can be derived.

In numerous publications, it has been suggested that concrete made of blast furnace slag cement shows a superb resistance to chloride ingress compared to concrete made of portland cement. In this thesis, over 100 cores are examined for chloride ingress. These cores were obtained from structures that were constructed in the 1940s and 1960s, with most likely CEM III/A cement. From the obtained chloride profiles it was concluded, in chapter 4, that the blast furnace slag cement shows a more or less similar resistance to chloride ingress as concrete made of portland cement. In general, superb resistance is observed for mortar specimens that are moist cured for 28 days under laboratory conditions.

The surface chloride concentration of concrete made of blast furnace slag cement is higher than that of concrete made of portland cement, which results in an increased chloride ingress.

The proposed model to determine spalling nicely fits the observed spalling at 81 bridges in the Netherlands, without the use of a model parameter. One could argue that the fit-procedure makes the model fit to the data, but the curvature of ogive shaped result of the model is also agrees with the observed data.

The results of the predictive model indicate that the amount of spalling at the concrete bridges in the Dutch highways will double in the coming decades. The sharp increase in the need for maintenance is caused by the sharp increase in the number of bridges that were constructed in the early 1970s and the use of de-icer salt since the early 1960s.

7.2. Recommendations

The ingress of chloride is reduced if the structure is not exposed to chlorides shortly after completion. The reduction of the chloride ingress is caused by the ongoing hydration which results in a reduced diffusion coefficient when the structure is first exposed to chlorides. However, the owner usually prefers to use the structure shortly after completion. When a coating or hydrophobic treatment protects a structure, the ingress of chlorides is strongly reduced during a period of at least longer than 5 years [Polder 2001]. It is emphasized that the period without damage to the concrete structure is extended with much more than the lifetime of the protective treatment because of the ongoing hydration.

The initial chloride concentration of concrete is inversely related to the condition of concrete structures. Although the most recent European Standard limits the amount of chlorides in the mixing water to 1.0g/l [NNI 2002], the maximum chloride concentration of concrete is limited to 0.4% by mass of cement [NNI 2001], The results in this thesis show that a chloride concentration of 0.4% by mass of cement will accelerate deterioration over time. Therefore it is recommended to limit the maximum chloride mixed-in concentration to 0.1% by mass of cement.

Concrete made of blast furnace slag cement showed similar performance, with respect to chloride ingress, as concrete made of portland cement. It is suggested to gain a better understanding of the processes that make blast furnace slag cement perform rather well under laboratory conditions, but rather poor on site.

References

1. Abramowitz, M., Stegun, I.A. (1970): *Handbook of Mathematical Functions*, Dover publications, New York.
2. ACI (1999): *ACI Building Code Requirements for Structural Concrete (318-99)*, American Concrete Institute, Farmington Hills.
3. Alonso, C., Andrade, C., Castellote, M., Castro, P. (2000): 'Chloride threshold values to depassivate reinforcing bars embedded in a standardized OPC mortar', in: *Cement and Concrete Research*, vol. 30, no. 7 (July), pp. 1047-1055.
4. Andrade, C., Sagrera, J.L., Sanjuán (2000): 'Several Years Study on Chloride Ion Penetration into Concrete Exposed to Atlantic Ocean Water', in: *Proceedings of 2nd International Workshop on Testing and Modelling the Chloride Ingress into Concrete* (Andrade, C., Kropp, J. eds.), Rilem, Paris.
5. Andrade, C., Castillo, A. (2003): 'Evolution of reinforcement corrosion due to climatic variations', in: *Materials and Corrosion*, vol. 54, no. 6 (June), pp. 379-386.
6. Arya, C., Buenfeld, N.R., Newman, J.B. (1990): 'Factors Influencing Chloride-Binding in Concrete', in: *Cement and Concrete Research*, vol. 20, no. 2 (March), pp. 291-300.
7. ASTM (1999): *Standard Test Method for Half-Cell Potentials of Uncoated Reinforcing steel in Concrete (C876-91)*, American Society for Testing and Materials, Philadelphia.
8. Bamforth, P.B. (1993): 'Concrete classification for r.c. structures exposed to marine and other salt-laden environments', in: *Proceedings of fifth international conference on structural faults and repair 1993 (Forde, M. ed.)*, vol. 2, pp. 31-40.
9. Bamforth, P.B. (1994): 'Prediction of the Onset of Reinforcement Corrosion Due to Chloride Ingress', in: Proceedings of Concrete across the Borders, Danish Concrete Association, Copenhagen.
10. Bamforth, P.B. (1999): 'The derivation of input data for modeling chloride ingress from eight year UK coastal exposure trials', in: *Magazine of Concrete Research*, vol. 51, no. 2 (April), pp. 87-96.
11. Barnes, B.D., Diamond, S., Dolch W.L. (1979): 'Micromorphology of the interfacial zone around aggregates in portland cement mortar', in: *Journal of the American Ceramic Society*, vol. 62, no. 1-2 (Jan.-Feb.), pp. 21-24.
12. Bažant, Z.P. (1979a): 'Physical model for steel corrosion in concrete sea structures – Theory', in: *Journal of the Structural Division*, vol. 108, no. ST6 (June), pp. 1137-1153.
13. Bažant, Z.P. (1979b): 'Physical model for steel corrosion in concrete sea structures – application', in: *Journal of the Structural Division*, vol. 108, no. ST6 (June), pp. 1154-1166.

14. Bentz, D.P. (1995): *A three-dimensional cement hydration and microstructure program. I. Hydration rate, heat of hydration, and chemical shrinkage (NISTIR 5756)*, Building and Fire Research Laboratory, Gaithersburg.
15. Berke, N.S., Weil, T.G. (1992): 'Worldwide review of corrosion inhibitors in concrete', in: *Advances in concrete technology* (Malhotra, V.M. ed.), Canada Centre for Mineral and Energy Technology, Ottawa, pp. 891-914.
16. Betoniek (1994): 'Blauwkleuring', in: *Betoniek* (Betonprisma, 's Hertogenbosch), vol. 9, nr. 24 (in Dutch).
17. Bijen, J.M.J.M. (1996): *Behoud en onderhoud van materialen en constructies*, Delft University of Technology, Delft (in Dutch).
18. Bijen, J.M.J.M. (1998): *Blast Furnace Slag Cement For Durable Marine Structures*, Betonprisma, 's-Hertogenbosch.
19. Bonavetti, V., Donza, H., Rahhal, V., Irassar, E. (2000): 'Influence of initial curing on the properties of concrete containing limestone blended cement', in: *Cement and Concrete Research*, vol. 30, no. 5 (May), pp. 703-708.
20. Boulfiza, M., Sakai, K., Banthia, N., Yoshida, H. (2003): 'Prediction of chloride ions ingress in uncracked and cracked concrete', in: *ACI Materials Journal*, vol. 100, no. 1 (Jan.-Feb.), pp. 38-48.
21. Breit, W. (1997): *Untersuchungen zum kritischen korrosionsauslösenden Chloridgehalt für Stahl in Beton (Ph.D. thesis)*, Institut für Bauforschung der Rheinisch-Westfälischen Technische Hochschule, Aachen.
22. Brodersen, H.A. (1982): *Zur Abhängigkeit der Transportvorgänge verschiedener Ionen im Beton von Struktur und Zusammensetzung des Zementsteins (Ph.D. thesis)*, Rheinisch-Westfälischen Technische Hochschule, Aachen.
23. BSI (1972), *Code of practice for the structural use of concrete: Design, materials and workmanship (CP 110)*, British Standards Institution.
24. Buenfeld, N.R., Newman, J.B. (1986): 'Permeability of marine concrete', in: *Marine Concrete, Papers for the International Conference on Concrete in the Marine Environment*, the Concrete Society, pp. 165-176.
25. Buist, W. (1982): *Beton I, Stabiliteit en duurzaamheid*, Stichting Postdoctoraal onderwijs in de civiele techniek, Delft (in Dutch).
26. Cady, P.D. (1977): 'Corrosion of reinforcing steel in concrete – a general overview of the problem', in: *Chloride corrosion of steel in concrete (ASTM STP 629)* (Tonini, D.E., Dean, S.W. eds.), American Society for Testing and Materials, pp. 3-11.
27. Cady, P.D., Weyers, R.E. (1983): 'Chloride penetration and the deterioration of concrete bridge decks', in: *Cement, Concrete and Aggregates*, vol. 5, no. 2, pp. 81-87.
28. Cady, P.D., Weyers, R.E. (1984): 'Deterioration rates of concrete bridge decks', in: *Journal of Transportation Engineers*, vol. 110, no. 1, pp. 34-44.
29. Carrier, E.C., Pu, D.C., Cady, P.D. (1975): 'Moisture distribution in concrete bridge decks and pavements', in: *Durability of concrete (SP 47-1)*, American Concrete Institute, Detroit.

30. CEB (1997): *New Approach to Durability Design, an example for carbonation induced corrosion (No. 238)*, Comité Euro-International du Béton, Lausanne.
31. Chisholm, D.H., Lee, N.P. (2001): 'Actual and Effective Diffusion Coefficients of Concrete Under Marine Exposure Conditions', in: *Proceedings of the 20th Biennial Conference of the Concrete Institute of Australia,* Concrete Institute of Australia.
32. Clifton, J.R. (1993): 'Predicting the Service Life of Concrete', in: *ACI Materials Journal*, vol. 90, no. 6 (Nov.-Dec.), pp. 611-617.
33. Collepardi, M., Marcialis, A., Turriziani, R. (1972): 'Penetration of Chloride Ions into Cement Pastes and Concretes', in: *Journal of American Ceramic Society*, vol. 55, nr. 10 (October), pp. 534-535.
34. Collepardi, M. (2003): 'A state-of-art review on delayed ettringite attack on concrete', in: *Cement and Concrete Composites*, vol. 25, no. 4-5, pp. 401-407.
35. Crank, J. (1975): *The Mathematics of Diffusion*, Clarendon press, Oxford.
36. CUR (1992), *Kritisch Chloridegehalte in gewapend beton (rapport 92-7)*, Gouda, (in Dutch).
37. CUR (1997), *Toelaatbaar chloridegehalte in gewapend beton (rapport 97-3)*, Gouda (in Dutch).
38. CUR (1998): *Duurzaamheid en onderhoud van betonconstructies (CUR-172),* Civieltechnisch Centrum Uitvoering Research en Onderzoek, Gouda (in Dutch).
39. CUR (1999): *DuraCrete – Compliance Testing for Probabilistic Design Purposes (R8)*, Civieltechnisch Centrum Uitvoering Research en Regelgeving, Gouda.
40. CUR (2000a): *DuraCrete – Statistical Quantification of the Variables in the Limit State Functions (R9)*, Civieltechnisch Centrum Uitvoering Research en Regelgeving, Gouda.
41. CUR (2000b): *DuraCrete – Final Technical Report (R17)*, Civieltechnisch Centrum Uitvoering Research en Regelgeving, Gouda.
42. CUR (2002): *Maatregelen ter voorkoming van betonschade door alkali-silicareactie (CUR-Aanbeveling 89)*, Civieltechnisch Centrum Uitvoering Research en Regelgeving, Gouda (in Dutch).
43. de Bruijn, W.A., Eggermont, P., Mulders, P.A.M. (1995): *Richtlijnen voor het ontwerpen van Betonnen Kunstwerken (ROBK versie 3)*, Rijkswaterstaat, Utrecht (in Dutch).
44. de Jong, H. (1983): *Over Bruggen*, Delft University Press, Delft (in Dutch).
45. de Lange, J.I. (1984): *Vergelijkend onderzoek naar het gedrag van gewapend betonnen prisma's in 2 en 8 jaar expositie in 5 en 100 meter diep Noordzeewater (report B-84-486/60.5.0400)*, Foundation for Materials Research in the Sea, Delft.
46. de Sitter, W.R., Bakker, R.F.M. (2001): 'Weerwoord op levensduur ontwerp en modellering wapeningscorrosie', in: *Cement*, vol. 53, no. 5 (August), pp. 64-71 (in Dutch).

47. Dhir, R.K., Jones, M.R., McCarthy, M.J. (1994): 'PFA concrete: chloride-induced reinforcement corrosion', in: *Magazine of Concrete Research*, vol. 46, no. 169, pp. 269-277.
48. Dunker, K.F., Rabbat, B.G. (1993): 'Why America's Bridges Are Crumbling', in: *Scientific American*, vol. 266, no. 3 (March), pp. 18-25.
49. Ellis, W.E., Riggs, E.H., Butler, W.B. (1991), 'Comparative results of utilization of fly ash, silica fume and ggbfs in reducing the chloride permeability of concrete', in: *Durability of concrete (SP-126)*, American Concrete Institute, pp. 443-458.
50. Estes, A.C., Frangopol, D.M. (1999): 'Repair Optimization of Highway Bridges Using System Reliability Approach', in: *Journal of Structural Engineering*, vol. 125, no. 7 (July), pp. 766-775.
51. FHWA (1995): *Recording and Coding Guide for the Structure Inventory and Appraisal of the Nation's Bridges (report no. FHWA-PD-96-001)*, Federal Highway Administration, Washington.
52. Fluge, F. (2001): 'Marine Chlorides – A probabilistic approach to derive provision for EN 206-1', in: *Proceedings of Duranet - Third workshop*, Tromsø, pp. 42-62.
53. Fraay, A.L.A. (1990): *Fly ash a pozzolan in concrete (Ph.D. thesis)*, Delft University of Technology, Delft.
54. François, R., Arliguie, G. (1999): 'Effect of microcracking and cracking on the development of corrosion in reinforced concrete members', in: *Magazine of Concrete Research*, vol. 51, no. 2 (Apr.), pp. 143-150.
55. Frangopol, D.M., Lin, K., Estes, A.(1997): 'Reliability of reinforced concrete girders under corrosion attack', in: *ASCE Journal of Structural Engineering*, vol. 123, no. 3 (March), pp. 286-297.
56. Gaal, G.C.M. (2001a): *Maintenance and Repair – Probability of Corrosion (report 25.5-01-26)*, Delft University of Technology, Delft.
57. Gaal, G.C.M., van der Veen, C., Djorai, M.H. (2001b): 'Deterioration of concrete bridges, in the Netherlands', in: *Proceedings of Structural Faults & Repair 2001* (Forde, M. ed.), London.
58. Gaal, G.C.M., van der Veen, C., Djorai, M.H. (2002): 'Prediction of Deterioration of Concrete Bridges in the Netherlands', in: *Proceedings of the First International Conference on Bridge Maintenance, Safety and Management* (Casas, J.R., Frangopol, D.M., Nowak, A.S. eds.), Barcelona, Spain.
59. Gaal, G.C.M., van der Veen, C., Walraven, J.C., Djorai, M.H. (2003a): 'Prediction of deterioration – start application of de-icing agent taken into account', in: *Proceedings 9th International bridge management conference*, Transportation Research Board, Orlando.
60. Gaal, G.C.M., van Beek, A. (2003b): 'Coefficient of Diffusion derived from structures exposed to chlorides up to 60 years old', in: *Proceedings 2nd International Workshop on Life Prediction and Aging Management of Concrete Structures (Rilem)* (Naus, D.J. ed.), Paris.

61. Gaal, G.C.M., Polder, R.B., van der Veen, C., Walraven, J.C. (2003c): 'Critical chloride content – state of the art', in: *Proceedings International symposium on Structural Faults & Repair 2003* (Forde, M. ed.), London.
62. Garboczi, E.J., Schwartz, L.M., Bentz, D.P. (1995): 'Modeling the influence of the Interfacial zone on the DC electrical conductivity of mortar', in: *Advanced cement based materials*, vol. 2, no. 5, pp. 169-181.
63. Gardiner, C.P., Melchers, R.E. (2002): 'Corrosion of mild steel in porous media', in: *Corrosion Science*, vol. 44, no. 11, pp. 2459-2478.
64. Gehlen, C. (2000): *Probabilistische Ledensdauerbemessung von Stahlbetonbauwerken, DAfStb 510' (Ph.D. thesis)*, Beuth Verlag, Berlin (in German).
65. Glass, G.K., Buenfeld, N.R. (1997): 'The presentation of the chloride threshold level for corrosion of steel in concrete', in: *Corrosion Science*, vol. 39, no. 5, pp. 1001-1013.
66. Glass, G.K., Reddy, B. (2002): 'The influence of the steel concrete interface on the risk of chloride induced corrosion initiation', in: *Proceedings of workshop Corrosion of steel in Reinforced Concrete Structures (COST 521)* (Weidert, R. ed.), pp. 227-232.
67. Goltermann, P. (2003): 'Chloride Ingress in Concrete Structures: Extrapolation of Observation', in: *ACI Materials Journal*, vol. 100, no. 2 (March-April), pp. 114-119.
68. González, J.A., López, W., Rodríquez, P. (1993): 'Effects of Moisture Availability on Corrosion Kinetics of Steel Embedded in Concrete', in: *Corrosion Engineering*, vol. 49, no. 12 (Dec.), pp. 1004-1010.
69. Gulikers, J.J.W., Polder, R.B., de Vries, J. (1996): *Aanbeveling voor de bepaling van het chloridegehalte in verhard cementbeton volgens de eisen van Bouwdienst Rijkswaterstaat (BSW 96-01)*, Bouwdienst Rijkswaterstaat, Utrecht.
70. Häkkinen, T. (1993): *Influence of high slag content on the basic mechanical properties and carbonation of concrete (Ph.D. thesis, VTT Publications 141)*, Technical Research Centre of Finland, Espoo.
71. Halamickova, P., Detwiler, P.H., Bentz, D.P., Garboczi, E.J. (1995): 'Water Permeability and Chloride Ion Diffusion in Portland Cement Mortars: Relationship to Sand Content and Critical Pore Diameter', in: *Cement and Concrete Research*, vol. 25, no. 4 (May), pp. 790-802.
72. Hausmann, D.A. (1967): 'Steel corrosion in concrete, How does it occur?', in: *Materials protection*, vol. 19, no. 6, pp. 19-23.
73. Hawk, H., Small, E.P. (1998), 'The Bridgit bridge management system, in: *Structural Engineering International*, vol. 8, no. 4, pp. 309-314.
74. Helland, S. (2001): 'Service life of concrete offshore structures', in: *Structural Concrete*, vol. 2, no. 3, pp. 121-125.
75. Helmuth, R., Stark, D. (1992): 'Alkali-Silica reactivity mechanisms', in: *Materials science of concrete III, vol. 2* (Skalny, J. ed.), American Ceramic Society, pp. 131-208.

76. Hobbs, D.W., Matthews, J.D. (1998): 'Minimum requirements for concrete to resist deterioration due to chloride-induced corrosion', in: *Minimum requirements for durable concrete* (Hobbs, D.W. ed.), British Cement Association, Crowthorne Berks.
77. Hogan, B. (2001): 'Anti-icing dates from the 30's', in: *Better Roads*, vol. 71, no. 1 (January).
78. Hooks, J.M., Cooper, J. (2000): 'Federal Sponsorship of innovative bridge programs', in: *Proceedings of Conference of High Performance Steel Bridges*, National Bridge Research Organization.
79. Hussain, S.E., Rasheeduzzafar, S., Al-Gahtani, A.S. (1994): 'Influence of Sulphates on Chloride Binding in Cements', in: *Cement and Concrete Research*, vol. 24, no. 1, pp. 8-24.
80. Hyman, W.A., Hughes, D.J. (1983): 'Computer model for life-cycle cost analysis of statewide bridge repair and replacement needs', in: *Transportation Research Record 899*, National Academy of Science, Washington D.C., pp. 52-61.
81. Jones, M.R., Newlands, M.D., Abbas, A.M.O., Dhir, R.K. (2001): 'Comparison of 2 year carbonation depth of common cement concretes using the modified draft CEN test', in: *Materials and Structures*, vol. 34, no. 241 (Aug.-Sept.), pp. 396-403.
82. Johnson, M.E. (1982): 'A comparison of Available Methods for Determining Salt Levels in Cheese', in: *Proceedings of 19th Annual Marschall Invitational Italian Cheese Seminar*, Madison.
83. Jooss, M., Reinhardt, H.W. (2002): 'Permeability and diffusivity of concrete as function of temperature', in: *Cement and Concrete Research*, vol. 32, no. 9 (Sept.), pp. 1497-1504.
84. Jung, W.Y., Yoon, Y.S., Sohn, Y.M. (2003): 'Predicting the remaining service life of land concrete by steel corrosion', in: *Cement and Concrete Research*, vol. 33, no. 5 (May), pp. 663-677.
85. Justnes, H. (1983): *Bounding and structure of some inorganic chlorides related to ziegler natta catalysis*, Norges Tekniske Høgskole, Trondheim.
86. Kawamura, M., Kayyali, O.A., Haque, M.N. (1988): 'Effects of a flyash on pore solution composition in calcium and sodium chloride-bearing mortars', in: *Cement and Concrete Research*, vol. 18, no. 5, pp. 763-773.
87. Khatib, J.M., Mangat, P.S. (2002): 'Influence of high-temperature and low-humidity curing on chloride penetration in blended cement concrete', in: *Cement and Concrete Research*, vol. 32, no. 11 (Nov.), pp. 1743-1753.
88. Kilareski, W.P. (1980): 'Corrosion induced deterioration of reinforced concrete – an overview', in: *Materials Performance*, vol. 19, no. 3 (March), pp. 48-50.
89. Kirkpatrick, T.J., Weyers, R.E., Anderson-Cook, C.M., Sprinkel, M.M. (2002): 'Probabilistic model for the chloride-induced corrosion service life of bridge decks', in: *Cement and Concrete Research*, vol. 32, pp. 1943-1960.

90. Kivi, Koninklijk Instituut van Ingenieurs, afd. voor Bouw- en Waterbouwkunde (1912): *Gewapend-Betonvoorschriften*. Amsterdam, L.J. Veen uitgever, (Dutch reinforced concrete standard 1912, in Dutch).
91. Kivi, Koninklijk Instituut van Ingenieurs, afd. voor Bouw- en Waterbouwkunde (1918): *Gewapend Betonvoorschriften 1918*. Amsterdam, L.J. Veen uitgever, (Dutch reinforced concrete standard 1918, in Dutch).
92. Kivi, Koninklijk Instituut van Ingenieurs, afd. voor Bouw- en Waterbouwkunde (1930): *Gewapend Betonvoorschriften 1930*. Amsterdam, L.J. Veen's uitgevers mij. N.V., (Dutch reinforced concrete standard 1930, in Dutch).
93. Kivi, Koninklijk Instituut van Ingenieurs, afd. voor Bouw- en Waterbouwkunde (1940): *Gewapend-Betonvoorschriften 1940 (N 1009)*. 's-Gravenhage, publisher unknown (Dutch reinforced concrete standard 1940, in Dutch).
94. Kivi, Koninklijk Instituut van Ingenieurs, afd. voor Bouw- en Waterbouwkunde (1954): *Gewapend-Betonvoorschriften 1950*. 's-Gravenhage, Uitgeverij Mouton & Co., (Dutch reinforced concrete standard 1950, in Dutch).
95. Kivi, Koninklijk Instituut van Ingenieurs, afd. voor Bouw- en Waterbouwkunde (1962): *Gewapend-Betonvoorschriften 1962 (NEN 1009)*. Amsterdam, L.J. Veen's uitgeversmaatschappij N.V., (Dutch reinforced concrete standard 1962, in Dutch).
96. Kropp, J., Hilsdorf, H.K., Grube, H., Andrade, C., Nilsson, L.O. (1995): 'Transportation mechanics and definitions', in: *Performance Criteria for Concrete Durability, Rilem report 12* (Kropp, J., Hilsdorf, H.K. eds.), Rilem, Paris.
97. Li, C.Q. (2002): 'Initiation of Chloride-Induced Reinforcement Corrosion in Concrete Structural Members – Prediction', in: *ACI Structural Journal*, vol. 99, no. 2 (March-April), pp. 133-141.
98. Lindvall, A., Andersen, A., Nilsson, L.O. (2000): 'Chloride ingress data from Danish and Swedish road bridges exposed to splash from de-icing salt', in: *Proceedings of 2nd International RILEM Workshop on Testing and Modelling the Chloride Ingress into Concrete* (Andrade, C., Kropp, J. eds.), Rilem, Paris.
99. Liu, Y., Weyers, R.E. (1998): 'Modeling the Time-to-Corrosion Cracking in Chloride Contaminated Reinforced Concrete Structures', in: *ACI Materials Journal*, vol. 95, no. 6 (Nov.-Dec.), pp. 675-681.
100. Locoge, P., Massat, M., Ollivier, J.P., Richet, C. (1992): 'Ion diffusion in microcracked concrete', in: *Cement and Concrete Research*, vol. 22, no. 2-3 (March-May), pp. 431-438.
101. Maage, M., Helland, S., Poulsen, E., Vennesland, Ø., Carlsen, J.E. (1996): 'Service Life Prediction of Existing Concrete Structures Exposed to Marine Environment' in: *ACI Materials Journal*, vol. 93, no. 6 (November-December), pp. 602-608.
102. Mammoliti, L.T., Brown, L.C., Hansson, C.M., Hope, B.B. (1996): 'The influence of surface finish of reinforcing steel and pH of the test solution on the chloride threshold concentration for Corrosion initiation in synthetic pore solutions' in: *Cement and Concrete Research*, vol. 26, no. 4 (April), pp. 545-550.

103. Mangat, P.S., Gurusamy, K. (1987a): 'Chloride diffusion in steel fibre reinforced concrete', in: *Cement and Concrete Research*, vol. 17, no. 3 (May), pp. 385-396.
104. Mangat, P.S., Gurusamy, K. (1987b): 'Chloride diffusion in steel fibre reinforced containing PFA', in: *Cement and Concrete Research*, vol. 17, no. 4 (July), pp. 640-650.
105. Mangat, P.S., Molloy, B.T. (1994a): 'Prediction of long term chloride concentration in concrete', in: *Materials and Structures*, vol. 27, no. 168 (May), pp. 338-346.
106. Mangat, P.S., Molloy, B.T. (1994b): 'Prediction of free chloride concentration in concrete using routine inspection data', in: *Magazine of Concrete Research*, vol. 46, no. 169 (Dec.), pp. 279-287.
107. Mangat, P.S., Limbachiya, M.C. (1999): 'Effect of initial curing on chloride diffusion in concrete repair materials', in: *Cement and Concrete Research*, vol. 29, no. 9 (Sept.), pp. 1475-1485.
108. Markow, M.J., Madanat, S.M., Gurenich, D.I. (1993): 'Optimal Rehabilitation Times for concrete bridge decks', in: *Maintenance of Roadway Pavement and Structures, Transportation Research Record 1392*, pp. 79-89.
109. McNeely, D.J., Lash, S.D. (1963): 'Tensile Strength of Concrete', in: *Journal of the American Concrete Institute*, vol. 60, no, 6 (June), pp. 751-761.
110. Mehta, P.K. (1992): Sulfate Attack on Concrete – A Critical Review, in: *Materials Science of Concrete III* (Skalny, J. ed.), The American Ceramic Society, pp. 105-130.
111. Meyer, A., Wierig, H.J., Husmann, K. (1967): 'Karbonatisierung von Schwerbeton', in: *Deutscher Ausschuss für Stahlbeton (Heft 182)*, pp. 1-33.
112. Mohammed, T.U., Hamada, H. (2001): 'A discussion of the paper "Chloride threshold values to depassivate reinforcing bars embedded in a standardized OPC mortar" by Alonso, C., Andrade, C., Castellote, M., Castro, P.' in: *Cement and Concrete Research*, vol. 31, no. 5 (May), pp. 835-838.
113. Mohammed, T.U., Hamada, H. (2003): 'Relationship between free chloride and total chloride contents in concrete', in: *Cement and Concrete Research*, vol. 33, no. 9 (Sept.), pp. 1487-1490.
114. Mori, Y., Ellingwood, B.R. (1994): 'Maintaining reliability of concrete structures. I: Role of inspection/repair', in: *Journal of Structural Engineering*, vol. 120, no. 3 (March), pp. 824-845.
115. Mutsuyoshi, H. (2001): 'Present Situation of durability of post-tensioned pc bridges in Japan', in: *Durability of post-tensioning tendons* (Taerwe, L. ed.), Fédération Internationale du Béton, Lausanne, pp. 75-88.
116. Neville, A. (1995): 'Chloride attack of reinforced concrete: an overview', in: *Materials and Structures*, vol. 28, pp. 63-70.
117. Nielsen, E.P., Geiker, M.R. (2003): 'Chloride diffusion in partially saturated cementitious material', in: *Cement and Concrete Research*, vol. 33, no. 1 (Jan.) pp. 133-138.

118. Nilsson, L.O., Andersen, A., Luping, T., Utgennannt, P. (2000): 'Chloride ingress data from field exposure in a Swedish road environment', in: *Proceedings of 2nd International Workshop on Testing and Modelling the Chloride Ingress into Concrete* (Andrade, C., Kropp, J. eds.), Rilem, Paris.
119. NNI (1984): *Voorschriften Beton VB 1974/1984 (NEN 3880)*. Nederlands Normalisatie-Instituut, Delft (in Dutch).
120. NNI (1995a): *Cement – Part 1: Composition, specifications and conformity criterial for common cements (NEN-EN 197-1)*, Nederlands Normalisatie Instituut, Delft.
121. NNI (1995b): *Voorschriften beton (NEN 6720)*, Nederlands Normalisatie Instituut, Delft (in Dutch).
122. NNI (2001): *Concrete – Part 1: Specification, performance, production, and conformity (NEN-EN 206-1)*, Nederlands Normalisatie Instituut, Delft.
123. NNI (2002): *Mixing water for concrete (NEN-EN 1008)*, Nederlands Normalisatie Instituut, Delft.
124. Nordtest (1995): *Accelerated Chloride Penetration (NT Build 443)*, Nordtest, Espoo.
125. Nordtest (1999): *Chloride Migration Coefficient from non-steady-state migration experiments (NT Build 492)*, Nordtest, Espoo.
126. Novak, P., Mala, R., Joska, L. (2001), 'Influence of pre-rusting on steel corrosion in concrete', in: *Cement and Concrete Research*, vol. 31, no. 4, pp. 589-593.
127. NSF (1999): Design of concrete structures, Norwegian Standards Association (Norges Standardiseringsforbund), Oslo.
128. O'Conner, J.P. (1994): 'Middle Eastern Concrete Deterioration: Unusual Case History', in: *Journal of Performance of Constructed Facilities*, vol. 8, no. 3 (Aug.), pp. 201-212.
129. Oshiro, T., Hamada, S. (1985): 'Structural Performance and Bending Test of Deteriorated Reinforced Concrete Bridges', in: *Strength Evaluation of Existing Concrete Bridges (SP-88)* (Liu, T.C. ed.), American Concrete Institute, Detroit.
130. Parrott, L.J. (1996): 'Some effects of cement and curing upon carbonation and reinforcement corrosion in concrete', in: *Materials and Structures*, vol. 29, no. 187 (April), pp. 164-173.
131. Patel, R.G., Parrott, L.J., Martin, J.A., Killoh, D.C. (1985): 'Gradients of Microstructure and Diffusion Properties in Cement Paste Caused by Drying', in: Cement and Concrete Research, vol. 15, no. 2, pp. 343-356.
132. Paulsson-Tralla, J., Silfwerbrand, J. (2002): 'Estimation of Chloride Ingress in Uncracked and Cracked Concrete Using Measured Surface Concentrations', in: *ACI Materials Journal*, vol. 99, no. 1 (Jan-Feb), pp. 27-36.
133. Petterson, K. (1994): 'Chloride thresholds value of the corrosion rate in reinforced concrete', in: *Corrosion and corrosion protection of steel in concrete* (Swamy, R.N. ed.), Academic Press, Sheffield, pp. 461-471.

134. Polder, R.B., Larbi, J.A. (1995): 'Investigation of concrete exposed to North Sea water submersion for 16 years', in: *Heron*, vol. 40, no. 1, pp. 31-56.
135. Polder, R.B., Borsje, H., de Vries, H. (2001): 'Prevention of reinforcement corrosion by hydrophobic treatment of concrete', in: *Heron*, vol. 46, no. 4, pp. 227-238.
136. Polder, R.B., Peelen, W., Bertolini, L., Guerrieri, M. (2002a): 'Corrosion rate of rebars from linear polarization resistance and destructive analysis in blended cement concrete after chloride loading', in: *Proceedings of ICC 15th International Corrosion Congress*. Granada.
137. Polder, R.B., Rooij, M.R. de (2002b): *Investigation of the concrete structure of the Pier of Scheveningen after 40 years of exposure to marine environment*, TNO Building and Construction Research, Delft.
138. Polder, R.B., de Rooij, M.R. (2003): *Duurzaamheid Maritieme Constructies*, TNO Building and Construction Research, Delft.
139. Powers, T.C. (1975): 'Freezing effects in concrete', in: *Durability of concrete (SP 47-1)*, American Concrete Institute, Detroit.
140. Rasheeduzzufar, Hussain, S.E., Al-Saadom, S.S. (1991): 'Effect of Cement Composition on chloride binding and corrosion of reinforcing steel in concrete', in: *Cement and Concrete Research*, vol. 21, no. 5 (Sept.), pp. 777-794.
141. Reddy, B., Glass, G.K., Lim, P.J., Buenfeld, N.R. (2002): 'On the corrosion risk presented by chloride bound in concrete', in: *Cement & Concrete composites*, vol. 24, no. 1 (Jan.), pp. 1-5.
142. Rehm, G., Moll, H.L. (1964): 'Versuche zum Studium des Einflusses der Rißbreite auf die Rostbildung an der Bewehrung von Stahlbetonbauteilen', in: *Deutscher Ausschuss für Stahlbeton (heft 169)*, pp. 5-23.
143. Reinhardt, H.W. (1985): *Beton als constructiemateriaal eigenschappen en duurzaamheid*, Delftse Universitaire Pers, Delft (in Dutch).
144. Rijkswaterstaat (2000): *Inspectierapport Kaagbruggen (30F-100)*. Rijkswaterstaat, Bouwdienst, Zoetermeer (in Dutch).
145. Roberts, M.B., Atkins, C., Hogg, V., Middleton, C. (2000): 'A proposed empirical corrosion model for reinforced concrete', in: *Proceedings of the Institution of Civil Engineers Structures and Buildings*, vol. 140, no. 1 (Feb.), pp. 1-11.
146. Roelfstra, G., Adey, B., Hajdin, R., Brühwiler, E. (2000): 'The condition evolution of concrete bridges based on a segmental approach, non-destructive testing and deterioration models', in: *TRB Transportation Research Circular 498*, Transportation Research Board, Washington, pp. C2/1-13.
147. Roskam: C. (1994): *Evaluatie van Schadebeelden aan betonnen kunstwerken*, Technische Universiteit Delft, Delft (in Dutch).
148. Roskam, C. (1996): *Analyse van schade aan kunstwerken*, Delft University of Technology, Delft (in Dutch).
149. SAA (1990): *Australian Standard for Concrete Structures (AS 3600)*, Standard Association of Australia.

150. Sagüés, A.A. (2001): *Metallurgical effects on chloride ion corrosion threshold of steel in concrete*, University of South Florida, Tampa (report WPI 05108906).
151. Sandberg, P., Tang, L., Andersen, A. (1998): 'Recurrent studies of chloride ingress in uncracked marine concrete at various exposure times and elevations', in: *Cement and Concrete Research*, vol. 28, no. 10 (Oct.), pp. 1489-1503.
152. Saremi, M., Mahallaoti E. (2002): 'A study on chloride induced depassivation of mild steel in simulated concrete pore solution', in: *Cement and Concrete Research*, vol. 32, pp. 1915-1921.
153. Schießl, P. (1986): 'Einfluß von Rissen auf die Dauerhaftigkeit von Stahlbeton- und Spannbetonbauteilen', in: *Deutscher Ausschuss für Stahlbeton (heft 370)*, Verlag Ernst & Sohn Berlin, pp. 9-52.
154. Schießl, P. (ed.) (1988), *Corrosion of steel in concrete (RILEM Technical report 60-CSC),* Chapman and Hall, London.
155. Scrivener, K.L. (1989): 'The Microstructure of Concrete', in *Materials of Science of Concrete I (Skalny, J. ed.)*, The American Ceramic Society.
156. Sedran, T., de Larrard, F., Angot, D. (1994): 'Prévisioin de la compacité des mélanges granulaires par le modèle de suspension solide. II: Validations cas des mélanges confinés', in: Bulletin de Liaison des Laboratoires des Ponts et Chaussées, no. 194 (Nov.-Dec.), pp. 71-86.
157. Siemes, A.J.M., Han, N., Visser, J.H.M. (2002): 'Onverwacht lage treksterkte in betonconstructies', in: *Cement*, vol. 54, no. 7, pp. 89-93 (in Dutch).
158. Söderqvist, M-K.(2000): 'Analysis of BMS Reference Bridges in Finland', in: *Transportation research circular (no. 498)*, Transportation Research Board, Washington, pp. C4/1-9.
159. Stanish, K.D., Hooton, R.D., Thomas, M.D.A. (2000): *Testing the Chloride Penetration Resistance of Concrete, A Literature Review*. University of Toronto, Toronto.
160. Stark, D., Morgan, B., Okamoto, P. (1993): *Eliminating or minimizing alkali-silica reactivity (SHRP-C-343)*, National Research Council, Washington DC.
161. Stern, M, Geary, A.L. (1957): 'Electrochemical Polarization, I. A Theoretical Analysis of the Shape of Polarization Curves', in: *Journal of Electrochemical Society*, vol. 104, no. 1, pp. 56-63.
162. Stewart, M.G., Rosowsky, D.V. (1998): 'Structural Safety and Serviceability of Concrete Bridges Subject to Corrosion', in: *Journal of Infrastructure Systems*, vol. 4, no. 4 (Dec.), pp. 146-155.
163. Stuvo (1989), *Levensduur van betonnen kunstwerken (Stuvo-rapport 88)*, Studievereniging Voorgespannen beton, 's-Hertogenbosch (in Dutch).
164. Suryavanshi, A.K., Swamy, R.N., Cardew, G.E. (2002): 'Estimation of Diffusion Coefficients for Chloride Ion Penetration into Structural Concrete', in: *ACI Materials Journal*, vol. 99, no. 5 (Sept-Oct), pp. 441-449.
165. Taheri, A. (1998): *Durability of Reinforced Structures in Aggressive Environment (Ph.D. thesis)*, Delft University Press, Delft.

166. Takewaka, K., Matsumoto, S. (1988), 'Quality and cover thickness of concrete based on the estimation of chloride penetration in marine environments', in: *Concrete in Marine Environment (SP-109)* (Malhotra, V.M. ed.), American Concrete Institute, Detroit, pp. 381-400.
167. Tang, L., Nilsson, L.O. (1993): 'Chloride binding capacity and binding isotherms of opc pastes and mortars', in: *Cement and Concrete Research*, vol. 23, no. 2, pp. 247-253.
168. Thoft-Christensen, P. (2000): 'Modeling of the Deterioration of Reinforced Concrete Structures', in: *Proceedings of 9th IFIP conference*, Ann Arbor.
169. Thomas, M.D.A, Matthews, J.D., Haynes, C.A. (1990): 'Chloride diffusion and reinforcement corrosion in marine exposed concretes containing Pulverized Fuel Ash', in: *Corrosion of Reinforcement in Concrete*, Elsevier, London, pp. 198-212.
170. Thomas, M.D.A, Matthews, J.D. (1996): 'Chloride penetration and reinforcement corrosion in fly ash concrete exposed to a marine environment', in: *Concrete marine environment, proceedings third CAMNET/ACI international conference (ACI SP-163)* (Malhotra, V.M. ed.), pp. 317-338.
171. Thomas, M.D.A., Bamforth, P.B. (1999): 'Modelling chloride diffusion in concrete, Effect of fly ash and slag', in: *Cement and Concrete Research*, vol. 29, no. 4 (April), pp. 487-495.
172. Thompson, P.D, Small, E.P., Johnson, M., Marshall, A.R. (1998): 'The Pontis bridge management system', in: *Structural Engineering International*, vol. 8, no. 4, pp. 303-308.
173. Tong, L., Gjørv, O.E. (2001): 'Chloride diffusivity based on migration testing' in: *Cement and Concrete Research*, vol. 31, no. 7 (July), pp. 973-982.
174. Tuutti, K. (1982): *Corrosion of steel in concrete*, Swedish Cement and Concrete Research Institute, Stockholm.
175. van Daveer, J.R. (1975): 'Techniques for Evaluating Reinforced Concrete Bridge Decks' in: *ACI Journal*, vol. 72, no. 12 (December), pp. 697-704.
176. van Noortwijk, J.M., Klatter, H.E. (2002): 'The use of lifetime distributions in bridge replacement modelling', in: *Proceedings of First International conference on Bridge Maintenance, Safety and Management*, Barcelona.
177. Vassie, P.R. (1984): 'Reinforcement corrosion and the durability of concrete bridges', in: *Proceedings of the Institution of Civil Engineers, Part 1*, vol. 76, pp. 713-723.
178. Vassie, P.R. (1986): *Corrosion of reinforcement: an assessment of twelve concrete bridges after 50 years service (TRRL research report # 78)*, Transport and Road Research Laboratory, Berkshire.
179. Verhey, B.A. (1912): *Handleiding voor berekening van uitvoering van eenvoudige gewapend betonconstructies met toepassing der gewapend betonvoorschriften van het koninklijk instituut van ingenieurs.* L.J. Veen, Amsterdam (in Dutch).
180. Visser, J.H.M., Gaal, G.C.M., de Rooij, M.R. (2002): 'Time dependency of chloride diffusion coefficients in concrete' in: *Proceedings of 3rd International*

RILEM Workshop on Testing and Modelling the Chloride Ingress into Concrete (Andrade, C., Kropp, J. eds.), Rilem, Paris.

181. Voortman, H.G. (2002): *User manual for the Fortran library 'Probmod'*, Delft University of Technology, Delft.
182. Vorster, M.C., Bafna, T., Weyers, R.E. (1991): 'Model for Determining the Optimum Rehabilitation Cycle for Concrete Bridge Decks', in: *Bridge and Hydrology research, Transportation Research Record 1319*, pp. 62-71.
183. Vu, K.A.T., Stewart, M.G. (2002): 'Service life prediction of reinforced concrete structures exposed to aggressive environments', in: *9th international conference on durability of building materials and components (CSIRO, BCE)*, Highett Australia.
184. Vulpen, T. van (2000): *Gladheid: preventie en bestrijding (publicatie 152)*, CROW, Ede (in Dutch).
185. Wardenier, P. (1995): *Onderzoek naar de bepaling van chloriden in beton (rapport 25.1.95.13)*, Delft University of Technology (in Dutch).
186. Wardenier, P. (1996): *Beton in marine omgeving / indringing chloride, deel I: voorbereidend onderzoek (report 25.1.96.23)*, Delft University of Technology (in Dutch).
187. Wardenier, P. (2003): *Chloridenprofiel in beton van wegdekken van diverse viaducten*, Delft University of Technology (in Dutch).
188. West, G. (1996): *Alkali-aggregate reaction in concrete roads and bridges*, Thomas Telford, London.
189. Weyers, R.E., Fitch, M.G., Larsen, E.P., Al-Qadi, I.L. (1994): *Concrete bridge protection and rehabilitation: Chemical and Physical Techniques (SHRP-S-668)*, Strategic Highway Research Program, National Research Council, Washington DC.
190. Wierig, H.J. (1965): 'Die Wasserdampfdurchlässigkeit von Zementmörtel und Beton', in: *Zement-Kalk-Gips*, vol. 18, no. 9, pp. 471-482 (in German).
191. Yalçyn, H., Ergun, M. (1996): 'The prediction of corrosion rates of reinforcing steels in concrete', in: *Cement and Concrete Research*, vol. 26, no. 10, pp. 1593-1599.

Notations and symbols

Roman lower case letters

a	CO_2 binding capacity of cement / concrete	[kg CO_2/m^3]
a_{por}	diameter of equivalent porous zone	[m]
b	diameter of porous zone plus cover depth	[m]
c	cover depth	[m]
c_{obser}	observed cover depth	[m]
c_{stand}	cover depth according to standard	[m]
d_{crit}	the thickness of the expansion at crack initiation	[m]
d_{por}	thickness of equivalent zone with porosity 1	[m]
d_r	diameter of the reinforcement	[m]
f_c'	compressive strength (cube)	[MPa]
f_{cm}	mean compressive strength of the concrete at the age of 28 days	[MPa]
f_t'	tensile strength of concrete	[MPa]
$f_{t;spl}$	tensile strength (split test)	[MPa]
h	change in hydraulic head over path l	[m]
i_{corr}	corrosion current	[$\mu A/cm^2$]
k	hydraulic conductivity	[m/s]
k_{rust}	rate of rust production	[kg·s/m]
l	flow path length	[m]
m_{CaO}	molar mass of calcium oxide (56.08)	[amu][18]
m_{CO2}	molar mass of carbon dioxide (44.01)	[amu][18]
m_{steel}	mass of corroded steel	[kg/m]
n	ageing parameter (n≥0)	[-]
t	time	[s]
t_{corr}	time of initiation of corrosion	[s]
t_{exp}	duration of exposure to deleterious environment	[s]
t_s	age at which exposure to de-icing agent started	[s]
$t_{service}$	service life	[s]
t_0	reference period (associated with $D_{cl;0}$)	[s]
w_{crit}	amount of corrosion products needed to cause cracking	[kg/m]
w_{expan}	amount of corrosion products needed to fill space due to expansion of concrete	[kg/m]
w_{porous}	amount of corrosion product necessary to fill the porous zone	[kg/m]
w_{rust}	mount of rust products	[kg/m]
w_{steel}	amount of corrosion products that causes actual cracking	[kg/m]
x	depth coordinate from the concrete surface into the concrete	[m]
x_{cb}	carbonation depth	[m]
y	depth coordinate from the concrete surface into the concrete	[m]

[18] atomic mass unit

z	depth coordinate from the concrete surface into the concrete	[m]

Greek lower case letters

α_h	degree of hydration	[-]
μ	mean value	[-]
ν_c	Poisson's ratio of the concrete	[-]
ξ_a	parameter relating to cement type (Häkkinen)	[-]
ξ_{air}	air content coefficient (Häkkinen)	[-]
ξ_b	parameter relating to cement type (Häkkinen)	[-]
ξ_{env}	environmental coefficient (Häkkinen)	[-]
ρ_{rust}	density of corrosion products	[kg/m^3]
ρ_{steel}	density of steel	[kg/m^3]
σ	standard deviation	[-]
ψ	parameter micro climatic conditions, wetting and drying (CEB)	[-]
ψ_1	parameter micro climatic conditions, mean moisture content (CEB)	[-]
ψ_2	parameter curing conditions (CEB)	[-]
ψ_3	parameter effect of water separation, local w/c-ratio (CEB)	[-]

Roman capital letters

A	flow area perpendicular to flow direction	[m^2]
C	concentration of diffusing substance	[kg/m^3]
C(x,t)	concentration of diffusing substance at depth x and time t	[kg/m^3]
C_c	content of cement in concrete	[kg]
C_{CaO}	content of calcium oxide in cement	[-]
$C_{cb;s}$	carbon dioxide concentration in the atmosphere	[kg/m^3]
$C_{cl}(x,t)$	concentration of chloride at depth x and time t	[%-binder mass]
$C_{cl}(x,y,t)$	concentration of chloride at depth x and y and time t	[%-binder mass]
$C_{cl;cr}$	critical chloride concentration	[%-binder mass]
$C_{cl;i}$	initial uniform chloride concentration in the concrete	[%-binder mass]
$C_{cl;s}$	concentration of chlorides at the surface	[%-binder mass]
D	diffusion coefficient	[m^2/s]
D_{cb}	(effective) carbon dioxide diffusion coefficient	[m^2/s]
D_{cl}	(effective) chloride diffusion coefficient	[m^2/s]
$D_{cl}(t)$	time-dependent chloride diffusion coefficient	[m^2/s]
$D_{cl;i}$	initial chloride diffusion coefficient	[m^2/s]
$D_{cl;0}$	reference chloride diffusion coefficient (associated with t_0)	[m^2/s]
D_{eff}	effective diffusion coefficient of heterogeneous material	[m^2/s]
D_{nt}	diffusion coefficient obtained with NT Build 443 test	[m^2/s]
D_p	potential chloride diffusion coefficient	[m^2/s]
D_{RCM}	chloride diffusion coefficient – by rapid chloride migration method	[m^2/s]
D_{ss}	steady state diffusion coefficient	[m^2/s]
E_{cf}	effective elastic modulus of concrete	[GPa]

F	rate of transfer per unit area of section	[m/s]
M	total amount of diffusing chlorides	[kg]
Q	amount of diffusing carbon dioxide	[kg]
Q	volumetric flow rate (D'Arcy)	[m^3/s]
V	concrete volume	[m^3]

Greek capital letters

ΔC_{cb}	difference between carbon dioxide concentration in the air and at the carbonation front	[kg CO_2/m^3]
Δt_{crack}	time from corrosion initiation to corrosion crack	[s]

Others

-

Abbreviations

BFSC	blast furnace slag cement
CSF	condensed silica fume
DOT	Department of Transportation (U.S.A.)
erf	error function
GGBS	ground granulated blast furnace slag
NBI	National Bridge Inventory
OPC	ordinary portland cement
PFA	portland fly ash cement (a.k.a. pulverized fuel ash)
SRPC	sulphate resistant portland cement

Appendices

APPENDIX A DIFFUSION EQUATIONS 117
APPENDIX B TERMS RELATED TO CHLORIDE INDUCED CORROSION 121
APPENDIX C DEFINITIONS FOR COEFFICIENT OF CHLORIDE DIFFUSION 127
APPENDIX D REVIEW MINIMUM COVER DEPTH (DUTCH STANDARDS) 129
APPENDIX E COVER DEPTH ACCORDING TO DUTCH STANDARDS 133
APPENDIX F COMPRESSIVE AND TENSILE STRENGTH 135
APPENDIX G HISTORY OF BLAST FURNACE SLAG CEMENT 137
APPENDIX H NATIONAL BRIDGE INVENTORY 139

appendix A Diffusion equations

Diffusion is the process by which matter is transported from one part of a system to another because of random molecular motions. Quantitative measurements of the rate at which a diffusion process occurs are usually expressed in terms of a diffusion coefficient. The diffusion coefficient, however, is not a true physical property but the proportionality constant in Fick's laws.

> *Diffusion coefficient*
> *Confining attention to one dimension only, the diffusion coefficient is defined as the rate of transfer of the diffusing substance across a unit area of a section, divided by the space gradient of concentration at the section [Crank 1975].*

There are two equations to describe the diffusion process; Fick's First en Second Law of Diffusion [Crank 1975, Stanish 2000].

Fick's First Law of Diffusion

The chloride diffusion into concrete which, in the one-dimensional situation normally considered, states:

$$F = -D\frac{\partial C}{\partial x} \qquad (49)$$

F	rate of transfer per unit area of section (flux)
C	concentration of diffusion substance
x	space coordinate measured normal to the section
D	diffusion coefficient

This equation is only useful after steady-state conditions have been reached, i.e. there is no change in concentration with time (flux is constant).

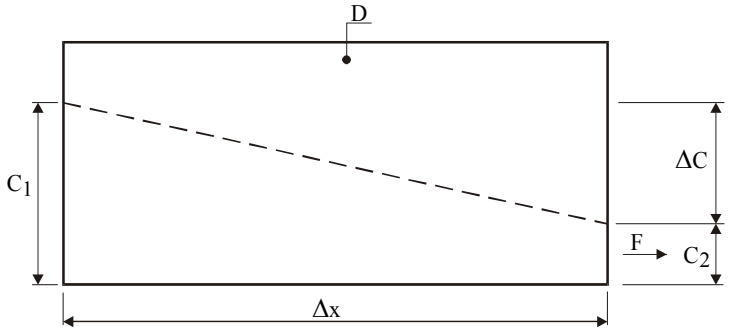

Figure 60: Fick's first law of diffusion

Fick's Second Law of Diffusion

A non steady state situation, where the concentration gradient changes in time, can be modelled by Fick's second law of diffusion. Consider an element of volume in the form of a rectangular parallelepiped whose sides are parallel to the axes of coordinates and are of lengths 2dx, 2dy and 2dz. The contribution to the rate of increase of diffusion substance in the element from two faces equals:

$$-8dxdydz\frac{\partial F_x}{\partial x} \tag{50}$$

$$-8dxdydz\frac{\partial F_y}{\partial y} \tag{51}$$

$$-8dxdydz\frac{\partial F_z}{\partial z} \tag{52}$$

The rate at which the amount of diffusing substance in the element increases is:

$$-8dxdydz\frac{\partial C}{\partial t} \tag{53}$$

hence we have immediately

$$\frac{\partial C}{\partial t}+\frac{\partial F_x}{\partial x}+\frac{\partial F_y}{\partial y}+\frac{\partial F_z}{\partial z}=0 \tag{54}$$

If the first law of Fick is applied

$$\frac{\partial C}{\partial t}=D\left(\frac{\partial^2 C}{\partial x^2}+\frac{\partial^2 C}{\partial y^2}+\frac{\partial^2 C}{\partial z^2}\right) \tag{55}$$

If diffusion is assumed as one-dimensional i.e. if there is a gradient of concentration only along the x-axis, the previous equation is reduced to:

$$\frac{\partial C}{\partial t}=D\frac{\partial^2 C}{\partial x^2} \tag{56}$$

The reduction is allowed because the concentration gradient normally exists in one direction only, which is from the external environment perpendicularly into the concrete. This is the relevant equation for non-steady conditions, often referred to as Fick's Second Law.

This has been solved using the following conditions:

- boundary condition $C_{x=0;\ t>0} = C_s$ (the surface concentration equals C_s at x=0)
- initial condition $C_{x>0;\ t=0} = 0$ (the initial concentration equals zero);
- infinite point condition $C_{x=\infty;\ t>0} = 0$ (far enough away from the surface, the concentration equals zero).

The solution is:

$$\frac{C(x,t)}{C_s}=1-erf\left(\frac{x}{\sqrt{4Dt}}\right) \tag{57}$$

C concentration of diffusing substance

C_s surface concentration of diffusion substance

D diffusion coefficient
t time
x space coordinate measured normal to the section

Second Law of Fick – solution time dependent diffusion coefficient

In this thesis the chloride ingress is determined with the solution of Fick's second law of diffusion where the time dependent coefficient of diffusion is taken into account. This section gives the derivation of the solution with the time dependent diffusion coefficient from the partial differential equation.

In chapter 3, the time dependent diffusion coefficient is discussed and modelled by equation 18.

$$D_{cl}(t) = D_{cl;0}\left(\frac{t_0}{t}\right)^n \tag{58}$$

Combining the equation of the time dependent diffusion coefficient (equation 18) with Fick's second law of diffusion (equation 56) gives:

$$\frac{\partial C}{\partial t} = D_{cl;0}\left(\frac{t_0}{t}\right)^n \frac{\partial^2 C}{\partial x^2} \tag{59}$$

therefore

$$\frac{1}{D_{cl;0}\left(\frac{t_0}{t}\right)^n}\frac{\partial C}{\partial t} = \frac{\partial^2 C}{\partial x^2} \tag{60}$$

Substituting equation 61 into equation 60 results in equation 62.

$$\partial T = D_{cl;0}\left(\frac{t_0}{t}\right)^n \partial t \tag{61}$$

$$\frac{\partial C}{\partial T} = \frac{\partial^2 C}{\partial x^2} \tag{62}$$

The standard solution of equation 62 is given in equation 63.

$$C(x,t) = C_s\left(1 - erf\left(\frac{x}{\sqrt{4T}}\right)\right) \tag{63}$$

Integrating equation 61 results in equation 20.

$$\int_0^t D_{cl}(t)dt = \frac{D_{cl;0}}{1-n}\left(\frac{t_0}{t}\right)^n t \tag{64}$$

Finally, equation 21 results from the substitution of equation 20 into equation 63.

$$C_{cl}(x,t) = C_{cl;s}\, erfc \frac{x}{\sqrt{4\frac{D_{cl;0}}{1-n}\left(\frac{t_0}{t}\right)^n t}} \qquad (0<n<1) \tag{65}$$

The initial chloride concentration is included in equation 21 by reducing the driving potential of the surface chloride concentration with the initial chloride concentration which is later added to the determined chloride concentration, as is presented in equation 66.

$$C_{cl}(x,t) = C_{cl;i} + (C_{cl;s} - C_{cl;i}) \cdot erfc \frac{x}{\sqrt{4 \cdot \frac{D_{cl;0}}{1-n}\left(\frac{t_0}{t}\right)^n \cdot t}} \qquad (0<n<1) \tag{66}$$

Second Law of Fick – limited supply of diffusion substance

Another solution is given for the 'instant plane source' for an instantaneous limited supply of diffusion substance, during a short period of time. The conditions are:

- boundary condition $C_{x=0;t=0} = M$ (the amount of substance M is deposited at t=0 in the plane x=0);
- initial condition $C_{x>0;\, t=0} = 0$ (the initial concentration equals zero);
- infinite point condition $C_{x=\infty;\, t>0} = 0$ (far enough away from the surface, the concentration equals zero).

The solution is:

$$C(x,t) = \frac{M}{\sqrt{\pi D t}} \exp\left(-\frac{x^2}{4Dt}\right) \tag{67}$$

It must be emphasised that the statement expressed mathematically by Fick's first law of diffusion is in general consistent only for an isotropic medium, whose structure and diffusion properties in the neighbourhood of any point are the same relative to all directions.

appendix B Terms related to Chloride induced corrosion

This appendix gives a glossary of terms related to chloride ingress and testing in concrete [e.g. Stanish 2000].

Absorption: Drawing of fluids into unsaturated pores by capillary suction.

Bridge A bridge is a structure that is erected over a depression or an obstruction, such as water, highway of railway, having a track or passageway for carrying traffic or other moving loads, and having an opening measured along the centre of the roadway of more than 6.1 metres [FHWA 1995]. Other countries use different span lengths.

BFSC Blast furnace slag cement is a portland cement of which 36 to 95% of the cement is replaced by blast furnace slag (upper and lower replacement boundaries differ from country to country). The main cement type of blast furnace slag cement is grouped into three sub-types as are tabulated in table 23.

Table 23: Product in the family of blast furnace slag cement [NNI 1995a]

cement type	clinker	blast furnace slag
CEM III/A	35 – 64	36 – 65
CEM III/B	20 – 34	66 – 80
CEM III/C	5 – 19	81 – 95

C_3A Tri-calcium aluminate

Cation A positively charged mon(o)atomic (Na^+, H^+, Ca^{2+}, Fe^{2+}) or polyatomic (NH_4^+, H_3O^+) ion.

Chloride binding The combination of chloride ions with the cement matrix of the concrete either through physical of chemical action. It reduces the effective chloride concentration in the pore solution, called the free chloride concentration.

Conductivity A material property describing the ease with which electrons or ions can pass through a unit length of that material of a unit cross-section, the inverse of resistivity.

Convection The movement of a fluid, including the dissolved species it may contain, through a porous body.

Corrosion current density

Corrosion is an electrochemical process involving electrons flowing from the anode to the cathode. Therefore the number of exchanged electrons is proportional to the number of oxidized iron atoms. The intensity of the flow of electrons, which gives an indication of the magnitude of corrosion, is called the corrosion current. However, the corrosion current cannot be measured directly, but is determined using the electrochemical polarization method. This current (i_{corr}) is calculated from the Stern-Geary equation $i_{corr}=B/R_p$ [Stern 1957]. Where: B is a constant, and R_p is the polarization resistance.

Diffusion

Transfer of mass by random motion of free molecules or ions in the pore solution resulting in a net flow from regions of higher concentration to regions of lower concentration of the diffusing substance [Kropp 1995].

Diffusion coefficient

For solids the diffusion coefficient describes the ability of transfer for a given substance.

Electrolyte

A solution in which current is carried by the movement of ions.

Error-function

The error function and complementary error function are special cases of the incomplete gamma function. Their definitions are [Abramowitz 1970]:

$$erf(x) = \frac{2}{\sqrt{\pi}} \cdot \int_0^x e^{-t^2} \cdot dt \tag{68}$$

$$erfc(x) = 1 - erf(x) \tag{69}$$

$$erf^{-1}(x) \approx \frac{\sqrt{\pi}}{2}\left(x + \frac{\pi x^3}{12} + \frac{7\pi^2 x^5}{480} + \frac{127\pi^3 x^7}{40320} + \frac{4369\pi^4 x^9}{5806080} + \frac{34807\pi^5 x^{11}}{182476800} + \frac{20036983\pi^6 x^{13}}{398529331200}\right) \tag{70}$$

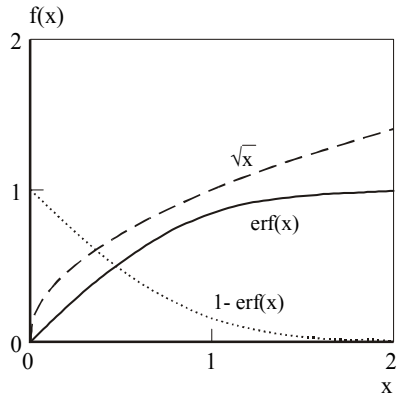

Figure 61: Error-function and √t-function

Failure — In this thesis failure is defined as the undesirable event of an intolerable amount of spalling.

Fick's Laws — The theoretical relationships governing diffusion. Fick's First Law states that: $F = -D\frac{dC}{dx}$. Fick's Second Law states that: $\frac{\partial C}{\partial t} = D\frac{\partial^2 C}{\partial x^2}$

Flux — Quantity of material that passes a unit area per unit of time.

Gradient — The change in value of a quantity per unit distance in a specified direction.

Half cell potential — A potential difference occurs between the anodic and cathodic areas of corroding reinforcement. As the rate of corrosion increases, the corrosion potential changes. The electrical potential difference between the anodic (half cell) and cathodic (half cell) may be measured by a voltmeter. The reading of the equipment gives the potential difference between the corroding reinforcement and a standard reference cell. Although interpretation of these potentials differences is disputed, it is generally agreed that a potential difference of –0.35 V versus $Cu/CuSO_4$, or more negative, is an indication of corrosion activity. The following guidelines are derived from U.S. bridge decks made of portland cement [ASTM 1999, van Daveer 1975]:

Table 24: Corrosion potential and corrosion probability for bridge decks [ASTM 1999]

potential [mV vs. Cu/$CuSO_4$]	**corrosion probability**
> -200	5%
-350 – -200	50%
< -350	95%

Migration — The movement of ions in a solution under an electrical potential gradient.

Permeation — Flow of liquids or gases caused by a pressure head [Kropp 1995].

Permeability (k) — The coefficient of permeability describes the permeation of gases or liquids through a porous material due to a pressure head. Frequently, the flow of water is evaluated according to the empirical formula of D'Arcy: $Q = k\frac{h}{l}A$, where Q = volumetric flow rate, A = flow area perpendicular to l, k = hydraulic conductivity, l = flow path length, h = change in hydraulic head over path l.

Porosity — The ratio, usually expressed as a percentage, of the volume of voids in a material to the total volume of the material, including voids.

Potential — The voltage difference between an anode and a cathode.

Sorptivity — Rate of absorption of water into an unsaturated surface of concrete by capillary action.

Spalling — The separation of a surface layer caused by thermal or mechanical stresses.

Structurally deficient — A bridge is structurally deficient if the superstructure or substructure requires immediate repairs or rehabilitation or if the ability to carry normal live loads is severely impaired.

Transport mechanisms — The different methods by which ions can travel from place to place, including but not necessarily limited to diffusion, permeation, wicking, sorption and migration.

Vapour diffusivity	The rate at which water vapour can travel through the unsaturated pores.
Wick-action	Evaporation of water in pores deposits salt and draws more solution to the evaporation front by absorption. Requires an air-exposed surface. Is dependent on humidity and on the vapour diffusivity of concrete.

appendix C Definitions for coefficient of chloride diffusion

In the numerous articles that are published about the coefficient of diffusion, many definitions are used [e.g. Chisholm 2001, Maage 1996]. This list of definitions is far from complete and is not more than a list to understand diffusion. There are two groups of diffusion coefficients; the steady state and the non-steady state diffusion coefficient. The non-steady state diffusion coefficient gives the diffusion coefficient as is defined by Fick's first law of diffusion. In a steady state test, specimens are exposed to a constant concentration gradient. The non-steady state gives the diffusion coefficient as is defined by Fick's second law of diffusion, where the driving difference in concentration changes in time.

D_{ss} steady state diffusion coefficient

D_{nt} diffusion coefficient obtained with NT Build 443 test
This coefficient is determined with a bulk immersion test, such as NT Build 443. During this test a completely water saturated specimen is submerged in a brine solution, 165 gr. sodium chloride per litre, during 35 days. The diffusion coefficient is obtained from the observed chloride profiles using non-linear regression analysis. This test is normally carried out on early-age (28 or 56 days) test specimens [Nordtest 1995].

D_{RCM} diffusion coefficient obtained with Rapid Chloride Migration test
During the rapid chloride migration test a completely water saturated specimen is submerged in a saline solution. The bottom of the specimen is in contact with a saline solution. Potential differences between electrodes that are attached to both ends of the specimen accomplish an increased migration of chlorides. After 6 to 96 hours of chloride exposure the specimen is split to determine the chloride ingress. The depth of the chloride ingress is determined with an indicator solution (silver nitrate). From the test-parameters (i.e. current, ingress depth, time of exposure) the coefficient of diffusion is calculated. The coefficient of diffusion that is determined with the RCM method agrees with the actual coefficient of diffusion [Nordtest 1999].

D_{eff} effective diffusion coefficient (a.k.a. apparent, achieved, bulk or in situ)
This coefficient is determined from a chloride profile by regression analysis, as is used in this research project. It reflects influences from all possible transport mechanisms that have contributed to the chloride profile and is an indication of the historical performance.

D_p potential diffusion coefficient (a.k.a. actual, intrinsic, measured)
The potential diffusion coefficient is determined from the virgin inner part of structures. In this way the concrete samples that are obtained are not 'contami-

nated' by chlorides. The diffusion coefficient is obtained by means of test methods like RCM or NT-443 method.

appendix D Review minimum cover depth (Dutch standards)

Usually the depth of the cover depends on the environment that the structure is exposed to during the period of use. The five types of environments that are used in this appendix are:

dry environment	the concrete surface is during the period of use not exposed to or in contact with ground, water or other atmospheric influences.
wet environment	the concrete surface is during the period of use exposed to water, ground and every kind of weather
wet environment + salt	the concrete surface is during the period of use exposed to wet environment plus de-icings salts.
marine environment	the concrete surface is during the period of use exposed to seawater or spray.
aggressive environment	the concrete is during the period of use exposed to a marine environment (also spray), aggressive liquids (acids), corrosive gas and vapor

Dutch reinforced concrete standard 1912 [Kivi 1912]

Table 25: Cover depth

structural member	cover on outer layer of reinforcement [mm]
	all environments
slab	10
beam	15
column	15

In the text of the standard, only one sentence is used to regulate the minimum concrete cover. This is remarkable because the writers of the standard were aware of the fact that there was a danger of corrosion and damage due to fire.

Dutch reinforced concrete standard 1918 [Kivi 1918]

Table 26: Cover depth

structural member	cover on main reinforcement [mm]	surcharges [mm]
	all environments	aggressive environment
slab	10	+10
beam	25 (17)	+10
column	35 (27)	+15

In this standard the cover is explicitly defined as the distance from the main reinforcement to the concrete surface. The diameter of the stirrups should be at least 8mm. The distance from the outer layer of reinforcement to the concrete surface is given between brackets.

Dutch reinforced concrete standard 1930 [Kivi 1930]

Table 27: Cover depth

structural member	cover on main reinforcement [mm]		surcharges [mm]
	all environments	uncontrollable surface	aggressive environment
slab	10	20	+10
beam	25 (17)	35	+10
column	35 (27)	-	+15

The explanation of this article warns for very large cover depth (50mm) in an aggressive environment, because of the risk of cracks due to shrinkage. This gives an idea how was thought about the concrete cover in those days.

Dutch reinforced concrete standard 1940 [Kivi 1940]

Table 28: Cover depth

structural member	cover on main reinforcement [mm]		surcharges [mm]	
	all environments	uncontrollable surface	aggressive environment	surface sandblasted
slab	10	20	+10	+10
beam	25 (17)	35 (27)	+10	+10
column	35 (27)	-	+10	+10

Dutch reinforced concrete standard 1950 [Kivi 1950]

The concrete cover measured from the bar closest to the concrete surface (this includes the stirrups) should be at least the values in the Table below:

Table 29: Cover depth

structural member	depth of member	cover on outer layer of reinforcement [mm]			surcharges [mm]	
		dry environment	wet environment	uncontrollable surface	aggressive environment	surface sandblasted
slab or wall	$h \leq 120$mm	10	15	20	+10	+10
	$h > 120$mm	15	15	20	+10	+10
beam	-	20	25	40	+10	+10
column	-	30	35	40	+10	+10

Dutch reinforced concrete standard 1962 [Kivi 1962]

Table 30: Cover depth

structural member	cover on outer layer of reinforcement [mm]			surcharges [mm]	
	dry environment	wet environment	uncontrollable surface	aggressive environment	surface sandblasted
floor slab	10	15	20	+10	+10
walls	15	20	25	+10	+10
beam	20	25	30	+10	+10
column	25	30	35	+10	+10

An aggressive environment is an environment with very high temperatures during a fire or contact with seawater (chlorides)

Dutch reinforced concrete standard 1974 and 1984 [NNI 1984]

In general, the cover has to be equal or larger than:
∅ if ∅ is equal to, or smaller than 25mm;
1.5·∅ if ∅ is larger than 25mm.

The concrete cover can be reduced by 5mm if the following conditions are met:
- the water-cement ratio is lower than 0.50 in dry environment or lower than 0.45 in a wet environment;
- 2/3 of the grain size is smaller than the cover.

These reductions may not lead to a cover that is lower than 25mm in case of a beam or 30mm in case of a column.

Table 31: Cover depth

structural member	**concrete grade**	**cover on outer layer of reinforcement [mm]**			**surcharges [mm]**			
		dry environment	**wet environment**	**aggressive environment**	**prestress steel**	**lightweight concrete**	**surface sand-blasted**	**uncontrollable surface**
slab or wall	B17,5 and lower	15	25	35	-	+5	+5	+5
	B 22.5 and higher	15	25	30	+10	+5	+5	+5
beam	B17,5 and lower	25	35	40	-	+5	+5	+5
	B 22.5 and higher	25	30	35	+10	+5	+5	+5
column	B17,5 and lower	30	40	45	-	+5	+5	+5
	B 22.5 and higher	30	35	40	+10	+5	+5	+5

Dutch reinforced concrete standard 1990/1995 [NNI 1995b]

Table 32: Cover depth (VBC 1990/1995)

structural member	**cover on outer layer of reinforcement [mm]**			**surcharges [mm]**		
	class 1	class 2	class 3, 4 and 5	surface sand-blasted	uncontrollable surface	f'_{ck}<25 N/mm^2
slab, wall	15	25	30	+5	+5	+5
beam, console	25	30	35	+5	+5	+5
column	30	35	40	+5	+5	+5

Table 33: Environmental classes (VBC 1990/1995)

class	**environment**
1	dry
2	wet
3	wet in combination with de-icing salts
4	marine
5 (a, b, c or d)	aggressive (weak, moderate, strong or very strong)

According to article 5.2.2, the cover should not be more than 5mm smaller than the regulated depth.

appendix E Cover depth according to Dutch standards

The results of the over 1100 determined cover depths are tabulated in table 34. In this table the cover depths are grouped by structural element and the standard according to which these elements are constructed. The cover depths have been determined with a cover meter,

Table 34: Actual cover depth at structures (mm)

structural member	standard	valid thru	standard cover depth	# data	mean value	standard deviation
beam	GBV 50/62	1950-1973	25	134	42.0	9.7
beam	VB 74/84	1974-1989	30	28	46.9	10.7
column	GBV 1962	1962-1973	30	38	37.9	6.1
column	VB 74/84	1974-1989	35	16	43.1	6.7
parapet	GBV 1950	1950-1961	15	43	44.4	11.4
parapet	GBV 1962	1962-1973	20	287	42.5	9.1
parapet	VB 74/84	1974-1989	25	91	48.2	8.7
parapet	VBC 90/95	1990-2000	30	10	53.2	10.7
slab	GBV 1950	1950-1961	15	32	36.5	11.7
slab	GBV 1962	1962-1973	20	97	36.0	5.9
slab	VB 74/84	1974-1989	25	40	46.6	5.6
wall	GBV 1950	1950-1961	15	60	36.6	12.2
wall	GBV 1962	1962-1973	20	161	39.9	5.5
wall	VB 74/84	1974-1989	25	103	48.5	6.7
wall	VBC 90/95	1990-2000	30	14	53.7	6.7

appendix F Compressive and tensile strength

The results of the compressive and tensile tests are tabulated in table 35. The cores were taken from the same bridges as the cores that were analysed for chloride concentration. The diameter of the cores was 75mm and the samples had a length of 150mm.

Table 35: Compressive and tensile strength

name	year	sample	$f'_{c;cyl}$	f'_{c_cube}	sample	$f_{t;uniaxial}$	sample	$f_{t;split}$	sample	$f_{t;split}$
unit			MPa	MPa		MPa		MPa		MPa
Reevliet	1963	R-D07	55,1	64,8	R-T07	1,1	R-D07	-	R-T07	-
		R-D08	71,2	83,8	R-T08	2,0	R-D08	4,3	R-T08	-
		R-D09	80,7	94,9	R-T09	2,0	R-D09	4,4	R-T09	-
		R-D10	55,8	65,6	R-T10	2,2	R-D10	4,5	R-T10	5,6
		R-D11	66,7	78,5	R-T11	2,2	R-D11	5,5	R-T11	-
		R-D12	56,1	66,0	R-T12	1,9	R-D12	4,8	R-T12	-
		R-D21	44,2	52,0	R-T21	-	R-D21	4,6	R-T21	-
		R-D22	68,7	80,8	R-T22	2,2	R-D22	-	R-T22	6,1
Mark	1940	BMD1	40,4	47,5	BMT1	1,2	BMD1	4,6	BMT1	-
		BMD2	45,0	52,9	BMT2	1,6	BMD2	4,1	BMT2	-
		BMD3	44,2	52,0	BMT3	1,1	BMD3	4,3	BMT3	-
		BMD4	46,8	55,1	BMT4	1,6	BMD4	3,9	BMT4	-
		BMD23	81,4	95,8	BMT23	1,6	BMD23	5,1	BMT23	-
		BMD24	78,6	92,5	BMT24	1,8	BMD24	5,7	BMT24	4,9
		BMD25	86,0	101,2	BMT25	2,0	BMD25	5,7	BMT25	-
Langeweg	1940	LGD1	52,7	62,0	LGT1	1,4	LGD1	3,7	LGT1	-
		LGD2	41,9	49,3	LGT2	0,6	LGD2	-	LGT2	3,0
Verlaten-dijk	1965	VD01	51,5	60,6	VT0	1,9	VD01	-	VT0	-
		VD02	47,4	55,8	VT02	2,2	VD02	-	VT02	4,5
Klein Overveld	1967	KD17	79,8	93,9	KT17	2,0	KD17	-	KT17	3,9
		KD18	57,0	67,1	KT18	2,4	KD18	-	KT18	5,3
average				70,5		1,75		4,69		
standard dev.				18,0		0,47		0,78		
var. coeff.				0,25		0,27		0,17		

appendix G History of Blast Furnace Slag Cement

It is important to know how the practice of slag in cement developed for bridge construction, because of the differences in resistance to ingress of chlorides between portland cement and blast furnace slag cement, when the durability of a bridge stock is assessed.

In 1888, the first blast furnace slag cement works was opened in Germany. The cement used in the Netherlands was imported from Germany. The Dutch iron and steel industry (Hoogovens) and the Dutch Portland Cement industry (ENCI), established a blast furnace slag cement factory, CEMIJ, at the blast furnace in IJmuiden, which started production in 1931 [Bijen 1998].

Over the years, the attitude of the standards about BFSC changed considerably. This section gives an overview of the attitude of the Dutch standards about BFSC.

GBV 1912	The use of blast furnace slag in cement is prohibited [Kivi 1912].
GBV 1918	The use of blast-furnace slag cement (replacement 75%) is prohibited for reinforced concrete. The use of iron-portland cement is allowed if the replacement is less than 30% [Kivi 1918].
GBV 1930	The use of BFSC is only permitted if principal and the contractor came to an agreement in advance [Kivi 1930].
GBV 1940	The regulation of cement are identical to GBV 1930 [Kivi 1940]
GBV 1950	The regulation of cement are still identical to GBV 1930. However, the clarification of the standard mentions that other cement types are not used to deliberately reduce of the quality of the concrete, but are frequently used for concrete in an aggressive environment [Kivi 1954].
GBV 1962	The contractor is free to choose the type of cements, and is no longer obliged to come to an agreement with the principal. The clarifications mention that the BFSC has better characteristics to offer resistance to an aggressive environment than PC [Kivi 1962].
VB 74/84	The regulation of cement still mentions that a certain type of cement can be banned to be used in concrete in an aggressive environment. This text has stayed the same for 50 years, but by now it means that the PC can be banned and not BFSC [NNI 1984].

Concrete made of blast furnace slag cement shows a temporary blue discolouration after removal of the mold. The blast furnace slag causes the discolouration when it reacts with water, because the slag contains iron, manganese and sulphur. These materials react to iron sulphide (FeS) and manganese sulphide (MnS) and give the blast furnace slag cement its blue colour. If the mold is removed, the blue colour will fade away in a few days due to oxidation. During the oxidation of iron sulphide and man-

ganese sulphide changes to respectively iron sulphate ($FeSO_4$) and manganese sulphate ($MnSO_4$) [Betoniek 1994].

The intensity of the discolouration gives an indication of the concrete quality. A concrete core of good quality is dark blue or purple. If the concrete has a high porosity, the near surface concrete may be oxidized to a depth of several centimetres within a few years.

appendix H National Bridge Inventory

The National Bridge Inventory is a database that catalogues the characteristics and tracks the condition of all bridges in the United States. This database was created after the collapse of the Silver Bridge. December the 15th 1967, the Silver Bridge across the Ohio River at Point Pleasant, West Virginia, collapsed under a load of bumper-to-bumper traffic. Thirty-one of the 37 vehicles on the bridge fell into the Ohio River or onto the Ohio Shore. Forty-six people were caught in their cars and died. At the time, there was no systematic maintenance program in place to monitor the condition of the nation's bridges. In fact, the exact number of bridges standing in the United States was not even known at that point in time [Hooks 2000].

To address this problem, the Federal Highway Act of 1968 created the National Bridge Inspection Program, which ordered state agencies to catalogue and track the condition of bridges on principal highways. The program set standards for state highway departments to conduct safety inspections, established the maximum time lapses between inspections and determined the qualifications of those responsible for carrying out the inspections. The data collected is submitted after every inspection period and maintained by the Federal Highway Administration in the National Bridge Inventory database.

Table 36: Number of concrete highway bridges in U.S. highways (year 2000)

span type	**number of bridges**
slab	34851
stringer / multi beam (cast in place)	7068
stringer / multi beam (precast)	44751
T-beam	22803
box beam cast in place (single / multiple)	8111
box beam cast in place (precast)	16376
frame	2278
arch	2035
segmental box girder	159
truss	5
orthotropic	4
other	2342
total	**140783**

The following figures will show the relative number of deficient concrete bridges of each type of span (slab, beam, t-beam, multiple of single box girder) in Interstate -, US numbered – and State highways.

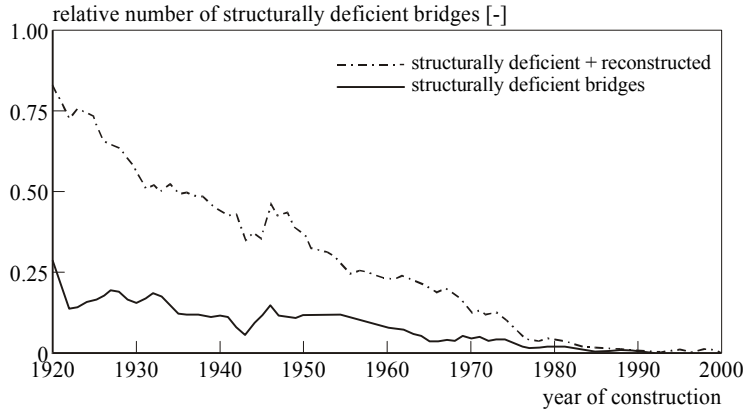

figure 62: Deficient slab bridges in US highways

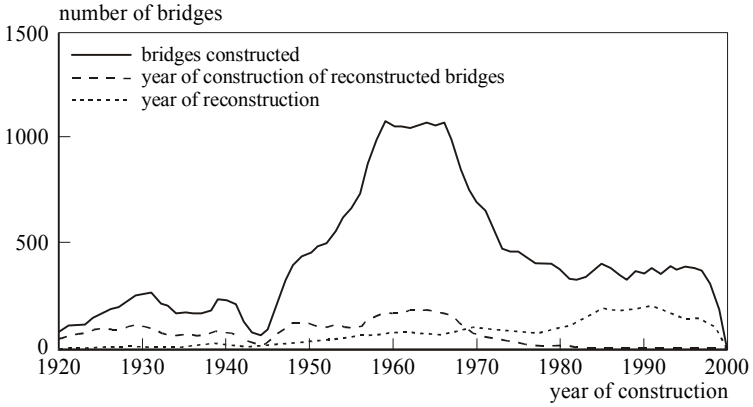

figure 63: Number of deficient slab bridges in US highways

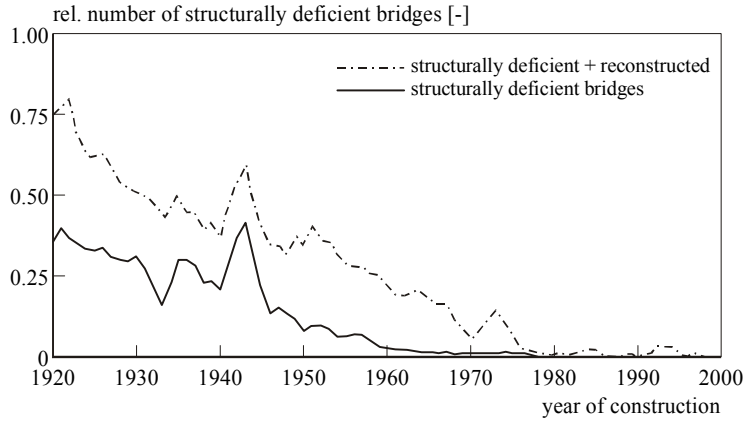

figure 64: Deficient cast in place girder bridges in US highways

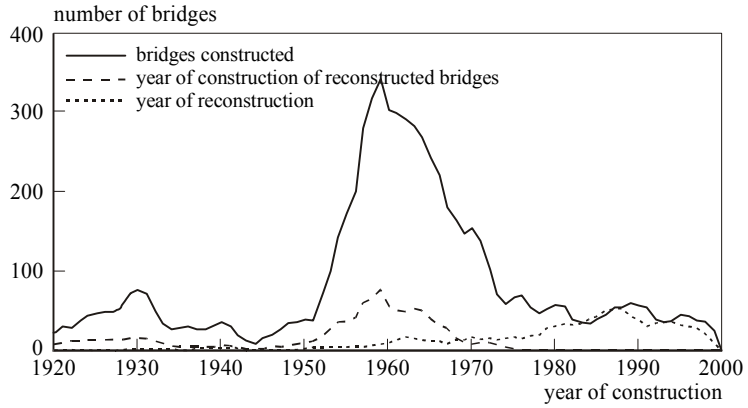

figure 65: Number of deficient cast in place girder bridges in US highways

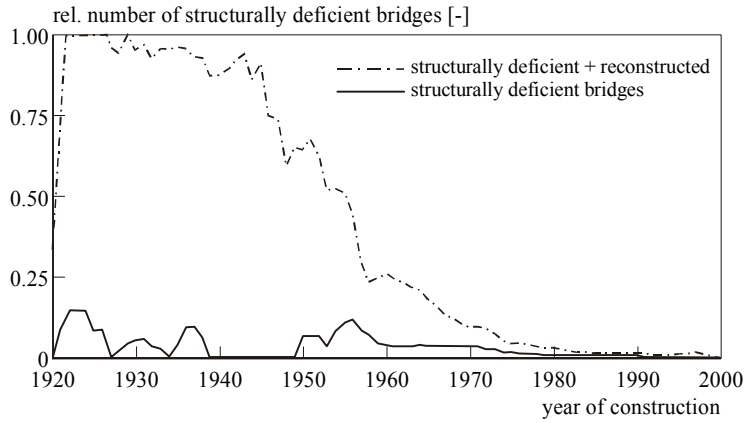

figure 66: Deficient precast girder bridges in US highways

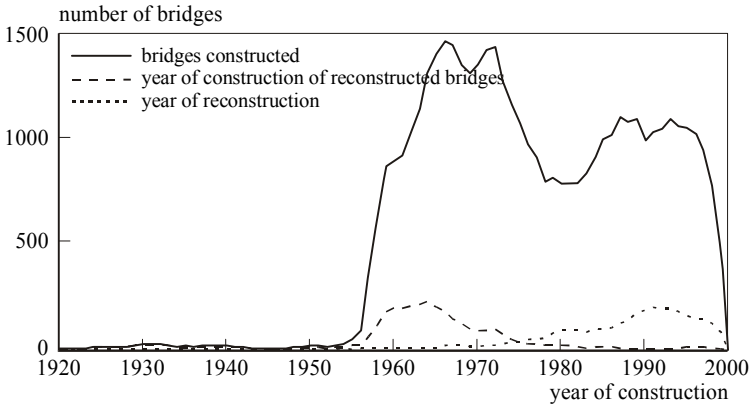

figure 67: Number of deficient precast girder bridges in US highways

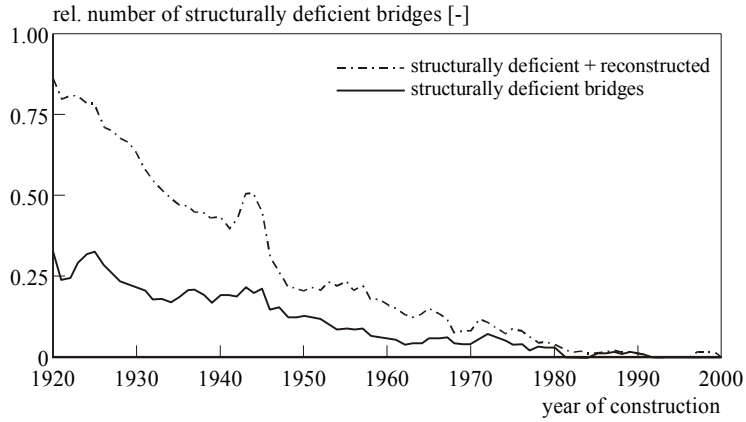

figure 68: Deficient T-beam bridges in US highways

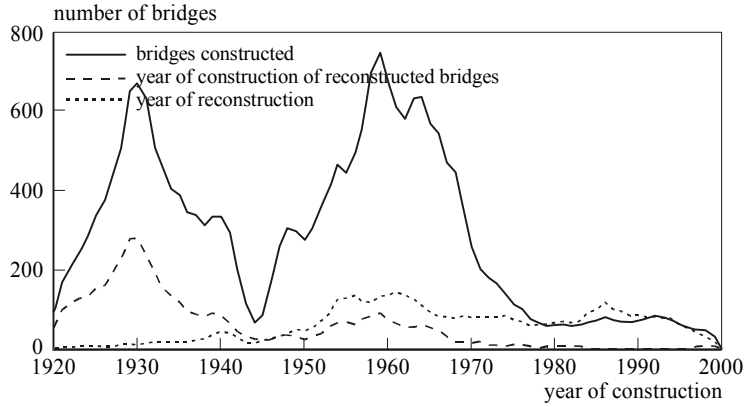

figure 69: Number of T-beam girder bridges in US highways

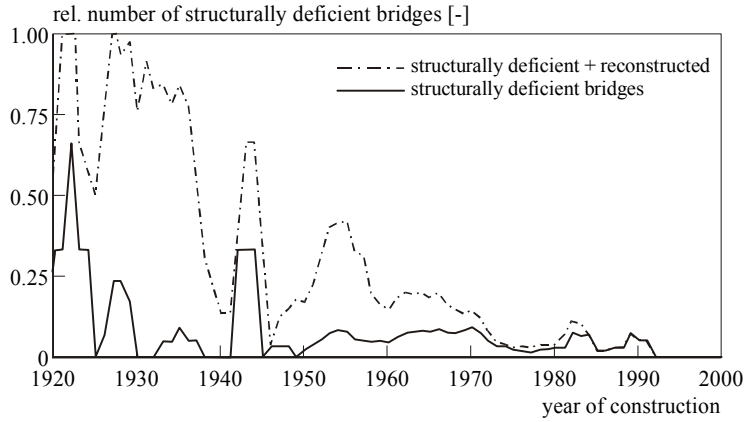

figure 70: Deficient cast in place box beam girder bridges in US highways

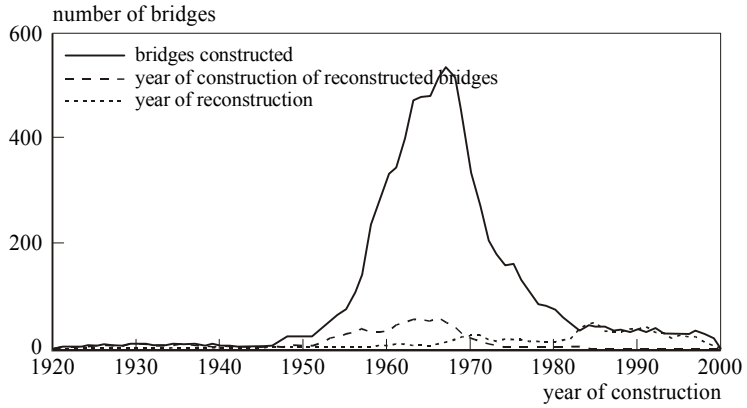

figure 71: Constructed cast in place box beam girder bridges in US highways

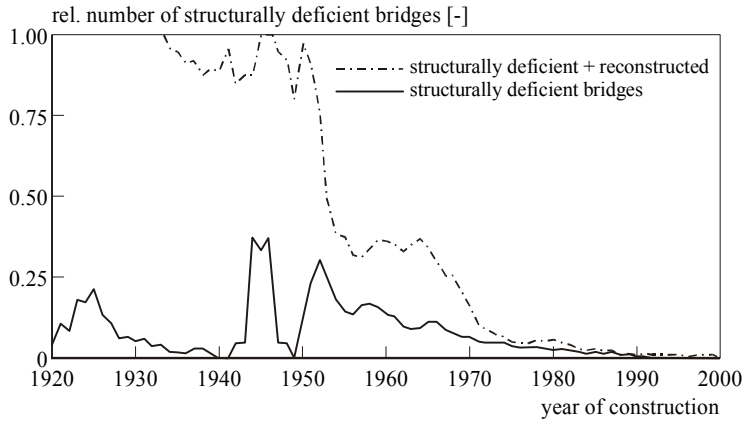

figure 72: Precast box beam girder bridges in US highways

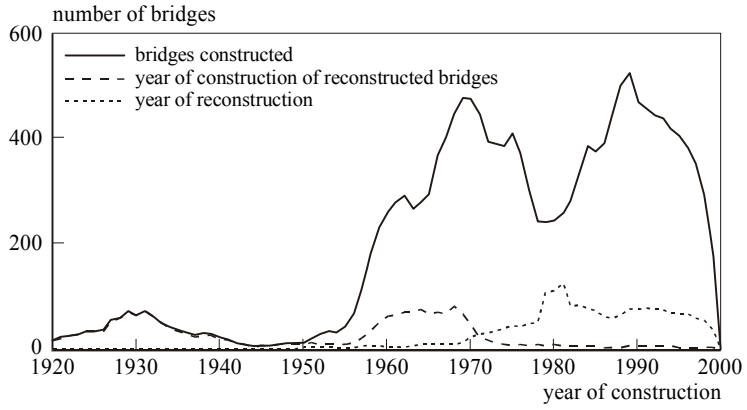

figure 73: Number of precast box beam girder bridges in US highways

Resume

Gerard Gaal was born on the 9th of March 1972 in Alkmaar. After graduation of the secondary school for lower general education (MAVO) in 1988 he started the education of Civil Engineering at the intermediate technical school (MTS). After completion of his study at the intermediate technical school in 1992 he continued the education of Civil Engineering at the secondary technical school (HTS).

As a result of the time scholarship he was forced to leave the secondary technical school after two years, to be able to finish the study of Civil Engineering at Delft University of Technology in time. In June 1999, he completed his study at Delft University of Technology with a graduation project about elevated highways for light weight traffic. This study was executed in assignment of the Ministry of Transport, Public Works and Water Management.

In August 1999, he started his Ph.D. project at the Concrete Structures Group of Delft University of Technology, concerning the durability of concrete highway bridges. The research was widely orientated and narrowly connected to the Dutch Ministry of Transport, Public Works and Water Management.

Since the first of May 2004, Gerard Gaal is working with Lloyd's Register Rail B.V. as a consultant. He is involved in various infrastructure related projects regarding asset management, risk and safety management, verification and validation.